CHARACTERISATION OF THE EFFECTS AND MECHANISM OF ACTION OF RAPAMYCIN AND GENISTEIN ON ACUTE MYELOID LEUKEMIA USING HIGH-THROUGHPUT TECHNIQUES

KARTHIK NARASIMHAN

(B.Tech, Biotechnology)

A THESIS SUBMITTED FOR THE DEGREE OF

DOCTOR OF PHILOSOPHY

DEPARTMENT OF BIOLOGICAL SCIENCES

NATIONAL UNIVERSITY OF SINGAPORE

2010

ACKNOWLEDGEMENTS

Words don't do justice to the heartfelt gratitude that I would like express to my supervisor, Dr.Lin Qingsong for the support, encouragement and invaluable guidance that he has provided me. He has been a friend, philosopher and guide, a constant source of encouragement, and a fountainhead of inspiration- in short the best supervisor one could possible ask for. I thank him for the confidence that he reposed in me and the scientific temper that he inculcated in me.

I would like to thank Dr.Prakash Kumar and Dr.Kunjithapadham Swaminathan for their mentorship and counsel. I'm deeply indebted to Dr.Paul Hutchinson of the 'Flow lab' of CeLS for his assistance and insights in performing the flow cytometry work. My previous supervisor Dr.Han Jin Hua was instrumental in helping me initiate my research, for which I'm very thankful to her.

I owe a great deal to the help and support of Lim Teck Kwang, our research assistant, Tay Bee Ling and all my lab mates for the stimulating research atmosphere that they provided in the lab. My thanks are due to Sarah Port and Aravind Menon, two excellent students, whom I had the pleasure of guiding and supervising.

My family has always believed in me and have been an unwavering source of support in all my endeavours. My father, mother, brother, grandparents, *mama* and *mami* have been my pillars of strength. It is the implicit faith and unconditional affection that they showered on me, which gave me the confidence and courage to brave the thrills and chills of research life.

'Some people go to priests; others to poetry'; and I to my friends- Aravind, Ayshwarya, Gauri, Pradeepa, Prasanna, Priya, Satish, Sheela, and Sravanthy. Life would not have been the same without them. I would like to thank them for all the hours spent in the canteen over mindless chats, days spent discussing science, and years spent looking out for each other through the thick and thin of time!

TABLE OF CONTENTS

SUMMARY

Acute Myeloid Leukemia (AML), caused by the uncontrolled proliferation of the leukocytes of the myeloid lineage, is a cancer with a very high mortality rate. Present therapies to treat AML include chemotherapy and bone marrow transplant. These methods suffer from certain inherent limitations such as heavy cytotoxicity and innocent bystander effects in the case of the former and acute allograft rejection in the latter. Hence there is an urgent need for more effective therapeutic strategies.

In this study, we have evaluated the efficacy of two such potential therapeutic drugs, namely Rapamycin (rapa) and Genistein (GEN) and have characterised their mechanism of action using high-throughput strategies. A combination of microarray and 4-plex iTRAQ based approach was adopted to study the effects of rapa on MV4-11 and THP-1 cells and an 8-plex iTRAQ based methodology was employed to profile the proteome of the MV4-11 and HL-60 cells treated with GEN.

We found that rapa had potent anti-proliferative effect on all the AML cell lines tested. We chose the cell lines with the lowest and highest IC_{50}, MV4-11 and THP-1 respectively, for functional characterisation. High-throughput studies indicated that rapa regulates Cell cycle, IGF-1 and FGF signalling, death receptor signalling, protein ubiquitination and hypoxia signalling pathways. Functional studies showed that rapa did not induce apoptosis but effected a time-dependent G1 arrest, with the peak inhibitory effect at 16 h. Interestingly, rapa down-regulated IGFBP2, usually elevated in AML patients. Our study showed that rapa represses Skp2, an important constituent of the protein ubiquitination pathway. Working on this clue, we identified that the time dependent G1 arrest is in fact the result of the inhibition of Skp2, leading to the accumulation of p27, which in turn causes repression of Cdk2 and Cdk4.

In the second study, we found that GEN had inhibitory effects on both the MV4-11 (IC_{50} 20µM) and HL-60 (IC_{50} 30µM) cells. We discovered that GEN inhibited the constitutive

phosphorylation of FLT3 in the MV4-11 cells, which carry the FLT3-ITD (Internal Tandem Duplication) mutations. However, GEN had potent anti-leukemic effects on the HL-60 cells too, in spite of them possessing the wild-type version of the gene.

A purely proteomic-based approach, using the 8-plex iTRAQ strategy, was employed to understand the dynamics of GEN's effects on the two subsets of AML. We found that GEN down-regulated the mTOR pathway, thus arresting protein synthesis in the AML cells. GEN up-regulated Akt, leading to elevation in the reactive oxygen species (ROS) levels which in turn caused apoptosis. While HL-60 underwent a caspase- mediated cell death, the apoptosis in MV4-11 was caspase independent. GEN induced arrest at the G2/M phase of the cell cycle in HL-60 while it caused a moderate G1 arrest in MV4-11. We can attribute these differences in the mechanism of action of GEN to the FLT3 mutational status of the two cell lines. Hence, we conclude that GEN has an all encompassing anti-proliferative effect on AML irrespective of its FLT3 mutational status and is an ideal candidate for clinical trials.

LIST OF TABLES

LIST OF FIGURES

LIST OF ABBREVIATIONS

2-D	Two- dimensional
2-DE	Two- dimensional electrophoresis
4EBP-1	4E binding protein 1
ACN	Acetonitrile
AML	Acute myeloid leukemia
APL	Acute promyelocytic leukemia
ATO	Arsenic trioxide
ATRA	All transretinoic acid
BSA	Bovine serum albumin
C.I	Confidence interval
CBF	Core binding factor
Cdk	Cyclin dependent kinase
CDKI	Cyclin dependent kinase inhibitor
Da	Dalton
DMSO	Dimethyl sulfoxide
ESI	Electrospray ionisation
FAB	French American British
FACS	Fluorescence activated cell sorting
FCS	Fetal calf serum
FITC	Fluorescein isothiocyanate
FLT3	Fms-like tyrosine kinase 3
FLT3-ITD	Fms-like tyrosine kinase 3- internal tandem duplication
GEN	Genistein
GO	Gene ontology
h	Hour
HAMMOC	Hydroxy Acid-Modified Metal Oxide Chromatography
HRP	Horse radish peroxidase
IC_{50}	Half maximal inhibitory concentration
ICAT	Isotope-Coded Affinity Tags

IPA	Ingenuity pathway analysis
IPI	International Protein Index
iTRAQ	isobaric Tag for Relative and Absolute Quantitation
LC/MS	Liquid chromatography/mass spectrometry
M	Molar
MAPK	Mitogen activated protein kinase
min	Minute
ml	Milli litre
mM	Milli molar
MMTS	Methylmethanethiosulphate
MS	Mass spectrometry
mTOR	mammalian Target Of Rapamycin
MTS	3-(4,5-dimethylthiazol-2-yl)-5-(3-carboxymethoxyphenyl)-2-(4-sulfophenyl)-2H-tetrazolium
nM	Nano molar
P.I	propidium iodide
p70S6K	p70S6 kinase
PBS	Phosphate buffered saline
PBS-T	Phosphate buffered saline- Tween
PEITC	β-phenylethyl isothiocyanate
PI3K	Phosphatidylinositol-3 kinase
PKM2	Pyruvate kinase M2
PS	Phosphatidylserine
PTK	Protein tyrosine kinase
PTM	Post-translational modification
PVDF	Polyvinylidene fluoride
Rapa	Rapamcyin
RC DC	Reducing agent and detergent compatible
ROS	Reactive oxygen species
rpm	Rotations per minute
RT	Real time

RTK	Receptor tyrosine kinase
RTKIII	Class III receptor tyrosine kinase family
s	Second
S/N	Signal to noise ratio
SDS	Sodium dodecyl sulphate
SDS-PAGE	Sodium dodecyl sulphate- polyacrylamide gel electrophoresis
SILAC	Stable isotope labelling by amino acid in cell culture
Skp2	S-phase kinase-associated protein 2
TCEP	Tris-(2-carboxyethyl) phosphine
TEAB	Triethylammonium bicarbonate Buffer
WBC	White blood cells
WHO	World health organisation
µ	Micron
µg	Microgram
µl	Microlitre
µM	Micro molar

CHAPTER 1

REVIEW OF LITERATURE

The literature review section comprises of an in-depth examination of the biology of acute myeloid leukemia, the drugs rapamycin and genistein, and an evaluation of the advantages of combining high-throughput approaches and functional analyses to study the mechanism of action of drugs.

1.1 Cancer

Cancer is a disease which is defined by the uncontrolled growth and proliferation of a group of cells. Cancer has afflicted humans for a long time. It is the leading cause of death in the western countries, second only to heart disease. According to the American Cancer Society's reports, the disease accounts for nearly 23.1% of all deaths in the United States of America alone. In Singapore too, the statistics show a similar trend, with cancer causing 25.6% of all deaths (Look, et al., 2001), making it one of the leading causes of mortality.

Cancer is a composite disease and is classified based on the individual organs and systems of the body where it develops. In clinical terms, cancer is defined as a collective term to include a large number of complex diseases, up to a hundred, that behave differently depending upon the cell types that they originate from. Cancers of the blood, liver, lung, breast, ovary, cervix, prostate, testis, colon, rectum, pancreas, lymph and kidney, are among the common manifestations of this disease.

Metastasis refers to the spreading of cancer from its primary site of origin to other parts of the body. The lethal combination of uncontrolled cell proliferation and metastasis makes cancer cells highly dangerous. Most cancers, with the notable exception of leukemia, are characterised by the formation of a tumour, a lesion like growth of an abnormal cluster of cells. Tumours could be benign (harmless, non-metastatic), pre-malign, or malign (harmful,

cancerous, and metastatic). While benign tumours can be surgically removed with no serious harm, malignant tumours are very difficult to treat.

Cancer is a genetic disease involving a multitude of genomic alterations such as single-nucleotide substitutions, large-scale chromosomal rearrangements, amplifications and deletions. The development of cancer is a multistep process and is influenced by a variety of risk factors such as age, sex, life style, diet, genetic makeup, etc. The causal factors contributing to cancer development are diverse. It is often a culmination of multiple factors that interact over a long period of time. On the one hand, the risk factors include heredity, abnormal genetic regulation and genetic makeup of some individuals. On the other hand, in many cases, the onset of the disease may be due to certain cancer causing agents called carcinogens such as tobacco and ionising radiations (Sasco, et al., 2004). It has been found that some viruses such as the human papillomavirus also induce tumours (zur Hausen, 2009). One of the most lethal among the various types of cancers is acute myeloid leukemia.

1.2 Acute Myeloid Leukemia

The etymology of the term 'leukemia' is derived from ancient Greek, 'leukos' meaning white and 'aima' meaning blood. It is the cancer of white blood cells (leukocytes). It is a hematopoietic stem cell disorder characterised by a block in differentiation of hematopoiesis, resulting in growth of a clonal population of neoplastic cells or blasts. It is broadly classified into 2 categories:

1) Acute Leukemia: This is the result of rapid increase in the levels of immature blood cells. It is the most common type of leukemia in children. It progresses fast and hence requires immediate treatment. The malignant cells if left untreated, pose the risk of metastasising through the bloodstream into other organs of the body.

2) Chronic Leukemia: This is characterised by the accumulation of relatively mature blood cells, over a period of months to years. In contrast with acute leukemia, chronic leukemia is

monitored over a period of time to ensure maximum effectiveness of the therapy. The frequency of affliction is greater among older people.

Additionally leukemia is subdivided based on the type of white blood cells (WBC) affected. Hence there are two subdivisions based on this classification method, namely:

a) Lymphocytic leukemia: The cancer develops in the lymphoid lineage of cells.

b) Myelogenous (myeloid) leukemia: The cancer occurs in the myeloid lineage of cells.

Hence by the combination of these two classification strategies, we recognise four types of leukemia (Table 1.1):

Table 1.1: Classification of leukemia by lineage and tumourigenicity

Affected cell lineage	Acute	Chronic
Lymphocytic	Acute lymphocytic leukemia	Chronic lymphocytic leukemia
Myelogenous (Myeloid)	Acute myelogenous leukemia	Chronic myelogenous leukemia

1.2.1 Biology of AML

Acute Myeloid Leukemia (AML) is a cancer of the leukocytes of myeloid lineage, distinguished by uncontrolled proliferation of hematopoietic precursor cells with decreased rate of self destruction and impaired differentiation. They comprise a heterogeneous group of malignancies of hematopoietic progenitor cells with different genetic abnormalities, clinical characteristics, and variable outcomes with currently available treatments (Gilliland and Tallman, 2002). The diagnosis of AML is now established when at least 20% of the cells identified in the blood or bone marrow are blasts of myeloid origin.

AML is principally classified based on the French-American-British (FAB) system, devised in 1976, which was later reviewed and revised in 1985. This is the most widely used system and the default methodology adopted to classify AML. AML is categorised eight-fold hence in Table 1.2.

Table 1.2: French-American-British (FAB) system of classification of AML

Category	Morphology	Incidence (%)
M0	AML with no differentiation	3
M1	AML without maturation	15-20
M2	AML with granulocytic maturation	25-30
M3	Hypergranular APML	5-10
M3 variant	Hypogranular variant APML	
M4	Acute myelomonocytic leukemia	25-30
M5a	Acute monoblastic leukemia	2-10
M5b	Acute monocytic leukemia	
M6	Erythroleukemia	3-5
M7	Megakaryoblastic leukemia	3-12

The classification depends on accurate morphological and cytochemical quantitation of the degree of differentiation and level of lineage commitment. The classification of AML in this system is defined by the presence of greater than 30% myeloid blasts in the bone marrow (Smith, et al., 2004) and their reactivity with histochemical stains, including myeloperoxidase, Sudan black, and the nonspecific esterases α-naphthylacetate and naphthylbutyrate.

An alternate system of classification is adopted by WHO which aims to demarcate distinct clinical entities within the spectrum of AML types as listed in Table 1.3. However this system is specialised and not used in common parlance.

Table 1.3: World Health Organisation (WHO) classification of AML

Category	**Morphology**	**Incidence (%)**
AML with recurrent cytogenetic translocations	AML with features of t(8;21)(q22;q22) AML with features of t(15;17)(q22;q12) AML with features of inv(16)(p13;q22) AML with 11q23	5–12 10–15 5 3-5
AML with MDS-related features	AML with multi-lineage dysplasia AML arising in previous MDS	10–15
Acute myeloid leukaemia, unspecified	AML minimally differentiated [M0] AML without maturation [M1] AML with maturation [M2] Acute myelomonocytic leukaemia [M4] Acute monocytic leukaemia [M5] Acute erythroid leukaemia [M6] Acute megakaryocytic leukaemia [M7] Acute basophilic leukaemia Acute panmyelosis with myelofibrosis	40–50
AML, therapy related	Alkylating agent-related Epipodophyllotoxin related Other types	5–10

1.2.2 Epidemiology of AML

AML accounts for 30% of all adult leukemia incidences. The epidemiology of AML shows some interesting trends. The disease has an incidence of 3.7 per 100,000 persons in the U.S.A. However it has an age-dependent mortality of 2.7 to nearly 18 per 100,000 persons. According to the American Cancer Society, 31,500 individuals in the U.S. will be diagnosed with leukemia annually. An estimated 21,500 patients will die of this disease. The annual incidence rates in Europe were between 2 and 4 per 100,000. In Singapore, leukemia is the tenth most common cancer among males (http://www.singaporecancersociety.org.sg/lac-gci-cancer-facts-n-figures.shtml). Although it is a relatively rare form of cancer, it has disproportionate survival rates in comparison to other cancer types. The incidence of acute leukemia is <3% of all cancers, and yet it constitutes the leading cause of death due to cancer in children and persons age <39 years (Deschler and Lübbert, 2006).

The median age of patients afflicted with this disease is 65. The survival rates of patients are age dependent. In Europe, five year relative survival decreased markedly with age. While 37% of patients between the 15–45 years age bracket survived, the rate among the oldest patients- aged 75 years and over was only 2% (Smith, et al., 2004).

1.2.3 Aetiology of the disease

There are many risk factors for AML. Age is an important factor among others as described earlier. It is a disease predominantly of later adulthood. Familial history of haematological disease is another factor. Genetic disorders including Down syndrome, Klinefelter syndrome, Patau syndrome, Ataxia telangiectasia, Shwachman syndrome, Kostman syndrome, Neurofibromatosis, Fanconi anemia, Li-Fraumeni syndrome, etc greatly increase the vulnerability to AML (Deschler and Lübbert, 2006).

Exposure to toxic chemical agents such as benzene, pesticides, cigarette smoking, embalming fluids, herbicides and radiation such as ionising rays from nuclear bombs, and medical procedures are high risk factors (Deschler and Lübbert, 2006) (Smith, et al., 2004). In some cases even certain kinds of drugs and chemotherapeutic agents have proven to increase the susceptibility to AML depending on the dosage and patient characteristics. These include alkylating agents, anthracyclines, taxanes, fludarabine, chlorambucil and cyclophosphamide (Morrison, et al., 2002; Verma, et al., 2009).

RNA retroviruses have been found to cause many neoplasms in many cancers including leukemia, albeit a clear link hasn't been identified yet. Parvovirus B19 seems to play a major role in the pathogenesis of AML (Kerr, et al., 2003).

1.2.4 Genetic abnormalities in AML

AML is characterised by many genetic translocations and mutations. They frequently occur in leukemia incidences. The Figure 1.1 lists the common mutations which predominate acute leukemias. Prominent among them is associated with t(1t5;17)(q22;q12) giving rise to the PML/RARα fusion in the case of acute promyelocytic leukemia. The AML1 and CBFβ components of the heterodimeric transcription factor core binding factor (CBF) are prone to translocations including t(8;21)(q22;q22) and inv(16)(p13q22). Activating point mutations in the genes such as RAS, FLT3, and c-KIT as well as loss of function mutations have been

frequently implicated in AML progression, survival and drug resistance (Gilliland and Tallman, 2002).

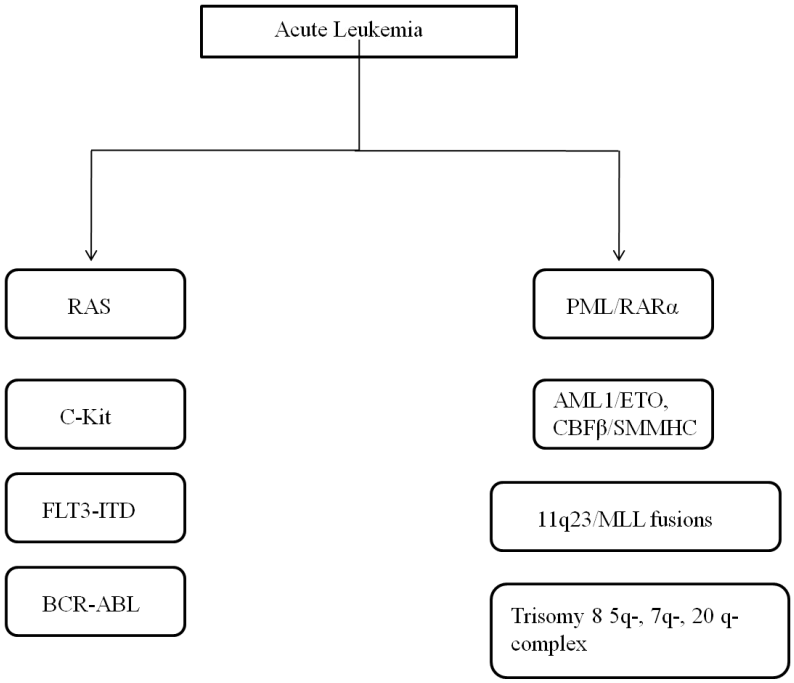

Figure 1.1: Common genetic abnormalities associated with AML (adapted from (zur Hausen, 2009)**)**

There are various genetic abnormalities including translocations and mutations which frequently occur in AML.

FLT3 (Fms-like tyrosine kinase 3), is a gene encoding a receptor tyrosine kinase belonging to the class III receptor tyrosine kinase family (RTKIII), which is 993 amino acids in length. It is expressed by immature hematopoietic cells and is crucial to the proliferation, differentiation and apoptosis of haematopoietic cells. In 1996, Nakao et.al identified that the FLT3 gene in certain AML cases possessed an internal tandem duplication in the juxtamembrane domain (Nakao, et al., 1996), rendering it constitutively active. It is the result of a head-to-tail duplication of 300–400 base pairs in exons 14 or 15. It is quite common in AML and occurs in around 24% of the cases. This mutation has not been detected in normal hematopoietic cells and is specific to AML. Subsequently it was reported that the point mutation D835 occurs in the activation loop of FLT3. It is relatively rare in comparison to the ITD mutation and is known to be present in 7% of all AML cases. These mutations might confer perpetuity to the activated status of FLT3 by relieving it of its autoinhibitory function (Gilliland and Griffin, 2002).

ITD mutations of FLT3 cause ligand-independent dimerisation and tyrosine autophosphorylation (Kiyoi, et al., 1998). Cells containing this mutation had an increased expression of STAT5 and RAS/MAPK pathways. The frequency of FLT3-ITDs in patients with AML increases with age, ranging from 5–15% in paediatric patients to 25–35% in adults. FLT3 has been found to be associated with poor prognosis in a number of studies. Clinical studies showed that patients with FLT3-ITD mutations had significantly smaller survival rates and died earlier than patients with wild type FLT3 gene. Hence there is a suggestion to classify patients with FLT3-ITD mutations as having high-risk disease (Abu-Duhier, et al., 2000) .

1.3 Current treatment strategies for AML

The acute nature of the disease makes it fatal if left untreated, over a period of days to weeks, depending on the blast count level in the peripheral blood. Hence immediate treatment is

essential. The current therapies for AML involve chemotherapy which combines therapeutic agents such as cytarabine (ara-C) and an anthracycline (daunorubicin or idarubicin) followed by multiple cycles of intensive post-remission therapy with elevated-dosage of ara-C (Gilliland and Tallman, 2002) (Mayer, et al., 1994). However, profound myelosuppression, frequent relapse of patients, poor response to therapy and development of resistance to the administered drugs are common deterrents to the treatment strategies.

With the advent of all transretinoic acid (ATRA) and arsenic trioxide (ATO), curing acute promyelocytic leukemia (APL), a subtype of AML (M3 and variant) has become a reality. In the case of ATRA therapy, the strategy involves early addition of chemotherapy such as ara-C to ATRA treatment and maintenance therapy, which involves continuous chemotherapy and intermittent ATRA treatment. Such an approach has been proven to reduce the incidence of relapse in APL and increase the chances of a disease free survival to 75-85% (Fenaux, et al., 1999). ATO when used alone in relapsed APL patients, a remission rate of greater than 80% and a 2-year survival rate of around 60% were observed. When ATO was used in combination with ATRA and gentuzumab, seven of eight patients achieved 100% remission. Six of eight patients remained in remission after 3 years (Quezada, et al., 2008).

Alternate therapies in development include gemtuzumab ozogamicin, an anti-CD33 monoclonal antibody chemically linked to the potent cytotoxic agent calicheamicin. This induces complete remission in CD33-positive AML (Sievers, et al., 2001).

Mutation in the FLT3 gene is the single most common genetic alteration in AML. This makes it a very attractive target for therapy. The FLT3 mutations make the cells refractory to most conventional drugs, necessitating alternate therapies for such patients. This has driven researchers to specifically design and develop drugs specifically to combat AML with FLT3-ITD mutations. Some of these are listed in Table 1.4.

Table 1.4: FLT3 inhibitors in different stages of development

Compound	Company	Receptor	Responses
CEP-701	Cephalon	FLT3 (wild-type and mutant)	1 of 8 patients: 5% blasts in bone marrow
SU5416	Sugen	FLT3 (wild-type and mutant) KIT, FMS and PDGFR	3 of 55 patients: partial remission with 6–25% bone-marrow blasts
SU11248	Sugen	FLT3 (wild-type and mutant) KIT, FMS and PDGFR	32 patients, 13 of 16 evaluable patients: >50% reduction in peripheral blasts
MLN518	Millenium	FLT3 (wild-type and mutant) KIT and PDGFR	8 patients, 2 out of 3 evaluable patients: >50% reduction in marrow blasts
PKC412	Novartis	FLT3 (wild-type and mutant) PKC, VEGFR and PDGFR	1 of 8 patients: >50% reduction in marrow blasts
L-000021649	Merck	FLT3 (wild-type and mutant) and VEGFR	Not reported yet

FLT3 inhibitors such as PKC412 are being tested in combination with conventional chemotherapeutic agents such as ara-c, doxorubicin, idarubicin, etoposide and vincristine with encouraging results in cell lines carrying a FLT3 mutation. They do not exert similar inhibitory effects in cells with wild-type FLT3 gene (Furukawa, et al., 2007) (Odgerel, et al., 2008).

However, the above mentioned strategies are restricted to the treatment of a subset of the disease, such as a particular subtype or cells carrying a particular mutation. The most potent generic therapy thus far is hematopoietic stem cell transplantation (HSCT) from a human leukocyte antigen (HLA)-matched donor (Gilliland and Tallman, 2002). Autologous as well as allogeneic bone marrow transplantation is found to result in better disease-free survival and reduced rate of relapse than intensive chemotherapy with high-dose cytarabine and daunorubicin (Zittoun, et al., 1995) (Gorin, 1998). However the overall survival was found to be marginally better in chemotherapy. The treatment-related mortality of HSCT was approximately 20% as observed in randomised clinical trials. This offsets any advantage that this approach offers (Cassileth, et al., 1998). The inherent drawbacks in each of these current treatment methods, necessitates the search for an effective, less toxic and more directed therapy for AML.

1.4 Rapamycin

1.4.1 Discovery and physical properties

Rapamycin (Rapa) also known as sirolimus, was first identified in 1975, as an antibiotic, produced by a strain of *Streptomyces hygroscopicus*, which was isolated from a soil sample collected from the Vai Atare region of Rapa Nui (commonly known as Easter islands). Rapa is a white crystalline solid with a melting range of 183° to 185°C. It is a lipophilic macrocyclic lactone, soluble in most organic solvents and virtually insoluble in water. It has a

molecular weight of 914. The structure of rapa was resolved with the aid of two-dimensional nuclear magnetic resonance studies (Figure 1.2).

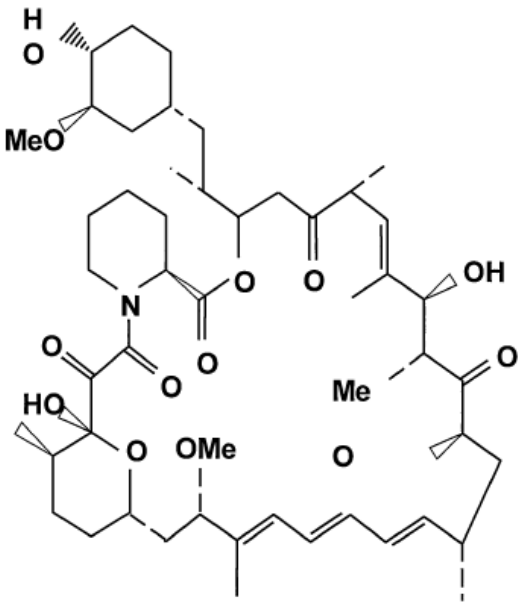

Figure 1.2: Chemical structure of rapamycin

Rapa was found to have strong anti-fungal action. It is a FDA approved immunosuppressant, and is capable of reversing acute active allograft rejection and enhancing long-term donor-specific allograft tolerance (Sehgal, 2003). Interestingly, it was observed that rapa showed promise as an anti-tumour drug. Studies pertaining to the anti-tumoural activity of rapa and its analogs (CCI-779, RAD001) and the possibility of using it as therapy for certain cancers are underway (Galanis, et al., 2005; Chan, et al., 2005; Agarwala and Case, 2010).

1.4.2 Rapamycin as an immunosuppressant

Rapa's immunosuppressive property was discovered when it was observed that it prevented experimental allergic encephalomyelitis and adjuvant arthritis and inhibited the production of antibodies. Rapa is a highly effective immunosuppressant in organ transplantation. This is due to rapa's unique mechanism of immunosuppression, favourable side effect profile with no end organ toxicity, and its synergistic action with other established immunosuppressants without overlapping toxicity (Sehgal, 2003).

Rapa belongs to a class of macrolide immunosuppressants whose activity is based on their binding to specific cytosolic binding proteins called immunophilins. Rapa specifically binds to the immunophilin FKBP12 (FK506 binding protein of 12 KDa). Other members of this class include cyclosporine A and FK506 (Sehgal, 1998).

1.4.3 Antifungal properties of rapamycin

Rapa exhibits strong antifungal effects and was initially discovered by virtue of this property. A number of other immunosuppressants of the same classification as rapa including cyclosporine A and FK506 possess similar potency against fungi. Rapa is mainly active against *Candida albicans* with a minimum inhibitory concentration range from 0.02 to 0.2 µg/ml, against ten strains. It is also effective against *Microsporum gypseum* and *Trichophyton granulosum, C. neoformans, C. albicans, Candida stelloidea, A. fumigatus,*

Aspergillus flavus, Aspergillus niger, Fusarium oxysporum, and *Penicillium sp*. It was found to be more potent than amphotericin B, the established fungicidal agent in use. Overall, rapa exerted its antifungal activity via FKBP12 and TOR homologs in *C.albicans* (Wong, et al., 1998; Cruz, et al., 2001).

1.4.4 Mechanism of action of rapa

Rapamycin is a known inhibitor of the mammalian Target Of Rapamycin (mTOR) pathway. The mechanism of this inhibition has been well established.

1.4.4.1 Structure of the mTOR protein

mTOR is known by several other names such as FK506-binding protein (FKBP12), rapamycin- associated protein (FRAP), rapamycin and FKBP12 target (RAFT1), rapamycin target (RAPT1), and sirolimus effector protein (SEP). The TOR proteins were identified originally in yeast, by virtue of mutations of two rapa target genes, which helped yeast escape the cell cycle arrest caused by rapa. The mammalian counterpart of this protein was identified subsequently to be a 289 kDa protein that has C-terminal homology to phosphatidylinositol-3 kinase (PI3K) and is therefore a member of the PI3K-related kinase family. Further studies revealed that rapa forms a complex with the immunophilin FKBP12 (Sabatini, et al., 1994). This complex then forms a ternary complex with mTOR. This binding leads to inhibition of the function of the mTOR protein, an atypical serine/threonine protein kinase. The structure of mTOR has been elucidated (Figure 1.3). It contains up to 20 tandem repeats of the HEAT domain (a protein-protein interaction structure of two tandem anti-parallel α-helices found in *h*untingtin, *e*longation factor 3, PR65/*A* and *T*OR) repeats at the N-terminal region, followed by *F*AT (*F*RAP, *A*TM, and *T*RRAP, all PIKK family members) domain. The ternary complex formation is due to the presence of the FRB (*F*KBP12/rapamycin *b*inding) domain. The kinase domain lies sandwiched between the FRB and the FATC domains, at the C-terminus of

the protein. The HEAT domain mediates protein-protein interactions, and the FATC domains mediate the kinase activity of mTOR (Yang and Guan, 2007) (Schmelzle and Hall, 2000).

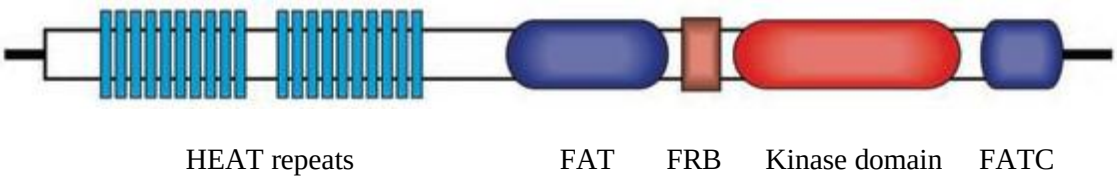

Figure 1.3: Architecture of the mTOR protein

1.4.4.2 Functional roles of mTOR

mTOR controls a number of functions related to cell growth, among which are cell cycle checkpoint regulation, translation, transcription, and protein kinase C signalling. The actions of mTOR are defined by its upstream and downstream effectors. Two very important mTOR downstream effectors are S6K1 (p70 ribosomal protein S6 kinase1) and 4E-BP1 (eIF4E binding protein 1). Usually, S6K1 and 4E-BP1 are bound to eIF3 (eukaryotic initiation factor 3) which renders them inactive. However, in response to stimulatory agents such as growth factors, mTOR binds to eIF3 and phosphorylates S6K1 and 4E-BP1. This releases S6K1 from eIF3, thus activating the kinase. The active S6K1 promotes translation and growth by phosphorylating cellular substrates such as S6. 4E-BP1 inhibits cap dependent mRNA translation via binding to the translation initiator eIF4E (eukaryotic translation initiation factor 4E). The phosphorylation of 4E-BP1 by mTOR frees it from eIF4E, relieves its inhibitory effect and stimulates translation initiation. Hence, active mTOR enhances cell growth by promoting protein translation, and increasing cell mass (Schmelzle and Hall, 2000). A key regulating partner of mTOR is the PI3K/Akt pathway. It interacts with growth factors and their receptors as well as other mitogenic stimuli. PI3K is usually activated in response to growth factors such as IGF-1.

1.4.5 Rapamycin as an anti-cancer agent

Hyper activity of mTOR is known to promote cancer. Rapa binds to mTOR by means of the FKBP12-rapa complex and inhibits the kinase action of mTOR. This abrogates the phosphorylation of S6K1 and 4E-BP1, which leads to arrest in the translation of proteins needed for cell cycle progression and cell growth. This confers rapa with profound anti-proliferative and tumour suppressive effects (Mita, et al., 2003) (Meric-Bernstam and Gonzalez-Angulo, 2009).

Rapa is hence a promising cure for cancer. A number of analogs of rapa such as CCI-779, RAD 001 and AP23573 are undergoing clinical trials for various cancers such as prostrate, breast, non- small cell carcinoma, glioblastoma and melanoma (Chan, et al., 2005) (Galanis, et al., 2005) (Mita, et al., 2008) (Johnson, et al., 2007) (Johnston, et al., 2010) (Hainsworth, et al., 2010), with encouraging results.

There have been very few studies investigating the anti-leukemic effects of rapa. The work by Récher et al (Récher, et al., 2005) attributes an anti-leukemic effect to rapa in blast cells. There are reports which suggest aberrant regulation of mTOR in leukemia, hence making it an attractive target for rapa mediated therapy (Panwalkar, et al., 2004) (zur Hausen, 2009). In spite of these studies, a thorough understanding of the regulatory effects of rapa on other molecules and pathways are still vague and not much is known about the perturbations caused by the drug treatment on the cell as a whole. All the previous studies pertaining to the anti-proliferative effects of rapa employed the traditional approach of investigating individual pathways, in this case just the mTOR and PI3K/Akt. We were interested in studying the effect of rapa on AML at the global level, by mapping all the transcriptomic and proteomic modulations caused by the drug. Such a study would go a long way in illustrating the mechanism of action of rapa in AML in its totality and in expanding our cognizance of the repertoire of its targets.

1.5 Genistein

1.5.1 Physical properties

Genistein (GEN) is a member of the family of chemicals called isoflavones, which are a class of estrogen like compounds found in soy. GEN is a natural tyrosine kinase (TK) inhibitor. In the search for specific inhibitors for tyrosine kinases, it was isolated from the fermentation broth of *Pseudomonas* sp.

Gen is the simplest of the isoflavonoid compounds of Leguminosae on a biosynthetic level (Dixon and Ferreira, 2002). Chemically known as 5, 7-Dihydroxy-3-(4-hydroxyphenyl)-4H-1-benzopyran-4-one or 4', 5,7-Trihydroxyisoflavone, its chemical formula is $C_{15}H_{10}O_{5n}$ (Figure 1.4).

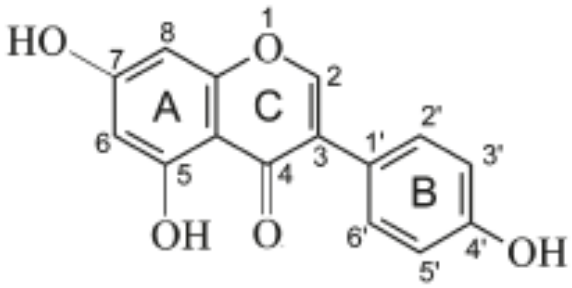

Figure 1.4: Chemical structure of genistein

1.5.2 Versatility of GEN

The major dietary sources of isoflavonoids are soy products, with one gram of soy protein containing nearly 250 mg of GEN. Processed soy products such as miso and soy sauce contain lower levels of GEN than tofu, which is the major source of isoflavones in the Asian diet.

The structure of GEN is similar to the potent estrogen estradiol-17β. In particular the phenolic ring and the distance (11.5 A) between its 40- and 7- hydroxyl groups share profound similarity. These features enable GEN to bind estrogen receptors and sex hormone binding proteins. It thus exerts both estrogenic and anti-estrogenic activity, the latter by competing for receptor binding by estradiol (Dixon and Ferreira, 2002). GEN is thus a phytoestrogen.

GEN has been known to exhibit many interesting properties. Like many other members of the isoflavonoid family, GEN exerts broad-spectrum antimicrobial activity and is therefore believed to help the plant fight microbial disease (Erasto, et al., 2004). Higher dietary intake of GEN is found to be responsible for reduced incidence of cardiovascular disease (Hwang, et al., 2001). It also seems to improve plasma lipids, resulting in lowered LDL cholesterol, the ratio of total cholesterol to HDL cholesterol, and the ratio of LDL to HDL cholesterol, in pre-menopausal women (Merz-Demlow, et al., 2000). An isoflavone rich diet also helps alleviate post-menopausal stress in women in addition to potentially reducing the risk of cardiovascular disease and osteoporosis (Alekel, et al., 2000). Interestingly GEN exhibited anti-cancer properties.

1.5.3 Anti-cancer properties of GEN

It is known that a significant correlation existed between an isoflavone rich soy-based diet and reduced incidence of breast cancer or mortality from prostate cancer in humans. A pioneering epidemiological study on Singapore Chinese women by Lee et al, (Lee, et al., 1991) showed that soy consumption directly correlated with reduced risk of breast cancer. In

another study, neonatal administration of GEN to rats proved to be effective in the control of chemically-induced mammary gland tumour. The study also confirmed that GEN in the diet at 'physiological level' greatly enabled cell differentiation, possibly by the up-regulation of the EGF pathway, with no observed toxic effects on the reproductive tracts of females. GEN is also known to reduce the risk of prostate cancer in men. Dietary GEN regulates sex steroid receptor and growth factor ligand and receptor mRNA expression, with a high degree of specificity (Lamartiniere, et al., 2002). It induces cell growth inhibition in prostate cancer through the suppression of telomerase activity by reducing the expression of human telomerase reverse transcriptase and c-myc and increasing the expression of p21, in a study 0performed on the prostate cancer cell line LNCaP (Ouchi, et al., 2005).

GEN has been show to have antioxidant effects and free radical scavenging properties. It thus protects cells against reactive oxygen species by inhibiting the expression of stress–response related genes and hence reduces carcinogenesis (Banerjee, et al., 2008) .

The prospects of developing GEN as a therapy for cancer is very bright and clinical trials are underway in this direction. There have been efforts to explore the possibility of enhancing the effects of GEN by means of combining it with prevailing chemotherapeutic agents. GEN has exhibited synergistic effects in inhibiting AML cells when combined with a chemotherapeutic agent such as cytosine arabinoside ara-c (Shen, et al., 2007). Interestingly, chemo-resistant colon cancer cells have been observed to respond to a combination of GEN and 5-fluorouracil *in vitro* (Hwang, et al., 2005).

1.5.4 GEN as a potential therapeutic agent for AML

GEN's potential as an anti-leukemic agent is of much interest to researchers. A number of studies have evaluated the effect of GEN on AML cell lines and in mouse models of leukemia. Most of these studies confirm that GEN indeed inhibits the proliferation of AML cells *in vitro* (Traganos, et al., 1992; Raynal, et al., 2008) .

A recent study by Sanchez et al., has detailed the mechanism by which GEN induced differentiation in AML cells as a ROS-independent process, mediated by the Raf-1/MEK/ERK axis, involving the PI3K pathway. The differentiation process is coupled and co-regulated with G2/M arrest, but uncoupled to the pro-apoptotic action of the drug (Sánchez, et al., 2009).

A high-throughput study by Shen et al., profiled the transcriptional changes induced by GEN treatment on the AML cell lines HL-60 and NB-4 (Shen, et al., 2007). The study observed that GEN down-regulated genes belonging to the MAPK pathway. The mode of inhibition employed by GEN includes cell cycle: G2/M arrest and apoptosis in varying degrees. Nude mice with established tumours showed a decrease in tumour volume when GEN was administered and an enhanced tumour reduction when GEN was combined with ara-c (Shen, et al., 2007). Thus the prospect of using GEN as a therapy for AML is highly promising.

Yet, unravelling the proteomic aspects of the dynamics of GEN action on AML is necessary for complete cognizance of its mechanism of action. A study by Zhang et al., attempted to map the proteome level changes caused by GEN in HL-60 cells, employing a two dimensional- gel electrophoresis (2D-GE) approach. However, they could conclusively identify only 14 proteins with altered levels from the study (Zhang, et al., 2007). This might be due to the inherent shortcomings of 2D-GE technique for protein separation and identification. Hence there is a great need to use a robust and advanced technology-based method to study the proteome of GEN-treated AML cells.

1.5.5 GEN- a potent tyrosine kinase inhibitor

GEN was reported to inhibit tyrosine-specific protein kinases in a landmark study by Akiyama et.al in 1987 (Akiyama, et al., 1987). It was identified that GEN had a highly specific inhibitory effect on tyrosine kinases, but little or no effect on the activity of serine and threonine kinases and other ATP analogue-related enzymes *in vitro*. The inhibitory effect

of GEN has been manifested in its inhibitory activity on c-src and v-abl, with an IC_{50} values of 7.4 and 22.2 µmol/L (2 and 6 µg/mL), respectively and EGFR's PTK activity at an IC_{50} of 2.6 µmol/L (Peterson, 1995). On the other hand, it does not have a generic inhibitory effect on all PTKs equally, and some of them such as p94 PTK are unaffected, underlining the specificity of GEN (Feller and Wong, 1992). Such high specificity is an interesting dimension to its characteristics.

Among the number of genetic abnormalities occurring in AML patients, FLT3-ITD is the most prominent, as detailed in section 1.2.4. FLT3 is a tyrosine kinase. Considering GEN's powerful inhibitory action on a number of PTKs, it is highly interesting to speculate on the effect of GEN on FLT3. However we could not find any previous study pertaining to this. Most of the studies described in section 2.4.4 establishing the anti-leukemic effects of GEN were performed on HL-60 and other cell lines possessing the wild-type FLT3 gene. None of the studies include MV4-11 or any other AML cell line with an ITD mutation. Since FLT3 mutations have a major role in leukemogenesis and resistance to drugs, it would be interesting to test whether GEN can exhibit anti-proliferative effects on cell lines possessing FLT3-ITD mutations as compared to those with the wild-type version of the gene. The fact that the drug has a potent PTK inhibitory effect makes it logical to expect a wide spread regulation at the proteomic level.

1.6 High-throughput approaches to mechanistic studies of drugs

The high-throughput approach of profiling the molecular response of cells to rapa therapy at both the transcriptomic and proteomic levels would provide a holistic perspective on the repercussions of drug treatment on the cell. The fact that we can profile the expression of most of the genes encoded by the human genome using microarray analyses is a boon to researchers (Bild, et al., 2006) (Clarke, et al., 2004) (Comuzzi and Sadar, 2006). Similarly, the advent of proteomic profiling technologies such as iTRAQ™ is catapulting translational

research into a whole new era and is paving the way for accelerated innovations in the field of cancer research (Hattori, et al., 2006) (Qian, et al., 2008). Such a two pronged approach, profiling the molecular level changes of mRNA and protein expression as a consequence of drug treatment has been proven to be effective in understanding the mechanism of action of drugs (Li, et al., 2007; Frolov, et al., 2003) (Nunoda, et al., 2007). Transcriptomic techniques can survey the expression levels of thousands of genes and can capture even the low copy number transcripts. On the other hand proteomic strategies, although not as sensitive as their transcriptomic counterparts, have the advantage of mirroring the protein levels, the eventual products of mRNA translation.

1.6.1 Transcriptomic profiling and microarray technology

The transcriptome of a cell is defined as the set of all messenger RNA (mRNA) molecules namely 'transcripts' produced in it. The transcriptome of cells are not fixed entities. They are highly dynamic and mRNA expression varies in accordance to the treatment conditions that the cells are subjected to. Hence studying the transcriptome of cells would provide deep insights into the effect of the drugs, dosages and time points.

Microarray is a very powerful technique to study the expression of thousands of genes simultaneously across samples, in response to treatment conditions. Hence one can obtain a global view of the transcriptome in one single shot. Microarrays have greatly aided cancer research by proving to be an invaluable tool to compare the expression levels of cancer vs. normal cells, classify tumours, obtain molecular signatures for cancer types, identify prognostic factors, conduct epidemiological studies and study the effects of drug treatment on cancer cells.

Studies identifying tumour biomarkers have skyrocketed due to the advent of microarrays. Comparative profiling of refractory and responsive tumours has been done to identify prognostic factors for many different cancers including AML and ALL (Ross, et al., 2004).

The gene expression profiles have been very useful in classification of tumours into genetically distinct subtypes with different prognostic values, which would be of great value in making therapeutic decisions (Valk, et al., 2004). A recent study by Kadara et al, identified a 6-gene signature that is capable of predicting the survival of lung adenocarcinoma by comparison of differential gene expression profiles of normal, immortalised, transformed, and tumourigenic lung epithelial cells (Kadara, et al., 2009).

A lot of such high-throughput microarray studies have been done in the field of leukemia biology too. Nowicki et al, have compared the profiles of CML patients (in different stages of tumour progression) with non-cancerous samples and identified a molecular signature for CML. The study also identifies that the gene expression patterns depend on the particular disease stage of the patient. Distinct expression signatures for the individual lineages of the leukemic blasts have been identified using microarrays. The study demonstrates the usefulness of gene expression monitoring in cancer classification and suggests the extension of this strategy for discovering and predicting cancer classes for other types of cancer, independent of previous biological knowledge (Golub, et al., 1999). Class prediction of AML into different subtypes is done by virtue of the characteristic gene expression profile of each of the subtype. Different genetic mutations and translocations are also identified by this method. NPM1 and FLT3-ITD gene mutations in AML have been shown to give rise to distinct gene clusters in AML. Hence the study of gene expression at a global level has greatly enhanced cancer research in general and leukemia studies in particular.

1.6.2 Affymetrix Genechip analysis

Genechip® is a product from Affymetrix which is one of the major providers of microarray solutions. DNA microarray is composed of thousands of DNA probes arranged as an array on a solid surface to interrogate the abundance and/or binding ability of DNA or RNA target molecules. The DNA probes that are used in a DNA microarray are usually amplified cDNA

fragments or synthesised oligonucleotide sequences that have sequences that complement the target sequences (Zhu, 2003).

The samples under study are labelled fluorescently. When samples are hybridised on the DNA microarray, the DNA probes will capture the nucleic-acid target molecules through sequence complementation. The strength of the fluorescent signal from the captured target is commensurate to the abundance of the target molecules and/or the binding compatibility between the probe and target molecules. A laser scanner is then used to capture this fluorescence and analyse it quantitatively. A microarray chip would contain thousands of such probes and hence can be used to analyse the expression pattern of a large number of genes in parallel.

Affymetrix human whole-genome microarrays can monitor the expression levels of upto 47,000 genes, including 38,500 well characterised genes and UniGenes. This in total amounts to more than 54,000 probe sets and 1,300,000 distinct oligonucleotide features. Each transcript is analysed by 11 probe pairs, each of which consists of a perfect match 25-mer oligonucleotide (PM) and a 25-mer mismatch oligonucleotide (MM), wherein a single base pair mismatch is in the central position. The PM/MM design is used for identification and subtraction of nonspecific hybridisation and background signals (Schinke-Braun and Couget, 2007).

GeneChip® is a specialised microarray that uses *in silico* synthesized DNA oligonucleotides as probes to detect the sequence similarity and abundance of target-DNA or -RNA molecules through complementary-sequence binding. The fabrication of chips is a highly standardised procedure. So are the target preparation, hybridisation, and processing protocols. This ensures consistency, high quality, reduced variability between samples, limited batch effects, ease of data mining and downstream analysis.

The arrays are manufactured by an innovative light-directed chemical synthesis process, which combines solid-phase chemical synthesis with photolithographic fabrication techniques

employed in the semiconductor industry. High-density oligonucleotide arrays are constructed using a series of photolithographic masks to define chip exposure sites, followed by specific chemical synthesis steps, with each probe in a predefined position in the array. Several such probe arrays are synthesised in parallel on a large glass wafer, hence enhancing the reproducibility and cost effectiveness. The wafers are then packed into injection-moulded plastic cartridges, which protect them from the environmental contaminants and serve as chambers for hybridisation. (http://www.ohsu.edu/xd/research/research-cores/gmsr/project-design/array-technology/affymetrix-genechip-arrays.cfm)

Genome expression analysis necessitates a wide, unbiased survey of the transcriptome. Hence it is imperative to provide a true global coverage of a complex genome in a single microarray and Genechip® succeeds in this respect. The technology has found wide acceptance and is used extensively in genomics research. An illustrative overview of the technology is shown in Figure 1.5.

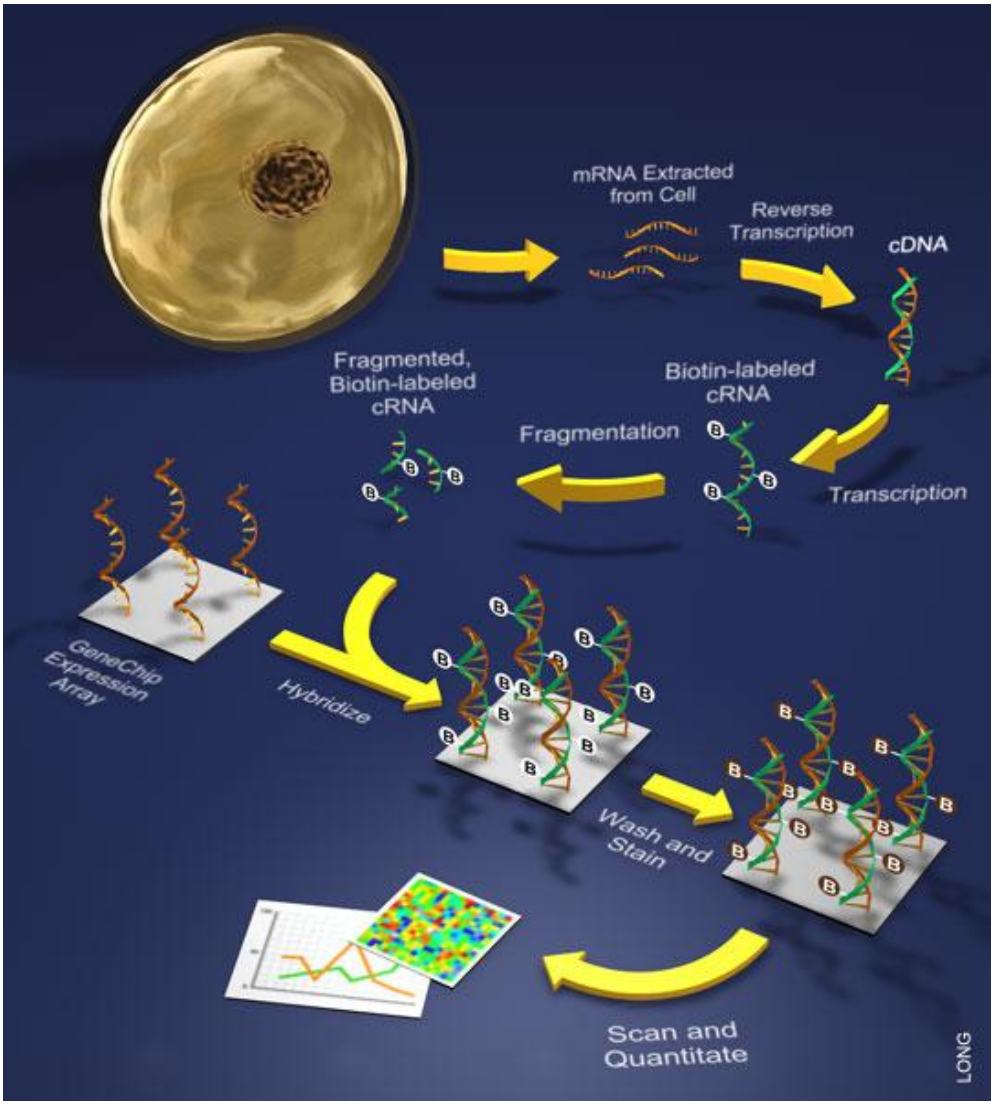

Figure 1.5: Overview of the Genechip microarray analysis

1.6.3 'Proteomics'- scope and definition

Proteome, as the name suggests, is the set of all the proteins expressed in a cell. The term 'proteome' was used for the first time in 1995, to describe the protein complement of a genome (Blackstock and Weir, 1999). 'Proteomics' can succinctly be defined as the study of protein properties (expression level, post-translational modification, interactions etc.) on a large scale to obtain a global, integrated view of disease processes, cellular processes and networks at the protein level (Blackstock and Weir, 1999).The goal of proteomics is, a comprehensive quantitative description of protein expression and its changes under the influence of biological perturbations such as disease or drug treatment (Anderson and Anderson, 1998). In many cases, transcriptomic data are not enough for a clear identification of a therapeutic target, mainly because proteins are the targets for the drug's mode-of-action. The effects seen on the gene expression level are only a response to drug effects on the gene level. However, it has been observed that there is not always a direct correlation between gene expression and protein expression patterns (Müllner, et al., 1998). Therefore, a major focus of current research in drug discovery and mechanism studies is to map the expression patterns of drug effects on the cell at both the nucleic acid and the protein levels.

1.6.3.1 Mass spectrometry- the magic wand of proteomics

In the past decade, the study of proteomics has blossomed into an extremely useful technique enabled by advances in the field of mass spectrometry. Mass spectrometry is a powerful analytical technique that is used to identify unknown compounds, to quantify known compounds, and to elucidate the structure and chemical properties of molecules. It has developed into an essential tool for biologists and chemists due to its versatility. It has several unique features spawning several applications including **accurate molecular weight measurements:** sample confirmation, sample purity determination, verification of amino acid substitutions, and detection of post-translational modifications; **reaction monitoring:** enzyme

reactions monitoring, chemical modification, protein digestion; **amino acid sequencing:** sequence confirmation, characterisation of peptides and protein identification; **oligonucleotide sequencing; protein structure:** protein folding studies enabled by monitoring H/D exchange and macromolecular structure determination.

A typical mass spectrometer consists of three parts 1) Ioniser 2) Ion Analyser 3) Detector (http://www.chemguide.co.uk/analysis/masspec/howitworks.html). The sample atom is ionised, usually to cations by the gain of a proton. The ions are sorted and separated according to their mass and charge. The separated ions are then detected and tallied, and the results are displayed on a chart. The ionisation methods include Electrospray Ionisation (ESI), Matrix Assisted Laser Desorption Ionisation (MALDI), Fast Atom Bombardment (FAB), Chemical Ionisation (CI), and Electron Impact (EI). (http://www.astbury.leeds.ac.uk/facil/MStut/mstutorial.htm).

ESI and MALDI are the two techniques most commonly used to ionise proteins. ESI ionises the analytes out of a solution. It is hence coupled to liquid-based separation tools. MALDI, on the other hand, sublimates and ionises the samples out of a dry, crystalline matrix via laser pulses. MALDI-MS is the preferred technique to analyse relatively simple peptide mixtures, whereas integrated liquid-chromatography ESI-MS systems (LC-MS) are better suited to analyse complex samples (Aebersold and Mann, 2003).

1.6.3.2 Proteome profiling techniques- an overview

The study of the proteome has helped solve many mysteries surrounding cancer and other human ailments (Jungblut, et al., 1999). This has been accelerated by the advent of a number of excellent techniques which enable a global study of the proteome. One can anticipate a modification of the expression of the proteins in a system in response to a perturbation such as drug treatment. Hence the proteomic profiling tool should be capable of capturing the relative difference caused by the drug in comparison to a reference control state. The most

popular of these techniques include 2- Dimensional Electrophoresis (2-DE), SILAC (Stable Isotope Labelling with Amino acids in Cell culture), ICAT (Isotope Coded Affinity Tag), iTRAQ (Isobaric Tag for Relative and Absolute Quantitation), etc. In general, these techniques involve protein labelling/separation followed by mass spectrometry based identification of the peptides. Each of these methods has its own inherent advantages and disadvantages.

2-DE involves separation of proteins on the basis of their isoelectric points and sizes. The first dimensional separation is achieved by isoelectric focussing (IEF), while the proteins are separated by mass using SDS-PAGE in the second dimension, in a direction 90˚ from the first. The resultant protein spots are excised and analysed by mass spectrometry. The strengths of this technique include identification of hundreds of proteins simultaneously and discernment of post translational modifications. However the pitfalls of this method are low reproducibility, limited dynamic range of isoelectric points and molecular weights, decreased rate of detection of low-abundance proteins and hydrophobic proteins.

ICAT is a method to relatively quantify cysteine containing peptides from tryptic digests of protein extracts and identify them using mass spectrometry. In this approach, two samples are labelled with a heavy and light pair of chemically identical tags that differ in the isotopic composition and contain a thiol-reactive and a biotin moiety. The thiol reactive group enables attachment to cysteine residues. Control and treated samples can be labelled with the heavy and light reagents respectively to enable relative quantification of the trypsin digested proteins. Although this method offers significant advantages over 2-DE in terms of reproducibility and automation of procedure, it cannot identify proteins without cysteine residues.

SILAC is a simple and straightforward approach for *in vivo* incorporation of a label into proteins for mass spectrometry (MS)-based quantitative proteomics. It relies on metabolic incorporation of a given 'light' or 'heavy' form of the amino acid into the proteins of actively

dividing cells in culture. Hence in an experiment two cell populations whose proteomes are to be quantified and compared, are cultured with the 'light' and 'heavy' versions of the same media. After a number of cell divisions, each instance of this particular amino acid will be replaced by its isotope labelled analogue. The cells are then combined, lysed and the differentially regulated proteins are quantitatively identified by mass spectrometry. SILAC is gaining popularity as the method of choice for accurately determining level of changes of proteins and PTMs. It has the inherent advantage of reduced sample complexity, increased efficiency and reproducibility owing to the introduction of the stable isotope early on in the procedure, while the cells are still dividing. However the success of the method is subject to 100% incorporation of the isotopic label. Also, the method currently suffers from the high cost of the labelled amino acids.

Hence in our study, we have used a method called iTRAQ which could be automated and whose power of identification is not restricted to any particular subset of proteins.

1.6.3.3 Isobaric Tag for Relative and Absolute Quantification (iTRAQ)

iTRAQ is a stable isotope labelling method for relative and absolute quantification of proteins. It involves the usage of reagents which were designed as isobaric tags consisting of a charged reporter group that is unique to each of the four reagents. The multiplexing capability of the method can be doubled to eight, by the usage of 8-plex iTRAQ reagents. The reagents contain a peptide reactive group, and a neutral balance portion to maintain an overall mass of 145 (305 in the case of 8-plex) (Zieske, 2006).

The 4-plex experimental design consists of labelling samples with four independent isobaric reagents which upon fragmentation in MS/MS would produce four unique reporter ions of *m/z*= 114-117 (Figure 1.8 a). The second generation of iTRAQ reagents can label 8 samples in one shot. The reporter ion masses are 113.1–119.1 Da and 121.1 Da (Figure 1.6 b). The mass at 120.1 is omitted in order to avoid contamination from phenylalanine immonium ion

(*m*/*z* 120.08). The peptide reactive group was designed to react with all primary amines which results in enhanced peptide coverage for any given protein. The reporter region was selected in the low mass area in order to keep the additive mass to the fragments negligible and hence eliminate any effect in either MS or MS/MS modes. This would also mean elimination of any interference with other immonium or fragments ions, enabling enhanced degree of confidence in interpretation (Zieske, 2006). In the case of the 8-plex strategy, the overall mass of the balance group was increased to provide for the additional channels. All mass differences are now encoded using ^{13}C and ^{15}N around a ring structure in the reporter group (Pierce, et al., 2008).

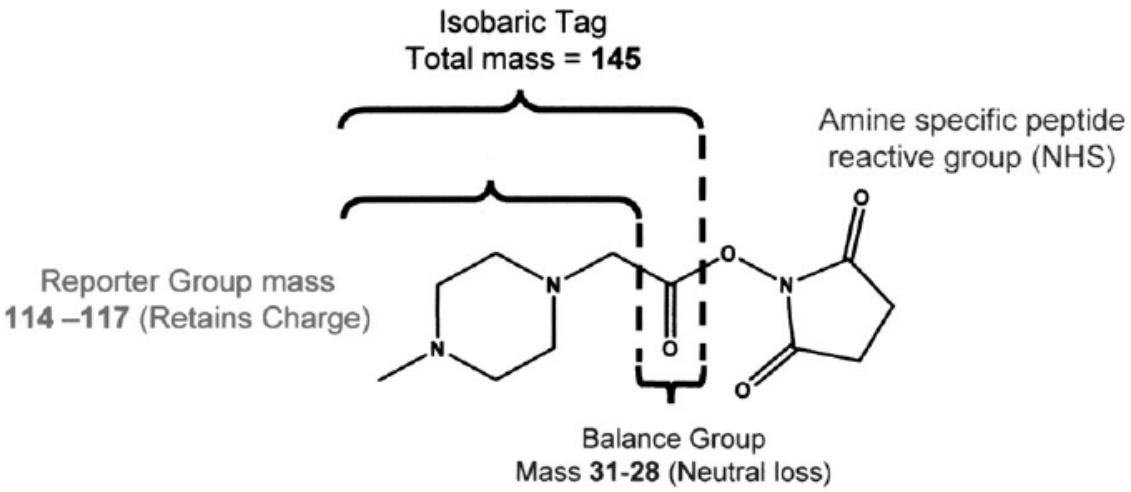

(a) 4-plex

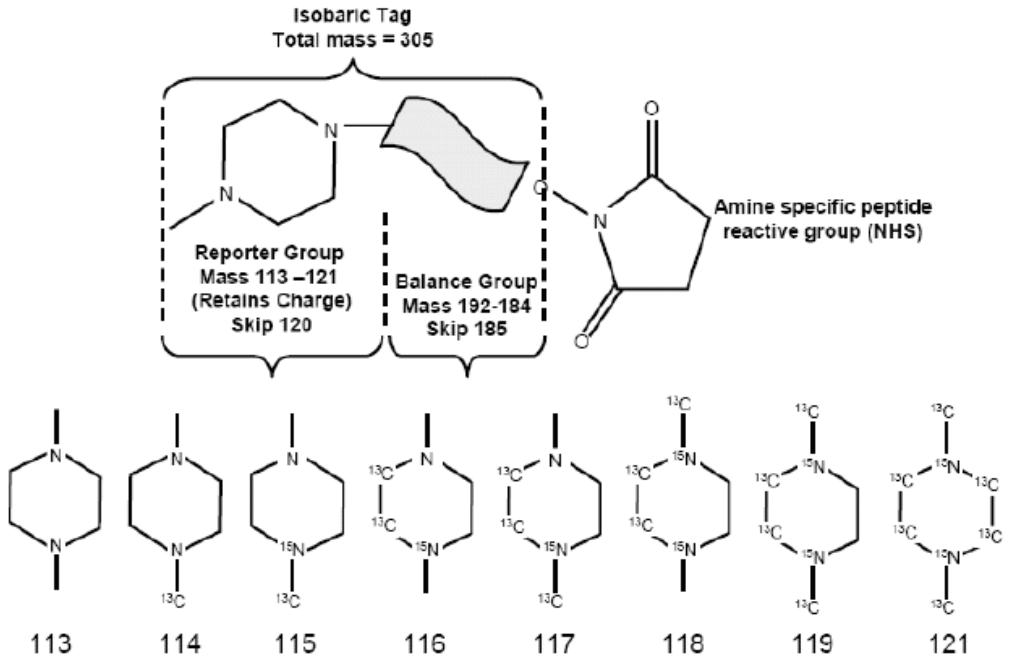

(b) 8-plex

Figure 1.6: Illustration of (a) 4-plex and (b) 8-plex iTRAQ reagent chemistry

The samples are independently reduced, alkylated, and enzymatically digested with trypsin. The ensuing pool of peptides from each sample is then labelled with one member of the multiplex set. The labelled peptides are then combined and subsequently analysed by LC-MS/MS. Quantitation is accomplished by comparison of the peak areas and the resultant peak ratios for the four MS/MS reporter ions. The isobaric nature of the reagents helps to pool the labelled peptides without increasing the complexity of the MS analysis. The workflow of the iTRAQ procedure is depicted in Figure 1.7.

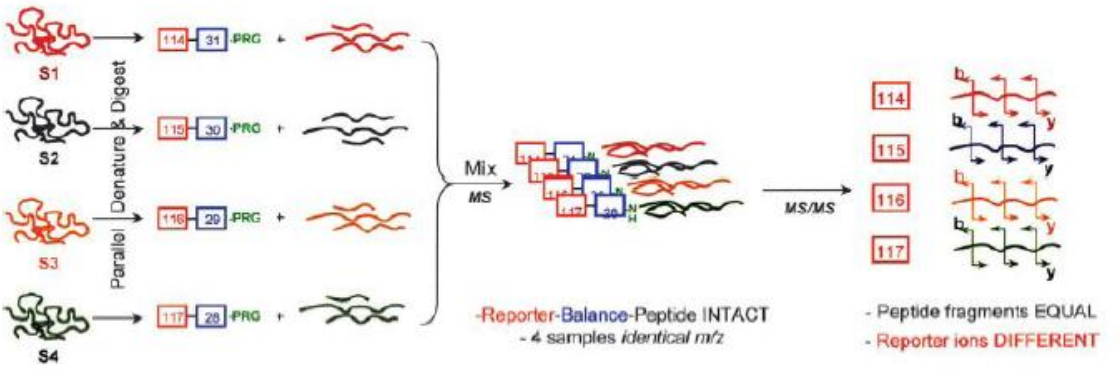

(a)

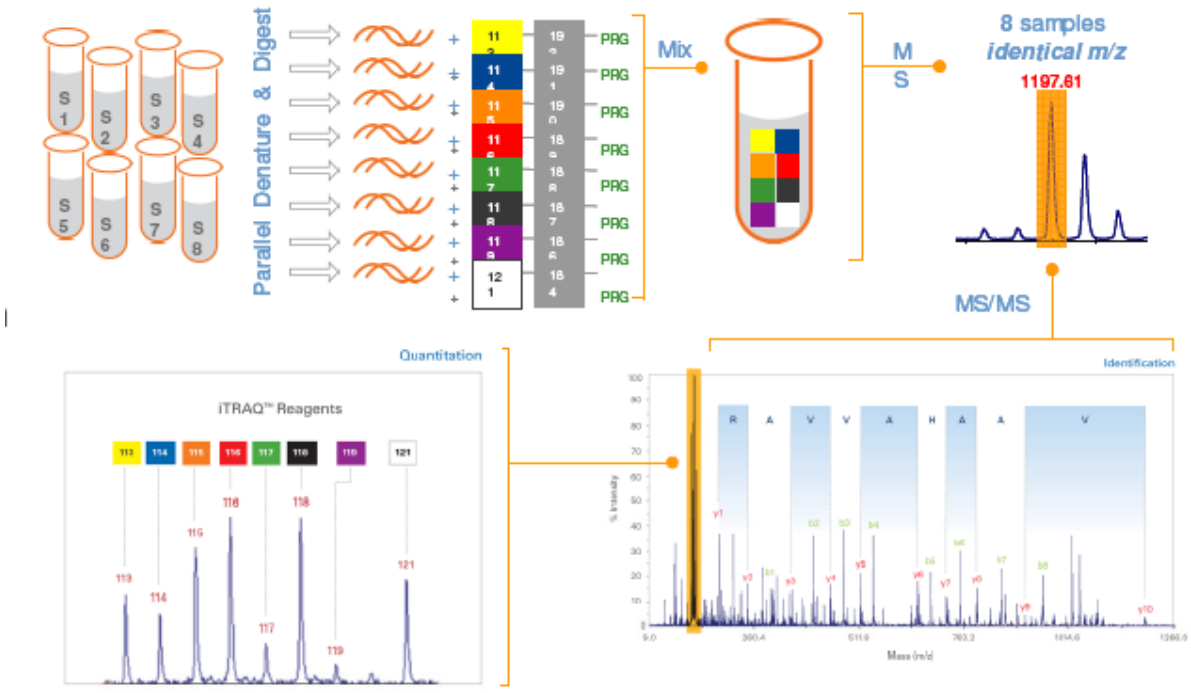

(b)

Figure 1.7: Workflow of (a) 4-plex and (b) 8-plex iTRAQ procedure

1.6.3.4 Critical evaluation of the iTRAQ technique

The iTRAQ technology offers certain significant improvements over other existing strategies for proteomic profiling. These include 1) Higher reproducibility due to the fact that the peptides from the same protein show similar relative quantification patterns in addition to biological replicates showing consistent conformity. 2) Higher confidence and quality of data because of the amine specificity of the isobaric tags which makes most peptides in a sample acquiescent to this labelling strategy with no loss of information from samples involving post-translational modifications. 3) Ease of cross comparison and improved statistical validation within experiments, enabled by the multiplexing capability of these reagents (Zieske, 2006). However the technique does have its own inherent pitfalls. Though it has enhanced sensitivity for quantitation, it is more susceptible to errors in precursor ion isolation. This indicates that the reliability of the technique could be hampered by mass spectrometer interference (Gan, et al., 2007). Yet, the method offers significant advantages which outweigh the negatives.

1.6.3.5 iTRAQ as a tool for oncoproteomic investigation

iTRAQ, in the recent years has especially proven to be a very effective tool for oncoproteomic evaluation. In many studies pertaining to cancer, it is imperative to compare the proteomic profiles of normal tissue/cell samples to their cancerous counterparts. This would shed light on the proteins which are abnormal in the tumour cells. On the same lines, in order to understand the effects of a drug on cancer, it is essential to compare the profiles of the treated and untreated cells.

Sensitive protein expression analysis has been difficult because amplification of proteins, unlike DNA or RNA is impossible. Relative quantification of proteins using iTRAQ is hence a bright prospect. Several studies have employed this strategy for oncoproteomic studies. Pierce et al, used an eight-plex iTRAQ based method to compare the activity of 6 leukemogenic tyrosine kinases (Pierce, et al., 2008). This technique was also exploited to

study the exact mechanism responsible for the anti-proliferative effects of the highly promising drug imatinib on chronic myeloid leukemia. The comparative profiling was performed across highly precious and relatively scarce clinical samples. The fact that iTRAQ could successfully identify a significantly large number of proteins bears testimony to the sensitivity and efficacy of the technique (Griffiths, et al., 2007).

The time dependent effects of butyrate, a fatty acid fermentation by-product, on colorectal cancer were critically evaluated by profiling the proteome of butyrate treated cells using iTRAQ 4-plex strategy. The multiplexing capability of iTRAQ proved invaluable in enabling the cross comparison across various time points within the same experiment. This eliminated the errors introduced by batch effects which seriously compromises the accuracy of the data (Tan, et al., 2008).

These examples thus illustrate the utility of iTRAQ as a tool for oncology research.

CHAPTER 2

AIMS OF THE STUDY

Cancer is a highly multifactorial disease. It is an umbrella term encompassing a huge gamut of ailments, which are characterised by uncontrolled proliferation of cells belonging to various body parts. This plurality is in fact the biggest hurdle in developing therapies to cure cancer. It is hence close to impossible to identify that elusive 'magic pill' that can cure cancer. Yet we endeavour to mitigate the deadly effects of the disease by developing lasting cures for certain types of cancer. In this respect, this thesis work attempts to add to the existing knowledge of AML and leukemia therapy.

We understand today that cancer is a result of a complex interplay of signalling and metabolic pathways acting in a deregulated state. Any drug designed to cure cancer would target these aberrant pathways. Hence, in order to design therapeutic agents for cancer treatment it is essential to understand the molecular mechanisms employed by the drug.

While there have been a number of studies in this direction, they suffer from the common fallacies of highly specified objectives and technology oriented constraints. We have studied the molecular mechanism of action of two drugs, with bright prospects as cure for AML. We have employed a combination of transcriptomic and proteomic based approaches to overcome the aforementioned pitfalls encountered in such studies. Such a top-down strategy hence provides a snapshot of the various pathways modulated by the drugs in AML.

The main aims of the project are:

1) Assess the prospects of using Rapamycin and Genistein as therapies for AML on a cell line based model of the disease.

2) Identify the pathways modulated by these drugs in AML using high-throughput strategies such as mRNA expression analysis and proteomics, in combination or alone.

3) Validate these findings using methods such as real-time PCR and western immunoblotting, to ascertain the veracity of the data.

4) Characterise the various novel pathways identified by the study by employing appropriate functional assays. (This is more like solving a jigsaw puzzle that is the mechanism of action of the drug, piece by piece, now that all the information that we need is at hand!)

This is the first concerted effort to extensively use high-throughput studies to study the effect of Rapa and GEN on AML. The study uncovers crucial information pertaining to the action of these drugs, which is fundamental in understanding its mode of action. The knowledge gleaned from this study provides a strong case for rapa and GEN to be considered for further clinical studies on human subjects and would pave the way for the successful alleviation of the misery of leukemia.

CHAPTER 3

MATERIALS AND METHODS

The Materials and Methods section encompasses detailed descriptions of all the methods employed and the protocols followed while performing the experiments. It also provides the source of all reagents and biological materials used in the research.

3.1 Cell Culture

The entire study was performed on immortal cell lines derived from AML patients. The cell lines used in this study are listed as follows and their FAB subtypes are indicated: MV4-11 (acute monocytic leukemia, FAB M5), THP-1 (acute monocytic leukemia, FAB M5), HL-60 (acute promyelocytic leukemia, FAB M2), HEL (erythroleukemia, FAB M6) and Kasumi-1 (FAB M2). All the cell lines were cultured in complete RPMI media supplemented with 10% FCS in a humidified incubator at 37˚C with 5% CO_2. Cells were grown in T-75 tissue culture flasks and aseptic conditions were strictly maintained. Cells were cultured according to the growth kinetics and doubling rates of each cell line.

3.2 *In vitro* cytotoxicity assay

Rapa was purchased from Calbiochem (Darmstadt, Germany) and dissolved in DMSO. 10mM stock solutions were made. GEN was purchased from Sigma- Aldrich (St.Louis, MO, USA) and stock solutions of 100mM were prepared. The aliquots were stored at -20˚C. Working solutions of the drugs were prepared by diluting the stock with RPMI (without FCS). The final concentration of DMSO in the *in vitro* assays was maintained at <0.05%.

In vitro cytotoxicity assays were performed using the MTS (3-(4, 5-dimethylthiazol-2-yl)-5-(3- carboxymethoxyphenyl)-2-(4-sulfophenyl)-2H-tetrazolium, inner salt assay reagent) - CellTiter 96® AQueous One Solution Cell Proliferation Assay (Promega, Madison, WI,

USA) to assess the inhibitory effect of rapa and GEN on the AML cells. It is a colorimetric assay for determining the number of viable and proliferating cells. It contains an electron coupling agent phenazine ethosulfate (PES), in addition to the above mentioned tetrazolium compound, fortifying the stability of the solution. The MTS tetrazolium compound is reduced by live cells into a coloured formazan product by the NADPH or NADH produced by dehydrogenase enzymes in metabolically active cells. Hence the colour change of the culture media is a direct indicator of the number of living cells and hence the cytotoxicity of the drug. Cells were seeded at a concentration of 2×10^5 cells/ml in 96-well plates and treated with increasing dosages of rapa for 48 h. The final volume was maintained at 100 µl. 20 µl of the MTS reagent was added to each well and the plate was incubated at 37˚C for 1-4 h. The absorbance of each well was measured at 490nm with a 96-well plate reader. The CalcuSyn software (Biosoft™) was used to calculate the IC_{50} dosage of rapa for each of the cell line used.

In the case of GEN treatment, the cytotoxicity was assessed using the trypan blue exclusion dye (Sigma-Aldrich). It is a vital dye which stains dead cells blue. Cells were treated with GEN at various dosages such as 10 µM, 20 µM and 40 µM, and for different time points including 0h, 24h, 48h and 72h. The dye was then loaded on to a small aliquot of the cells and counted under a microscope. The total number of viable cells in the treated and control cells were calculated to assess the cytotoxicity of GEN, accounting for the dilution introduced in the previous step by mixing the dye with the cell.

3.3 Transcriptomic analysis using microarray

3.3.1 RNA extraction

The MV4-11 and THP-1 cells were cultured at a seeding density of 2×10^5 cells/ml. The MV4-11 cells were treated with 50nM and 500nM of rapa while the THP-1 cells were treated

with 500nM of the drug for 48 h. The control was subjected to treatment with the same amount of DMSO used to dilute the drug, to normalise the effects of DMSO on the cells.

The cells were harvested after 48 h of drug treatment and RNA was extracted using the RNeasy kit (Qiagen, GmbH, Hilden, Germany). The manufacturer's instruction was followed and pure RNA was eluted out using a binding column to remove DNA and protein contaminants. The RNA was quantified using the NanoDrop® ND-1000 UV-Vis Spectrophotometer (Nanodrop Technologies, Wilmington, DE, USA). The RNA was stored at -80˚C.

The quality of the RNA was assessed using the RNA 6000 Nano LabChip kit on the Agilent 2100 Bioanalyzer (Agilent Technologies, Inc., Palo Alto, CA, USA). The Agilent 2100 Bioanalyzer is a microfluidics-based platform for sizing, quantification and quality control of DNA, RNA, proteins and cells on a single platform. This instrument offers several significant advantages over the traditional methods of RNA quality detection using gel electrophoresis. It enables rapid quality checking possible with a sample preparation and running time of only 30-40 min. It also has multiplexing capabilities, allowing up to 10-12 samples in one chip. The data is highly reproducible and the quality of the output is very neat. The method is very easy to adopt. Hence it was used in our experiment.

The RNA 6000 Nano kit was employed. The electrodes were decontaminated with RNaseZAP® (Ambion/Applied Biosystems, Austin, TX, USA). The chip priming station was set up in the required position for RNA analysis. After equilibrating the reagents to room temperature, the gel matrix was filtered through a spin column by centrifugation. The filtered gel matrix would be in excess. It can be stored at 4˚C and should be used within a month after preparation. 1 µl of the dye concentrate is then added to a 65µl aliquot of filtered gel matrix. After thorough mixing, it is subjected to centrifugation at 13,000 g for 10 min at room temperature. The gel-dye mix is then added to a new RNA Nano chip, which is placed in the correct position on the chip priming station. The gel-dye mix is added in a particular sequence on the chip, as mentioned in the user manual supplied by the manufacturer and the chip is

pressurised using the syringe on the chip priming station. This is followed by addition of RNA Nano marker to the ladder and sample wells. Heat denatured RNA ladder is then added to the ladder well. 1 µl of the RNA samples whose quality is to be tested are then added to the sample wells. The sample is vortexed using the special vortex provided and the chip is analysed within 5 min of preparation on the bioanalyzer.

3.3.2 Affymetrix Genechip analysis

The gene expression profiling was done using the Affymetrix Human Genome U133 2.0 arrays (GeneChip®, Affymetrix, Santa Clara, USA). The samples were prepared and run as biological replicates, strictly adhering to the Affymetrix GeneChip® Expression Analysis Technical Manual for the eukaryotic sample and array processing. The general flow of work is illustrated in Fig 3.1.

The GeneChip® Human Genome U133A 2.0 Array is a single array comprising of 14,500 well-characterised human genes and 18,400 transcripts. The salient features of this chip are many. It provides transcripts of well substantiated genes. It involves 22,000 probe sets and 500,000 distinct oligonucleotide features.

Sequences used in the design of the array are obtained from databases such as GenBank®, dbEST, and RefSeq. The sequence clusters were fashioned from the UniGene database and then refined by analysis and comparison with a number of other publicly available databases. Oligonucleotide probes complementary to each corresponding sequence are synthesised *in situ* on the array. Eleven pairs of oligonucleotide 25-mer probes are used to measure the level of transcription of each sequence represented on the GeneChip Human Genome U133A 2.0 Array (HG-U133A 2.0). The GeneChip arrays are manufactured by a very sophisticated process wherein synthesised photolithographic masks are used to direct light onto the surface of a wafer. The oligonucleotide probes are then synthesised on the surface one base at a time.

The samples were prepared as suggested by the manufacturer strictly adhering to the instructions provided. 2µg of RNA was used as the starting material for each of the samples. The samples which were hybridised to the chips are as follows: MV4-11- 50nM rapa, MV4-11- 500nM rapa; THP-1- 500 nM rapa. All the samples were prepared as biological duplicates.

One-cycle target labelling procedure was followed. Poly-A RNA Controls (Spike-in Controls) were added to the sample to include exogenous positive controls to monitor the labelling process. Double stranded cDNA is synthesized and cleaned up to remove all possible nucleic acid and other contaminants. This is followed by preparation of biotin-labelled cRNA by *in vitro* transcription. The cRNA thus obtained is again cleaned up and its quality and integrity is verified using the Agilent 2100 Bioanalyzer. The cRNA is subjected to fragmentation for target preparation. This is done to obtain optimal assay sensitivity. The fragmented cRNA is again tested using the Bioanalyzer for complete and proper fragmentation. Once the efficiency of the process is verified, the sample is hybridised onto the chip. This is performed by injecting the samples processed for hybridisation (hybridisation cocktail) into the HG U133 2.0 array, which is then sealed and incubated in a rotating hybridisation chamber set at 60 rpm at 45˚C for 16 hr. The volume of the cocktail prepared depends on the format of the array. In this case we used the 10 Format (Midi) array. The hybridised arrays were washed and stained with the SAPE station (Streptavidin Phycoerythrin) on the GeneChip® Fluidics station 450 using the appropriate protocols. The stained arrays were scanned using the GeneChip® Scanner 3000 7G.

Figure 3.1 illustrates the process of preparing samples for Affymetrix genechip analysis in a step-by step manner.
(http://media.affymetrix.com/support/downloads/manuals/expression_analysis_technical_manual.pdf)

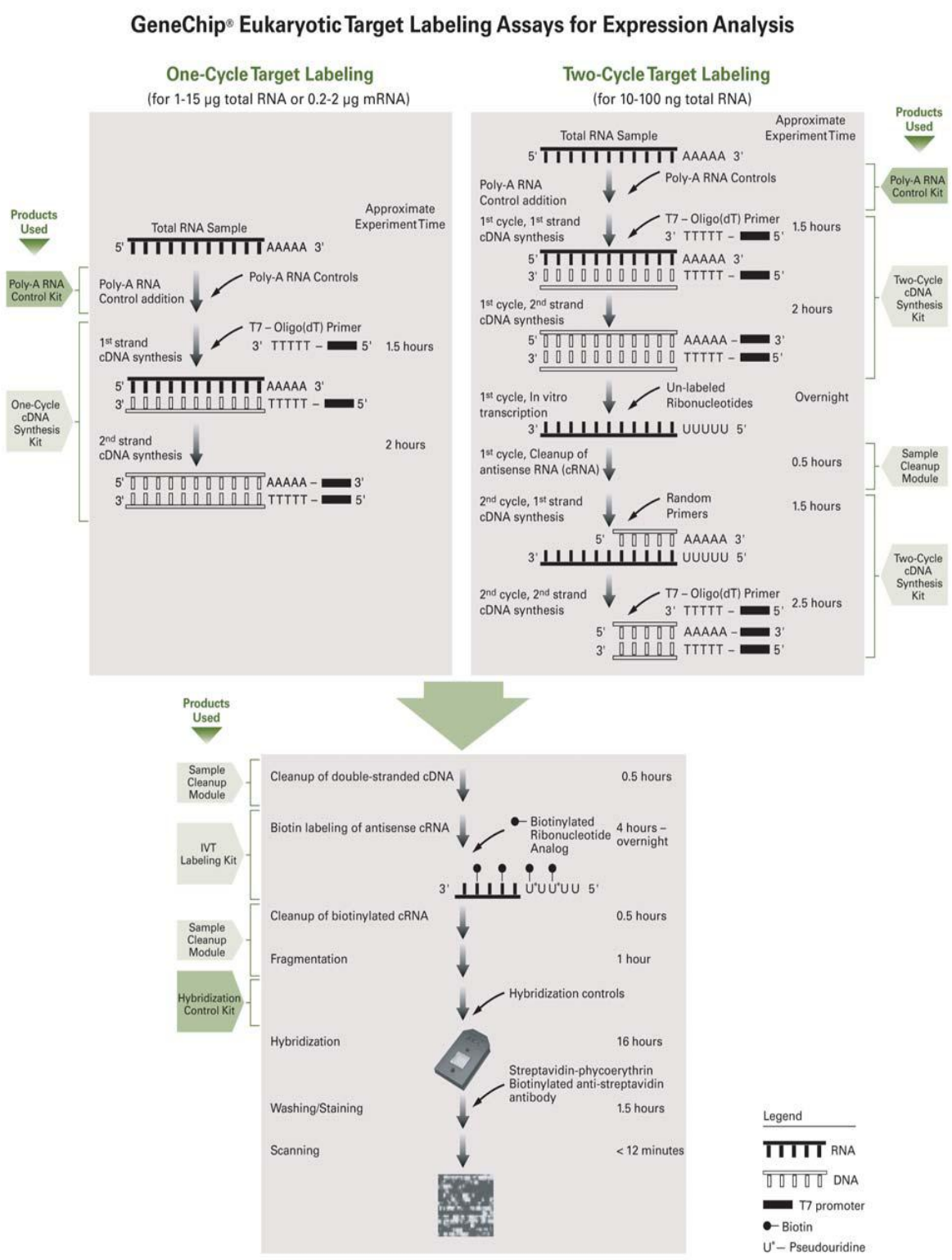

Figure 3.1: Workflow of Genechip array sample processing and array scanning

3.4 Data analysis

The microarray data was deposited in the public database ArrayExpress. The accession number is E-MEXP-2170 and is open for public use. The raw image files were generated by scaling the global factor to 500 using the Affymetrix GeneChip® Operating Software 1.2 (GCOS). The quality of the microarray data was verified by checking the parameters such as sig (3'/5') value of house-keeping controls, which have been inserted as an internal control of quality control by the manufacturers. The spiked in control levels were assessed to judge the labelling and hybridisation efficiencies.

Scatter plots of each of the replicates were generated to confirm the reproducibility of duplicate chips. The data was subsequently analysed using Genespring 7.3.1 (Silicon Genetics, USA). It provides a complete suite of statistical and visualisation tools for microarray data analysis. The data was normalised on 'Per Chip: Normalise to 50^{th} percentile' and 'Per Gene: Normalise to specific samples' basis. The normalised data was filtered for 'Flags: Present or Marginal' and 'Fold Change cut off of +/-1.5'.

One-way ANOVA was performed to obtain statistically significant genes with p-value$\leq$0.05. The genes were classified according to their 'Gene ontology'. Hierarchical clustering was performed to visualise the expression difference among the different treatment conditions and across the two cell lines.

3.5 isobaric Tag for Relative and Absolute Quantification (iTRAQ) labelling

The proteomic profiling of rapa treated cells was done using the 4-plex iTRAQ™ labelling strategy (Applied Biosystems, Life Technologies Corporation, Carlsbad, CA, USA) while the proteome of the GEN treated cells was probed using an 8-plex iTRAQ method. The difference between the methods as suggested by their nomenclature lies in the fact that the 8-plex method essentially doubles the number of samples that can be studied in a batch experiment. It has 4 more tags to accommodate these extra samples.

3.5.1 Protein extraction and sample preparation for iTRAQ labelling

The proteome profiles of cells treated with rapa and GEN were generated using the iTRAQ labelling technique. The cells were harvested and lysed for protein extraction with 0.5M Triethylammonium bicarbonate Buffer (TEAB), pH 8.5 containing 1% SDS and protease inhibitor. The cells were pelleted and incubated with this lysis buffer at room temperature for 15 min and at 100˚C for 20 min. Protein separation was achieved by centrifuging at 4˚C for 1 h at 14,000 rpm, and the supernatant was separated. The samples were quantified using the RC DC™ Protein Assay (Bio-Rad, Hercules, CA, USA). 100µg of each sample was used for the iTRAQ labelling.

The protein samples were diluted 10 times with 0.5M TAEB, pH 8.5 and subjected to reduction with 5 mM tris-(2-carboxyethyl) phosphine (TCEP) at 60 °C for 1 h followed by alkylation with 10 mM methyl methanethiosulfonate (MMTS) for 10 min. Cysteine blocking was performed on the sample, each of which was diluted to 0.05% (w/v) SDS. The samples were then trypsinised with 25 µl trypsin at 37˚C for 16 h.

Following this, each tryptic digest was labelled for 1 h with one of the four isobaric amine-reactive tags for the 4-plex study. The pattern adopted for labelling the tags for the rapa study is as depicted in Table 3.1:

Table: 3.1: iTRAQ labelling plan for rapa treated samples

LABEL	SAMPLE
114	MV4-11- Control
115	MV4-11- 50nM rapa
116	THP-1- Control
117	THP-1- 500nM rapa

For the GEN study, an 8-plex method was adopted. Hence the samples were prepared as biological duplicates and labelled with one of the eight isobaric tags for 2 h using the labelling pattern as shown in Table 3.2:

Table: 3.2: iTRAQ labelling plan for GEN treated samples

LABEL	**SAMPLE**
113	MV4-11- Control 1
114	MV4-11- Control 2
115	MV4-11- 20 µM 1
116	MV4-11- 20 µM 2
117	HL-60- Control 1
121	HL-60- Control 2
118	HL-60- 30 µM 1
119	HL-60- 30 µM 2

3.5.2 Cation exchange, purification and desalting of labelled samples

These iTRAQ-derivatised samples (4 or 8, based on the protocol followed) were then pooled and passed through a strong cation exchange (SCX) cartridge as recommended by the manufacturer (AB SCIEX, Foster City, CA, USA). The bound peptides were eluted with 5 % NH_4OH in 30 % methanol. This eluate (from the ion exchange step) was desalted using a C_{18} column Sep-Pak cartridge (Millipore, Billerica, MA, USA). It was then subjected to vacuum-drying, and reconstituted for 2D-LC (two dimensional liquid chromatography). The reconstitution was done using 20µl of 5 mM KH_2PO_4 buffer containing 5 % ACN, pH 3.0.

3.5.3 2D-LC separation of Labelled Peptides

The iTRAQ-labelled peptide mixtures were separated using an Ultimate™ dual gradient LC system (Dionex-LC Packings, Sunnyvale, CA, USA) provided with a Probot™ MALDI spotting device. The 2-D LC separation was performed in the following manner. The labelled peptide mixture was dissolved in 2% ACN with 0.05% TFA. It was then injected into a 0.3 × 150-mm strong cation exchange column (FUS-15-CP, POROS 10S) (Dionex-LC Packings, Sunnyvale, CA, USA) for separation. This constituted the first dimension of separation. In the case of the 8-plex study, the sample was initially reconstituted to 50 µl, of which 12 µl was injected by microliter pickup injection into a 0.5 × 23.5 mm strong cation-exchange (SCX) NanoEase™ trap column (WATERS Corp., Milford, MA, USA) for first dimensional separation. The Mobile phase A used was 5 mM KH_2PO_4 buffer, pH 3, 5% ACN, and mobile phase B used was 5 mM KH_2PO_4 buffer, pH 3, 5% ACN, 100 mM KCl, respectively. A steady flow rate of 6 µl/min was maintained. A total of nine fractions were obtained using step gradients of mobile phase B: unbound, 0–5, 5–10, 10–15, 15–20, 20–30, 30–40, 40–50, and 50–100%. The eluting fractions were captured alternatively onto two 0.3 × 1-mm trap columns (3-µm C_{18} PepMapTM, 100 Å) (Dionex-LC Packings) and washed with 0.05% TFA followed by gradient elution in a 0.2 × 50-mm reverse phase column (monolithic polystyrene-

divinylbenzene) (Dionex-LC Packings).In the case of the 8-plex study, the reverse phase (C_{18}) and trap columns were both purchased from Waters Corporation. The mobile phases used for this second dimensional separation were 2% ACN with 0.05% TFA (A) and 80% ACN with 0.04% TFA (B). The gradient elution step was 0–60% B in 15 min at a flow rate of 2.7 µl/min. The LC fractions were mixed directly with MALDI matrix solution (7 mg/ml α-cyano-4-hydroxycinnamic acid and 130 µg/ml ammonium citrate in 75% ACN) at a flow rate of 5.4 µl/min via a 25-nl mixing tee (Upchurch Scientific, IDEX Health & Science, Oak Harbour, WA, USA) before they were spotted onto a 192-well stainless steel MALDI target plate (Applied Biosystems, Life Technologies Corporation) using a Probot Micro Precision Fraction Collector (Dionex-LC Packings) at a speed of 5 s/well. 50 fmol of ACTH peptide (m/z = 2465.199) was spiked into each well as internal standard.

3.5.4 Mass Spectrometry Analysis and Database search

3.5.4.1 4-plex iTRAQ study

The 4700 Proteomics Analyzer mass spectrometer (Applied Biosystems) was used in the analysis of the samples on the MALDI target plates for the 4-plex study. Nitrogen at a collision energy of 1 kV and a collision gas pressure of 1×10^{-6} torr was used to do the MS/MS analyses. The peptide and protein identifications were performed by using the GPS Explorer™ software version 3.6 (Applied Biosystems, Life Technologies Corporation) to create and search files with the MASCOT search engine (version 2.1; Matrix Science). The International Protein Index (IPI) human database *(version 3.30, 67,922 sequences)* was used for the search, and this was restricted to tryptic peptides.

One thousand shots were accumulated for each MS spectrum. For MS/MS, 6,000 shots were combined for each precursor ion with signal to noise (S/N) ratio greater or equal to 100. For precursors with S/N ratio between 50 and 100, 10,000 shots were acquired. The resolution used to select the parent ion was 200. No smoothing was applied before peak detection for

both MS and MS/MS, and the peaks were deisotoped. For MS/MS, only the peaks from 60 to 20 Da below each precursor mass and with S/N ≥ 10 were selected. Peak density was limited to 30 peaks per 200 Da, and the maximum number of peaks was set to 125. Cysteine methanethiolation, N-terminal iTRAQ labeling, and iTRAQ-labeled lysine were selected as fixed modifications; methionine oxidation was considered as a variable modification. One missed cleavage was allowed. Precursor error tolerance was set to 100 ppm; MS/MS fragment error tolerance was set to 0.4 Da. Maximum peptide rank was set to 2. iTRAQ quantification was performed using the GPS Explorer™ software and normalized among samples. iTRAQ ratios were calculated based on the cluster areas of the iTRAQ reporter fragment peaks (114, 115, 116, and 117), and the calculation of ratios included only peptides identified with C.I. percent above cut-off thresholds as described below. The average iTRAQ ratio and standard deviation were determined using the GPS Explorer™ software (version 3.6).

3.5.4.2 8-plex iTRAQ study

In the case of the iTRAQ study, mass spectrometry was performed on a 4800 MALDI-TOF/TOF Analyser (Applied Biosystems/MDS Sciex) operating in positive mode. The laser intensity was adjusted to 4000 for MS and 4300 for MS/MS acquisition. One thousand shots were accumulated in each spot. MS spectra were acquired between *m/z* 800-3000. The 7 precursor ions with the highest peak intensity of each spot with at least S/N of 50 were automatically selected for MS/MS acquisition. MS/MS was performed using air as the collision gas at collision energy of 1 kV and collision gas pressure of ~1.4×10^{-6} Torr, with an accumulation of 5000 shots for each spectrum.

ProteinPilot™ 2.0.1 (Applied Biosystems, Life Technologies Corporation) was employed for protein identification which uses the Paragon™ algorithm to perform database searches. The IPI database version 3.65 was the relevant human protein repository used for the search.

Redundancy was eliminated by grouping the identified proteins using the ProGroup algorithm in the software.

A decoy database search strategy was adopted to estimate the false discovery rate (FDR) for peptide identification. A corresponding randomized database was generated using the Proteomics System Performance Evaluation Pipeline (PSPEP) feature in the ProteinPilot™ Software 2.0.1. The results were then exported into Microsoft Excel for manual data interpretation.

3.5.5 Determination of the significant cut-off threshold for fold-change

To determine the cut-off threshold for the fold change of proteins identified from the iTRAQ study to be considered as significantly regulated, two equal amounts of six-protein mixtures (Applied Biosystems) were trypsin digested and labelled with the iTRAQ reagents (Tan, et al., 2008). The standard deviation (S.D) of all the ratios of the labelled peptides was computed to be 0.15. Thus by using a 1 + 2 S.D formula the fold-change cut-off thresholds were set as 1.3 for up-regulated proteins and reciprocally 0.77 for down-regulated proteins. This strategy was adopted for the 8-plex iTRAQ GEN study.

In the case of the 4-plex rapa study, the S.D of the ratios of the proteins identified from the iTRAQ study was computed to be 0.12. Hence cut-off thresholds of 1.24 and 0.80 were applied for up and down-regulated proteins respectively.

3.5.6 Estimation of false positive rate to determine cut-off score

A randomized database generated using IPI human database Version 3.31 (generated using a Pearl script downloaded from http://www.matrixscience.com/help/decoy_help.html) was used, in addition to the IPI human database for the purpose of weeding out false positives from the iTRAQ results. The false positive rate was calculated by comparing the peptide hits

obtained from these 2 databases at different ion score C.I % (peptide). The minimum ion score C.I % was set such that no more than 5% false positive rate is achieved. Based on this cut-off threshold, all the proteins identified from the random database search were matched to a single-peptide. Hence, proteins identified from the human database that are matched to at least 2 peptides are statistically confident. For single-peptide matched proteins, only those with ion score C.I % greater than the highest C.I % attained from the random database search were considered as significant.

For the 8-plex study, the ProteinPilot™ software was used for the data visualisation. Among the various parameters used to classify the data, the unused score is of significance. An unused score greater than 2 corresponds to a confidence of greater than 99%. This corresponds to an accepted false discovery rate (FDR) of 1%. Hence this cut-off score was used to pick proteins of high confidence.

3.6 Quantitative Real-Time PCR validation of microarray and iTRAQ data

The microarray and iTRAQ data were validated using quantitative real-time PCR technique. 8 genes of interest were chosen from the microarray data for this purpose. The criteria applied in the choice of these genes were two-fold. They were selected on the basis of their level and direction of fold change and their potential implications in explaining the mechanism of effects of rapa on MV4-11 and THP-1 cell lines.

cDNA was synthesised from total RNA using the High-Capacity cDNA Archive Kit (Applied Biosystems). The RNA was reverse transcribed using reverse transcriptase enzyme. 2 µg of RNA was converted to cDNA using the following procedure. The 2× RT master mix was prepared hence as shown in Table 3.3:

Table 3.3: 2X Reverse transcription master mix recipe

Component	**Volume (µl) /Reaction**
10X Reverse Transcription Buffer	5
25X dNTPs	2
10X random primers	5
MultiScribe™ Reverse Transcriptase	2.5
Nuclease-free H2O	10.5
Total per Reaction	**25**

2 µg of RNA was diluted to 25 µl and was mixed with the 2× RT master mix. The mixture was placed in a thermocycler set to the following conditions (Table 3.4):

Table 3.4: PCR program for reverse transcription reaction

	Step 1	**Step 2**
Temperature	25˚ C	37˚ C
Time	10 min	120 min

The cDNA was stored at -20˚C. The qRT-PCR was performed on the ABI Prism 7000 thermocycler. SYBR Green (Applied Biosystems) was the choice of fluorescent detection system used. Primers were designed using the Primer Express® Version 2.0 program and the sequences are listed in Table 3.5. β2M gene was used as the endogenous control for the study as its levels remain unchanged due to rapa treatment. Equal amount of cDNA was used in all the reactions and the samples were run on ABI PRISM® 7000 Sequence Detection System. SYBR Green reagent (Applied Biosystems) was the employed to quantify the expression

levels of the selected genes. The data was analysed using the ABI PRISM® 7000 SDS Software. The comparative C_T ($\Delta\Delta C_T$) method was used to calculate the fold-change values.

Table 3.5: List of primers used for real-time PCR

Gene	Forward Primer	Reverse Primer	Product (bp)
FOS	TCACCCGCAGACTCCTTCTC	AGTGACCGTGGGAATGAAGTTG	102
FRAT1	TCCTCGGTTCAAGGTCACTGTT	ACCGGCAGAACCTGGCTACT	71
IGFBP2	CGGAGCAGGTTGCAGACA	GTTCTCCACCAGGCCTCCTT	56
IL8Rβ	CCAGCGACCCAGTCAGGAT	TTCAAAGCTGTCACTCTCCATGTTA	70
SKP2	TGCTAAAGGTCTCTGGTGTTTGTAA	AAGGTCTGCCATAGAGACTCATCA	70
TGFβI	CTGTCCAGCAGCCCTACCA	TCCGTGCGGTCCGTGTA	90
TIEG	GCTCAACTTCGGTGCCTCTCT	CTTTTGGCCTTTCAGAAATCATTT	71
TNFSF7	CTGCCGCTCGAGTCACTTG	GCTGAGGTCCTGTGTGATTCAG	64

3.7 Pathway Analysis

The genes and proteins showing significant differences in fold change values from the microarray and iTRAQ studies were analysed using the Ingenuity Pathway Analysis software (Ingenuity® Systems, Redwood city, CA, USA), Version 5.5.1 (IPA). It is highly useful to study the pathways and networks each candidate gene or protein is involved in.

An excel file containing the list of genes/proteins showing up/down regulation due to rapa treatment was uploaded into IPA. The software maps each of the gene/protein to the repository of information in the Ingenuity Pathways Knowledge base. Molecular networks regulated by the drugs in AML were obtained using these focus genes and proteins. The canonical pathways and functions were also ranked based upon their significance.

The gene ontology analysis for the proteomic profile was done using STRAP, an open source software tool for protein annotation. (http://cpctools.sourceforge.net). Protein lists were submitted as text documents, upon which GO was generated for each protein.

3.8 Protein Extraction for western blot analysis

AML cells were treated with the drugs and harvested. The time of harvest was specific to individual experiments. The cells were washed twice with ice-cold PBS and lysed with buffer containing 50 mM Tris-HCl (pH 7.5), 150 mM NaCl, 1% Triton X-100, protease inhibitor and phosphatase inhibitor cocktails (Roche, Basel, Switzerland). The cells were incubated with the lysis buffer for 30 min on ice. The mixture was then centrifuged for 30 min at 4˚C at 14,000 rpm. The supernatant was carefully extracted and stored at -80˚C. Aliquots were stored at -20˚C.

3.9 Western Blot

The protocol suggested by the company was followed to perform western immunoblotting. The antibodies were purchased from the commercial vendors listed in Table 3.6. The expression level of the loading control actin was used to ensure equal loading in each well. The proteins were separated on 12% SDS-PAGE gel. The proteins thus separated were then transferred on to PVDF membrane (Bio Rad, Hercules, CA). The membrane was activated by methanol treatment for 15 sec, prior to the transfer protocol. The transfer was conducted in a cold room, on ice for 90 min at a constant voltage of 100V. The membrane was then blocked with 5% milk (in 1× PBS-T) for 1 h at room temperature with gentle shaking. In some cases overnight blocking at 4˚C was performed.

The membrane was then washed well with 1× PBS and incubated overnight with the primary antibody diluted to the appropriate quantity in 5% BSA. After vigorous washing, the membrane was incubated for 1 h at room temperature with the appropriate secondary antibody. This was followed by successive washing in 1× PBS-T. Table 3.6 summarises the conditions used for each antibody. The membranes were then incubated with HRP substrate Western Lightning (Perkin Elmer, Waltham, MA, USA) and the signals were detected on Amersham hyperfilm X-ray films (GE Healthcare, UK).

Table 3.6: Antibody dilutions and blocking conditions used for western immunoblotting

Antibody	Source	Dilution	Blocking
Actin	BD Biosciences, Franklin Lakes (NJ, USA	1:4000, 1 h- room temp	1 h- room temp
p-FLT3	Cell Signaling Technology (Danvers, MA, USA)	1:500, Overnight- 4˚C	2 h- room temp
4E-BP1	Cell Signaling Technology (Danvers, MA, USA)	1:1000, Overnight- 4˚C	1 h- room temp
p-4E-BP1	Cell Signaling Technology (Danvers, MA, USA)	1:1000, Overnight- 4˚C	2 h- room temp
p70S6K	Cell Signaling Technology (Danvers, MA, USA)	1:1000, Overnight- 4˚C	2 h- room temp
Cyclin D1	Cell Signaling Technology (Danvers, MA, USA)	1:1000, Overnight- 4˚C	1 h- room temp
Cyclin E	Cell Signaling Technology (Danvers, MA, USA)	1:1000, Overnight- 4˚C	1 h- room temp
Cdk 2	Santa Cruz Biotechnology (Santa Cruz, CA, USA)	1:200, Overnight- 4˚C	1 h- room temp
Cdk 4	Santa Cruz Biotechnology (Santa Cruz, CA, USA)	1:200, Overnight- 4˚C	1 h- room temp
p27	Santa Cruz Biotechnology (Santa Cruz, CA, USA)	1:200, Overnight- 4˚C	1 h- room temp
Skp2	Invitrogen (CA, USA)	1:1000, Overnight- 4˚C	1 h- room temp
Akt	Cell Signaling Technology (Danvers, MA, USA)	1:1000, Overnight- 4˚C	1 h- room temp
IGFBP2	Abcam (Cambridge, MA, USA)	1:1000, Overnight- 4˚C	2 h- room temp
Anti-mouse (secondary antibody	BD Pharmingen (San Jose, CA, USA)	1:2500, 1 h- room temp	N.A
Anti-rabbit (secondary antibody)	Chemicon, Millipore (Billerica, MA, USA)	1:5000, 1 h- room temp	N.A

3.10 Cell Cycle Analysis

We used flow cytometry analysis to study the change in the cell cycle distribution of the cells after rapa treatment. The cells were treated with GEN and harvested at 0 h, 8 h, 24 h, 48 h and 72h time points after drug treatment. Time points of 0 h, 8 h, 16h, 24 h and 48 h were adopted for the rapa study. The cells were washed twice with 1× PBS and fixed in ice cold 70% ethanol. The fixed cells were then stored at -20˚C until staining and analysis.

The cells were stained with staining solution containing 0.1% Triton-X-100 in PBS, 200 µg/ml of RNaseA and 20 µg/ml of propidium iodide (PI) for half an hour before flow cytometry analysis. The DNA content of the samples was studied by running the samples on CyAn Flow Cytometer (Dako, Denmark). 50,000 relevant cells were collected in each sample. The DNA content distribution was obtained by analysis using the Summit 4.3 software (Dako, Denmark).

3.11 Caspase 3/7 Assay

The MV4-11 and THP-1 cells were treated with rapa for 0 h, 12 h and 20 h time points. In the case of GEN treatment, the drug treated MV4-11 and HL-60 cells were incubated for 0 h, 24 h, 48 h and 72 h and assayed for apoptosis as follows. The treatments were carried out in 96 well plates. The cells were incubated with equal volumes of Caspase-Glo®3/7 reagent (Promega, Madison, WI, USA) for 1 h along with the necessary controls. The assay is designed as a homogenous, luminescence based method to study caspase 3/7 activity. The assay reagent contains the tetrapeptide sequence DEVD, provided in a solution pack optimized for caspase activity, luciferase activity and cell lysis. The Caspase 3/7 levels were proportional to the luminescence recorded and apoptosis was assessed hence.

3.12 Annexin V-FITC apoptosis detection

MV4-11 and THP-1 cells were treated with rapa and harvested after 48 h. A time course study was done in the case of GEN treatment, involving the following time points: 0h, 8h, 24h, 48h, and 72h. The cells were stained with annexin V-FITC and propidium iodide (PI) to detect apoptosis. During apoptosis, the membrane phospholipid phosphatidylserine (PS) is translocated from the inner to the outer leaflet of the plasma membrane. Annexin V is a Ca^{2+} protein which binds to PS with high-affinity and binds to cells with exposed PS. When Annexin V is bound to a fluorochrome FITC, the structure can be used to detect apoptotic cells on a flow cytometer. Double staining of cells with PI was done to select for early apoptotic cells, which would stain positive for Annexin V FITC but not for PI. Cells displaying double positive staining patterns represent dead or late apoptotic cells. Cells which stain only for PI and not for Annexin V FITC are necrotic. Double negative staining represents viable cells.

The harvested cells were washed twice with ice cold 1× PBS and resuspended in 1× binding buffer at a concentration of 1×10^6 cells/ml. 100 µl of the solution (1×10^5 cells) was then transferred to a 5 ml culture tube (Dako). To this, 5 µl of Annexin V-FITC and 5 µl of PI were added, to ensure equal double staining. The cell-stain cocktail was vortexed gently and the ensuing mixture was incubated at room temperature for 15 min in the dark. 400 µl of 1X binding buffer was added to each tube and the sample was analysed by flow cytometry immediately. The flow cytometers used were CyAn (Rapa study) and BD FACS Calibur (GEN study). 50,000 relevant cells were collected in each case. The data was analysed using the FlowJo software (Version 7.6) (Tree Star, Inc.) and Summit v4.3 (Dako) to assess the percentage of cells undergoing apoptosis.

3.13 Measurement of ROS levels in cells

MV4-11 and HL-60 cells were treated with GEN for the following time points: 8h, 24h, 48h and 72h. The treatment was carried out in 6-well plates and the cells were seeded at a density of 2×10^5 cells/ ml. The cells were harvested at each time point and assayed for the inherent reactive oxygen species (ROS) levels using the ROS detection reagent 5-(and-6)-carboxy-2′,7′-dichlorodihydrofluorescein diacetate (carboxy-H_2DCFDA) (Molecular Probes, Invitrogen, Eugene, OR, USA).

The derivatives of reduced fluorescein and calcein act as cell-permeant indicators for ROS detection. The unique property of the reduced and acetylated forms of 2′, 7′-dichlorofluorescein (DCF) and calcein to become fluorescent upon removal of the acetate groups by intracellular esterases in the event of oxidation is used to mirror the ROS levels inside the cells. The carboxy derivative of fluorescein, carboxy-H_2DCFDA, carries additional negative charges that improve its intracellular retention compared to noncarboxylated forms.

A concentrated stock solution of the probe was prepared and kept tightly sealed. The probe was diluted shortly before use in pre warmed PBS. The harvested cells were resuspended in 1×PBS containing 5 µM of the probe dye. The cells were loaded with the dye by incubating them with the dye solution for 45 min at 37˚C. The cells were then incubated in the growth medium for 15 min to enable their recovery. Oxidation of the probe was detected by measuring the increase in fluorescence intensity using the CyAn flow cytometer. 20,000 relevant cells were collected for each run.

3.14 Nascent protein synthesis quantification using Click chemistry

The amount of nascent proteins produced by MV4-11 and HL-60 cells treated with GEN in comparison to the untreated cells was studied to understand the effects of GEN on protein synthesis. The Click-iT® Metabolic Labeling Reagents for Proteins and Click-iT® Cell

Reaction Buffer Kit (Molecular Probes, Invitrogen) were used for this purpose. Cells were treated with GEN and harvested at 24h, 48h and 72 h time points. The treatment was performed as explained in section 3.13.

The click chemistry incorporates a new class of chemical reactions that use bio-orthogonal or biologically unique moieties to label and detect proteins using a two step procedure. In the first step, a biomolecule containing an azide- or alkyne is actively incorporated into the protein(s) of interest. This is followed by the detection step, wherein the chemoselective ligation or "click" reaction between an azide and an alkyne occurs. In the click reaction, the modified protein is detected with a corresponding azide- or alkyne-containing dye or hapten. The proteins thus labelled with the Click-iT® metabolic labelling reagent are detected using the Click-iT® Cell Reaction Buffer Kit by flow cytometry.

The metabolic labelling reagent used was Click-iT® AHA (L-azidohomoalanine), a methionine alternative. The detection molecule used was Alexa Fluor 488 (alkyne). The effect of GEN on nascent protein synthesis is studied by assaying the incorporation of AHA in newly translated proteins. The AHA was solubilised with DMSO to make a 1000x stock solution, which was stored at -20˚C. The cells were harvested and washed with 1×PBS. The cells were depleted of their methionine reserves by incubating them in methionine-free RPMI for 45 min. The cells were then transferred to the normal growth medium. 50 µM of AHA was added to the growth medium and the cells were incubated for 2 hours. The cells were then harvested and fixed in 4% PFA for 15 min. This was followed by permeabilisation with 0.1% saponin for 15 min. 3% BSA was used to wash the cells. The Click-iT® reaction cocktail was prepared as shown in Table 3.7 (volumes indicated per reaction).

0.5ml of the click-iT reaction cocktail was added to each sample and incubated for 30 min at room temperature. The cells were washed once with 3% BSA and the fluorescence was measured using a BD FACS Calibur flow cytometer, set to capture the fluorescence of Alexa Fluor 488 dye.

Table 3.7: Click-iT® reaction cocktail preparation methodology

Reaction components	**1 reaction**
1x Click-iT reaction buffer	440 µl
$CuSO_4$	10 µl
Click-iT cell buffer additive	50 µl
Alexa Fluor 488 dye	Add to 1-5 µM final concentration
Total volume	500 µl

CHAPTER 4

HIGH-THROUGHPUT CHARACTERISATION OF THE EFFECTS OF RAPA ON AML

This chapter delves deep into the elucidation of the anti-proliferative effects of rapa on AML cell lines and attempts to explore the possible reasons for such a phenomenon. The chapter weaves a laconic justification for a combinatorial approach to study the transcriptome and proteome of rapamycin treated cells and describes the results obtained from the study in great detail.

4.1 Introduction

Rapa, a macrolide antibiotic, is a potent FDA approved immunosuppressant, capable of reversing acute active allograft rejection and enhancing long-term donor-specific allograft tolerance (Calne, et al., 1989). Interestingly, it was found to exhibit anti-cancer effects. Studies pertaining to the anti-tumoral activity of rapa and its analogs (CCI-779, RAD001) and the possibility of using it as therapy for certain cancers are underway (Chan, et al., 2005; Galanis, et al., 2005; Mita, et al., 2008). Recent studies indicate that rapa controls the proliferation of AML cells (Récher, et al., 2005). Thus rapa is a prospective alternate therapy for AML.

Rapa is a key regulator of the mTOR pathway which is responsible for cell growth and proliferation. Rapa arrests this critical pathway by binding to mTOR as a complex with FKBP12 and thus abrogating the phosphorylation of the downstream effectors S6K1 and 4E-BP1 (Sehgal, 1998; Sehgal, 2003) . Rapa also represses the PI3K/Akt pathway in AML cells, which is activated in AML blasts (Martelli, et al., 2006) and is known to control AML survival (Xu, et al., 2003). This pathway lies upstream of mTOR and controls essential cellular processes such as cell growth, cell cycle progression, transcription and apoptosis (Song, et al., 2005).

Since all the previous studies pertaining to the anti-proliferative effects of rapa employed the traditional approach of investigating individual pathways, namely mTOR and PI3K/Akt, crucial information about the repercussions of rapa treatment on the cell as a whole is lacking. Hence we consider it imperative to study the effects of rapa on AML at the global level, by obtaining a bird's eye view of the modulations caused by the drug by employing a high-throughput approach.

We have profiled the transcriptomic and proteomic level changes induced by rapa in AML with the aid of microarray and iTRAQ™ techniques respectively. Transcriptomic techniques can survey the expression levels of thousands of genes and can capture even the low copy number transcripts. On the other hand proteomic strategies, although not as sensitive as their mRNA counterparts, have the advantage of mirroring the protein levels, the eventual products of mRNA translation. We have also performed functional studies to bolster the findings from the high-throughput technologies. Thus we present here for the first time, a comprehensive snapshot of the key functional pathways and networks regulated by rapa in AML.

This chapter explicates the results obtained from the high-throughput study and the meaning derived from it. It proceeds to provide new evidence on novel activities of rapa and how it can be exploited for AML therapy.

4.2 Results

4.2.1 Rapa has cell line specific growth inhibitory effects on different AML cells

The sensitivity of a spectrum of AML cell lines, namely MV4-11, THP-1, HL-60, Kasumi-1 and HEL to rapa treatment was tested. The *in vitro* cytotoxicity assays were carried out in 96-well plates using the MTS assay protocol as described in Chapter 3.

Rapa was found to inhibit the growth of all the cell lines, but to varying degrees as inferred from their respective IC_{50} values (Table 4.1). MV4-11 was the most sensitive with an IC_{50} of

50nM. THP-1 was the least responsive with the inhibitory effect reaching a plateau at around 500nM (IC_{50} 755nM, estimated value) (Figure 4.1). This implies a static effect in the cytotoxicity of THP-1 to rapa treatment beyond a certain threshold. Nevertheless it is still sensitive enough to respond to drug treatment. MV4-11 and THP-1 cell lines were used as models for all further studies.

Table 4.1: IC_{50} concentration for various AML cell lines after 48 h treatment of rapa

Cell Line	AML subclass (FAB)	IC_{50}, nM
MV4-11	M5	50
Kasumi-1	M2	87
HEL	M6	97
HL-60	M2	173
THP-1	M5	755*

*= Estimated value

All cell lines were treated with increasing dosages of rapa and the cytotoxicity was analysed using the MTS assay. The IC_{50} values were calculated using the CalcuSyn software. All values are mean of triplicate experiments.

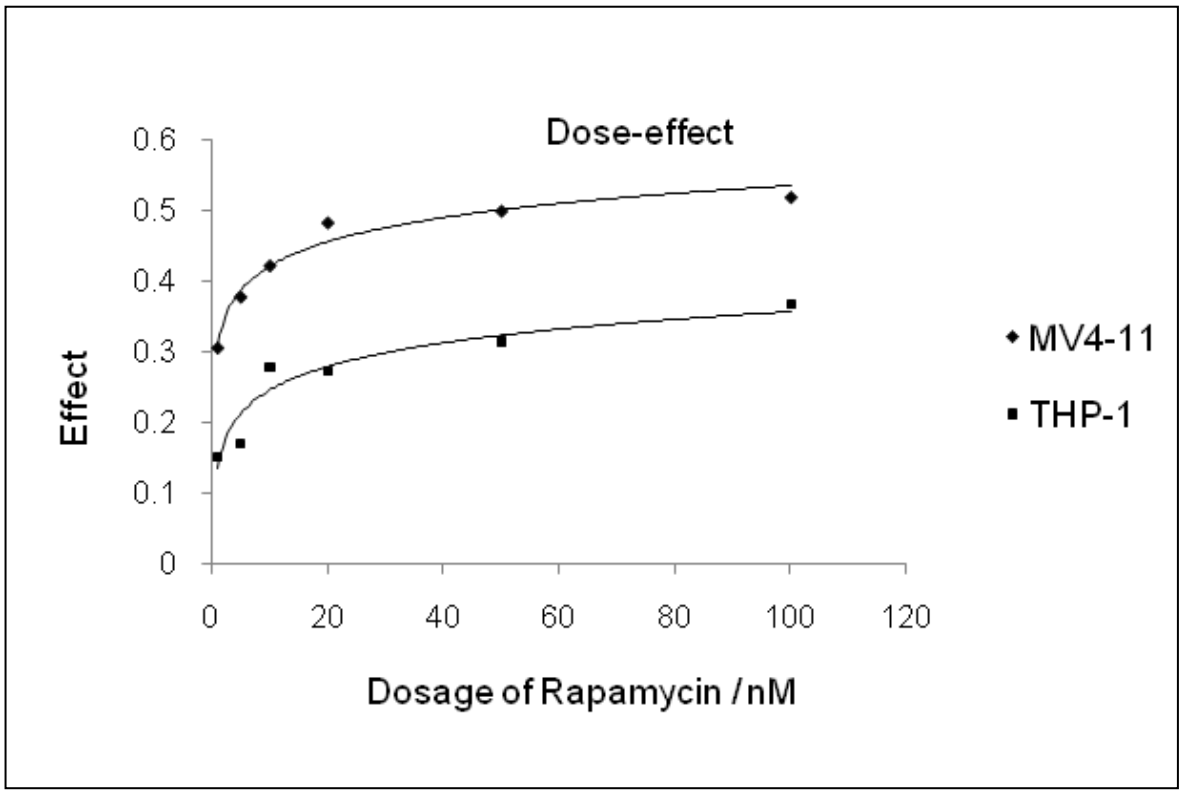

Figure 4.1: Dose-response curves of cell lines after 48 h of rapa treatment

Dose-response curves for MV4-11 and THP-1, the most and the least rapa-sensitive cell lines are shown. The inhibitory effect of rapa was studied by growing the cells with increasing dosages of the drug. All cell lines were treated with increasing dosages of rapa and the cytotoxicity was analysed using the MTS assay. The IC_{50} values were calculated using the CalcuSyn software. All values are mean of triplicate experiments.

4.2.2 Gene expression profiles of AML cells treated with rapa

The key to understanding the real mechanism of action of the drug is to analyse the molecular level changes orchestrated by it on the AML cells. Hence, the transcriptome of the MV4-11 cells treated with 50nM and 500nM of rapa, and THP-1 cells treated with 500nM of rapa were profiled. The Affymetrix GeneChip based cDNA microarray was the technology of choice. It offered several advantages such as wide coverage, ease of application, standardised downstream analysis, etc. The technology is described in detail in Chapters 1 and 3.

The samples were run as biological duplicates. Performing the experiment in replicates increases the confidence in the data due to increased sample size and reduces the chances of error due to chance. The Control samples in this study were cells which were not treated with the drug. However the control samples were treated with the same quantity of DMSO used in the dilution of the drug. This process subtracts the background observed due to DMSO.

The data obtained from the study was analysed using Genespring™ 7.3.1 software. Transcriptome analysis indicated a significant similarity and yet a profound contrast in the expression patterns of the two cell lines (Figure 4.2). The expression profiles of the MV4-11 cells treated with 50nM and 500nM concentrations of rapa do not show major differences. The two treatment conditions showed an overlap of 201 up-regulated genes and 186 down-regulated genes, reiterating the fact. Hence elevated levels of rapa do not significantly alter the transcriptome of AML cells. However, we could observe marked deviations in the profiles of MV4-11 cells and THP-1 cells which might explain the reason for their differential sensitivity to the drug. Only 35 up-regulated genes and 32 down-regulated genes were observed to overlap. 129 up-regulated genes and 158 down-regulated were unique to THP-1 alone.

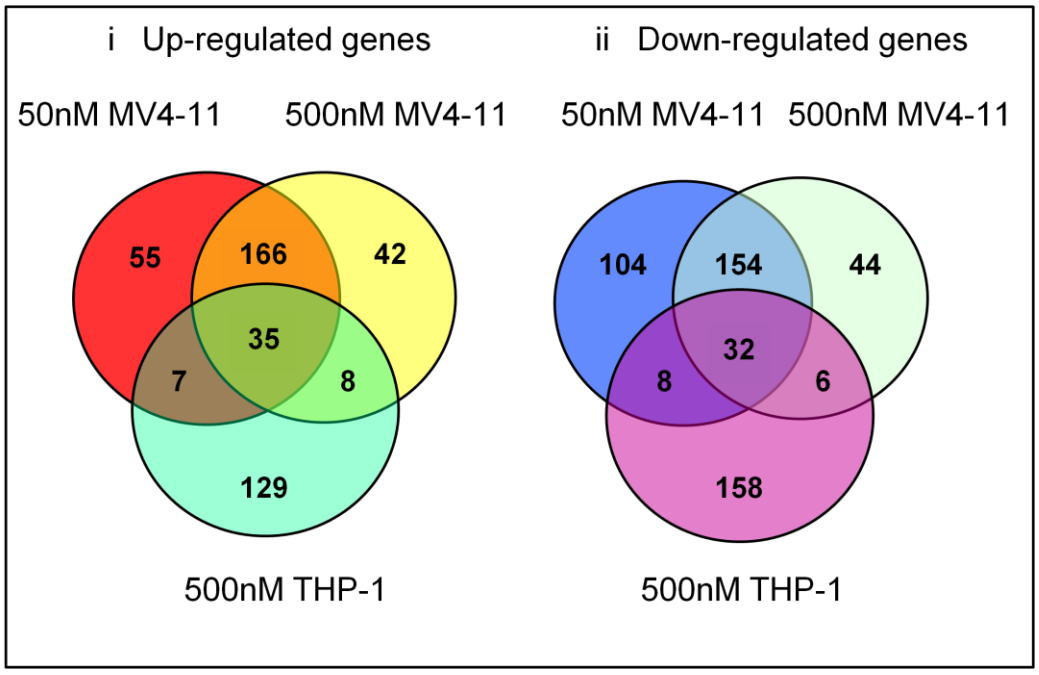

Figure 4.2: Venn Diagrammatic comparison of transcriptome profiles of MV4-11 and THP-1

Venn diagrammatic comparison of the (i) Up-regulated genes (ii) Down-regulated genes, of MV4-11 and THP-1, which cleared the p-value cut-off and fold-change cut-off.

The fold-change cut-off of 1.5 was used to filter the genes and identify those regulated by rapa treatment (Table 4.2).

Table 4.2: Rapa regulates a large number of genes in AML

Sample	Number of up-regulated genes	Number of down-regulated genes
MV4-11 50nM	263	298
MV4-11 500nM	251	236
THP-1 500nM	179	204

The genes were filtered on flags and fold-change (cut-off 1.5). The genes were then subjected to statistical tests. The genes listed above are those which cleared the stringent quality check.

The expression profiles of the two cell lines were subjected to hierarchical clustering using Genespring. The profiles clustered in accordance to the cell line type and treatment conditions (Figure 4.3). The MV4-11 samples clustered together and the THP-1 samples formed another subgroup. Among the MV4-11 samples, the treated samples clustered closer to each other and branched away from the control. This indicates a stark difference between the control and treated samples.

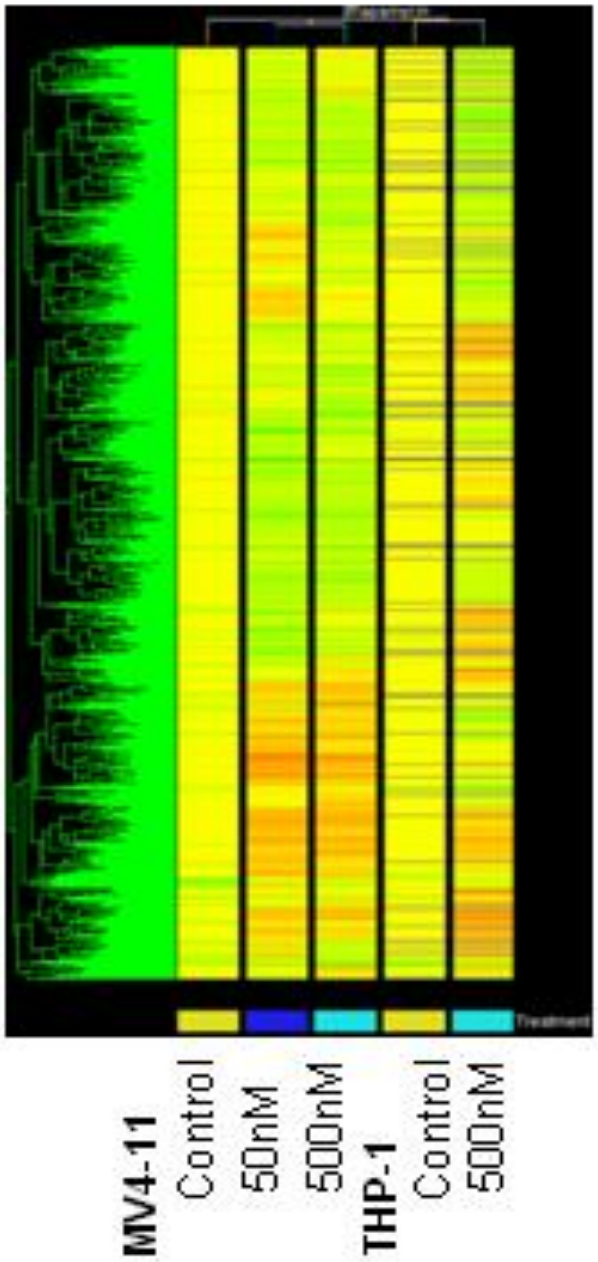

Figure 4.3: Hierarchical clustering of transcriptomic profiles of microarray data

Hierarchical clustering of the transcriptomic profiles indicate that samples cluster according to cell type and dosage. Thus MV4-11 samples cluster together, away from THP-1 samples.

4.2.3 Mapping the alterations in the proteome using iTRAQ labelling

Rapa treatment had a pronounced effect on the proteome of AML cells. The proteomic study was conducted on a 4-plex iTRAQ platform. The samples were labelled as described the in the Chapter 3, section 3.5.1. The study identified 24 proteins with altered levels in MV4-11 and 73 in THP-1. All proteins with Total Score C.I % of greater than 99 and a change in expression of at least 1.24 folds are listed in the Table 4.3.

Table 4.3: Proteins regulated by rapa in (A) MV4-11, (B) THP-1, as identified from the iTRAQ study

(A) MV4-11

Protein Name	Accession Number	Avg iTRAQ ratio * (115/114)
IMMT Isoform 3 of Mitochondrial inner membrane protein	IPI00470829	1.642439636
FEN1 Flap endonuclease 1	IPI00026215	1.521590774
SERPINB6 serine (or cysteine) proteinase inhibitor, clade B (ovalbumin), me	IPI00749398	1.385402845
MARCKS Myristoylated alanine-rich C-kinase substrate	IPI00219301	1.347752825
GSN Isoform 2 of Gelsolin precursor	IPI00646773	1.309421037
RPS27 40S ribosomal protein S27	IPI00513971	1.298915161
GPX1 glutathione peroxidase 1 isoform 2	IPI00398780	1.289065272
RAB5B Ras-related protein Rab-5B	IPI00017344	1.288308742
GNAI2 Galphai2 protein	IPI00465121	1.284414535
NARS 33 kDa protein	IPI00643900	1.241839687
AHSA1 Activator of 90 kDa heat shock protein ATPase homolog 1	IPI00030706	0.803412596
CYB5B Hypothetical protein DKFZp686M0619	IPI00641334	0.801761495
FUBP1 69 kDa protein	IPI00644386	0.801565742
HIST1H4G H4 histone family, member L	IPI00020618	0.793182978
CYC1 Cytochrome c1 heme protein, mitochondrial precursor	IPI00029264	0.79034019
UBQLN1 Isoform 1 of Ubiquilin-1	IPI00099550	0.783455955
XTP3TPA CDNA: FLJ21190 fis, clone CAS12333	IPI00012197	0.778186963
VASP Vasodilator-stimulated phosphoprotein	IPI00301058	0.77590876
BCLAF1 Isoform 2 of Bcl-2-associated transcription factor 1	IPI00413671	0.745287285
ATP5J ATP synthase, H+ transporting, mitochondrial F0 complex, subunit F6 i	IPI00456008	0.730890893
FAM10A5 Protein FAM10A5	IPI00168839	0.715983233
LSP1 50 kDa protein	IPI00554652	0.696898312
MTDH Protein LYRIC	IPI00328715	0.61510525
PRSS1 Trypsin-1 precursor	IPI00011694	0.554801634

(B) THP-1

Protein Name	Accession Number	Avg iTRAQ ratio * (117/116)
GSN Isoform 2 of Gelsolin precursor	IPI00646773	1.879134992
NUCKS1 Isoform 1 of Nuclear ubiquitous casein and cyclin-dependent kinases	IPI00022145	1.780701265
TMSB4X Thymosin beta-4	IPI00220828	1.551528455
MARCKS Myristoylated alanine-rich C-kinase substrate	IPI00219301	1.539001055
IMMT Isoform 3 of Mitochondrial inner membrane protein	IPI00470829	1.529509401
- 20 kDa protein	IPI00397828	1.519899869
COX17 11 kDa protein	IPI00796062	1.460314786
TKT Transketolase variant (Fragment)	IPI00788802	1.4074547
ATP6V1G1 Vacuolar ATP synthase subunit G 1	IPI00025285	1.390577733
TMSB10 Thymosin beta-10	IPI00220827	1.38045995
DPP7 Dipeptidyl-peptidase II variant (Fragment)	IPI00555697	1.359279234
RAB11A Ras-related protein Rab-11A	IPI00429190	1.316931985
CAPG Macrophage-capping protein	IPI00027341	1.304971846
TPP1 Isoform 3 of Tripeptidyl-peptidase 1 precursor	IPI00554538	1.304063292
GARS Glycyl-tRNA synthetase	IPI00783097	1.302716562
HCLS1 Hematopoietic lineage cell-specific protein	IPI00026156	1.297388367
DDB1 127 kDa protein	IPI00784120	1.29624959
VASP Vasodilator-stimulated phosphoprotein	IPI00301058	1.295950569
CSE1L Isoform 3 of Exportin-2	IPI00219994	1.295364442
ANXA5 Annexin A5	IPI00329801	1.293687483
SOD2 manganese superoxide dismutase isoform B precursor	IPI00607577	1.287521235
CA2 Carbonic anhydrase 2	IPI00218414	1.286970854
DBNL Isoform 2 of Drebrin-like protein	IPI00396437	1.275614289
CYC1 Cytochrome c1 heme protein, mitochondrial precursor	IPI00029264	1.262771413
PTPRC Protein tyrosine phosphatase, receptor type, C	IPI00306325	1.254756992
CD44 Isoform CD44 of CD44 antigen precursor	IPI00305064	1.247395793
SERPINB6 serine (or cysteine) proteinase inhibitor, clade B (ovalbumin), me	IPI00749398	1.243512064
NUCB2 Nucb2 splice variant	IPI00746961	1.24329333
AHNAK 313 kDa protein	IPI00555610	1.240159991
RPS21 Ribosomal protein S21	IPI00387084	0.80516512
EIF4G1 eukaryotic translation initiation factor 4 gamma, 1 isoform 2	IPI00384463	0.804817869
PRMT1 HRMT1L2 protein	IPI00215734	0.803250774
RPS29 ribosomal protein S29 isoform 2	IPI00639942	0.80307878
DUT Isoform DUT-N of Deoxyuridine 5'-triphosphate nucleotidohydrolase, mito	IPI00375015	0.800780657
TCP1 T-complex protein 1 subunit alpha	IPI00290566	0.800773139
EIF3S7 Eukaryotic translation initiation factor 3 subunit 7	IPI00006181	0.800393334
RPL27A 60S ribosomal protein L27a	IPI00456758	0.797303968
ACAT1 ACAT1 protein	IPI00440499	0.7970036
LOC732066;LOC730004 similar to 60S ribosomal protein L22	IPI00787417	0.796638334

MCM5 DNA replication licensing factor MCM5	IPI00018350	0.794889315
PCNA Proliferating cell nuclear antigen	IPI00021700	0.794596819
- 140 kDa protein	IPI00829641	0.793113132
YARS Tyrosyl-tRNA synthetase, cytoplasmic	IPI00007074	0.791402626
MCM6 DNA replication licensing factor MCM6	IPI00031517	0.790651597
LOC143244 similar to eukaryotic translation initiation factor 5A	IPI00218084	0.784781249
EIF4G3 Isoform 1 of Eukaryotic translation initiation factor 4 gamma 3	IPI00646377	0.783896456
KHSRP KH-type splicing regulatory protein	IPI00479786	0.782626467
S100A9 Protein S100-A9	IPI00027462	0.775027952
HSP90AB1 Heat shock protein HSP 90-beta	IPI00414676	0.768882981
EIF3S9 Isoform 2 of Eukaryotic translation initiation factor 3 subunit 9	IPI00719752	0.763462937
SSBP1 Single-stranded DNA-binding protein, mitochondrial precursor	IPI00029744	0.762615947
MCM3 DNA replication licensing factor MCM3	IPI00013214	0.757531381
IRF2BP2 interferon regulatory factor 2 binding protein 2 isoform B	IPI00646970	0.755749949
TRAP1 57 kDa protein	IPI00646055	0.753481402
DDOST dolichyl-diphosphooligosaccharide-protein glycosyltransferase precurs	IPI00297084	0.742141434
TOMM22 Mitochondrial import receptor subunit TOM22 homolog	IPI00024976	0.739267539
hCG_1983058 similar to eukaryotic translation elongation factor 1 beta 2	IPI00414723	0.738043368
RPS27 40S ribosomal protein S27	IPI00513971	0.737534975
CSTB Cystatin-B	IPI00021828	0.735548498
PA2G4 41 kDa protein	IPI00794875	0.734318582
CDC37 Hsp90 co-chaperone Cdc37	IPI00013122	0.730410383
HSPH1 Heat shock 105kDa/110kDa protein 1	IPI00513743	0.730409178
- Eukaryotic translation elongation factor 1 alpha-like 3	IPI00472724	0.727433009
COX6C Cytochrome c oxidase polypeptide VIc precursor	IPI00015972	0.720914829
G3BP2 Isoform B of Ras GTPase-activating protein-binding protein 2	IPI00179890	0.719958259
S100A8 Protein S100-A8	IPI00007047	0.719737255
NUDC 24 kDa protein	IPI00646767	0.712462089
SSR4 Protein	IPI00646864	0.697726854
HNRPF Heterogeneous nuclear ribonucleoprotein F	IPI00003881	0.69545242
EEF1G 50 kDa protein	IPI00747497	0.66634367
hCG_1644239 similar to ribosomal protein L31	IPI00243278	0.609338211
SAE1 33 kDa protein	IPI00640965	0.592283434
LYZ Lysozyme C precursor	IPI00019038	0.589455535

The proteins listed above cleared the fold-change cut-off of +/- 1.24 with a confidence of more than 95%.

4.2.4 Rapa regulates a variety of pathways in AML

Ingenuity Pathway Analysis software was employed to analyse the microarray and iTRAQ data and hence unearth the variety of canonical pathways regulated by rapa in AML. In the MV4-11 microarray study, 542 genes mapped to the Ingenuity Knowledge Database and 407 genes were deemed network eligible, while in the iTRAQ analysis, 24 proteins mapped and 10 were found to be network eligible. Among the genes showing regulation by rapa in the THP-1 cell line, in the microarray study, 372 mapped to the Ingenuity Knowledge database and 279 genes were classified as network eligible, while in the iTRAQ study for this cell line, 66 proteins mapped to the database and 27 of them were network eligible.

The biological functions regulated by the drug are a reflection on the key processes targeted by the drug. The major functions modulated hence by the drug are cancer, cell cycle, cellular growth and proliferation and cell death (Table 4.4).

Table 4.4: Biological functions regulated by rapa in AML

Functions	Number of Molecules regulated		Significance of the pathway: p-value score	
	# of genes-from microarray	# of proteins-from iTRAQ	Microarray	iTRAQ
Cancer	215	25	5.02E-09-8.24E-03	1.87E-03-2.95E-02
Cellular Growth and Proliferation	204	6	1.64E-05-7.78E-03	8.14E-03-2.69E-02
Cell death	162	8	1.16E-06-8.24E-03	1.87E-03-2.95E-02
Gene Expression	129	3	2.78E-04-8.08E-03	6.3E-03-8.14E-03
Cellular development	100	8	2.18E-05-7.78E-03	1.27E-03-2.16E-02
Haematological system development and function	93	9	7.68E-07-8.24E-03	2.12E-03-2.69E-02
Cell-To-Cell Signalling and Interaction	92	6	5.19E-07-8.24E-03	4.27E-05-2.56E-02
Immune and lymphatic system development and function	85	5	6.03E-07-8.24E-03	2.72E-03-2.69E-02
Immune response	83	6	1.78E-05-8.08E-03	2.72E-03-2.88E-02
Inflammatory Disease	83	2	8.52E-05-7.19E-03	3.17E-04-2.95E-02
Tissue morphology	81	8	2.59E-04-7.19E-03	5.21E-05-2.69E-02
Cell Cycle	81	4	1.52E-03-8.13E-03	2.72E-03-2.95E-02
Cell morphology	69	10	8.44E-05-8.14E-03	1.25E-04-2.92E-02

Comparison of data from microarray and iTRAQ study. The microarray data and iTRAQ data of both the cell lines were merged and compared to obtain the overall picture.

Canonical pathways are well studied established pathways. They include signalling as well as metabolic pathways. The most important and relevant pathways regulated by rapa in AML as identified from the microarray study include IGF-1 signalling, PI3K/Akt, insulin receptor signalling, cell cycle: G1/S checkpoint regulation, death receptor signalling, hypoxia signalling, FGF signalling and protein ubiquitination (Table 4.5).

Networks are key regulatory interactions between genes/proteins. Although they do not constitute a standardised pathway, they influence key functions. The 50nM dosage of rapa regulated 42 networks in MV4-11 and the 500nM dosage modulated 41 networks. In the case of THP-1 cells, 30 networks were regulated.

Table 4.5: Key canonical pathways regulated by rapa in AML

Pathway	Sample	Genes regulated (fold change)
Cell cycle G1/S arrest	MV4-11- Rapa 50nM	**ATM** (1.744), RBL2 (1.833), ***SKP2*** (-2.507), SUV39H1 (-1.557)
	MV4-11- Rapa 500nM	**ATM** (1.5), E2F3 (1.626), ***SKP2*** (-2.063)
	THP-1- Rapa 500nM	CDK4 (-1.622), ***SKP2*** (-1.594)
Death receptor signalling	MV4-11- Rapa 50nM	**CFLAR** (1.676), **HTRA2** (-1.648), *MAP3K5* (1.544), **TNF** (2.606), **TNFSF10** (-2.078)
	MV4-11- Rapa 500nM	**CFLAR** (1.663), **HTRA2** (-1.530), **TNF** (3.066), **TNFSF10** (-2.496)
	THP-1- Rapa 500nM	*MAP3K5* (1.741), TNFRSF1B (1.947)
IGF-1 signaling	MV4-11- Rapa 50nM	BAD (-1.563), **FOXO3** (1.658), **IGFBP2** (-3.024), **IGFBP7** (-1.580)
	MV4-11- Rapa 500nM	FOS (1.781), **FOXO3** (1.674), **IGFBP2** (-2.419), **IGFBP7** (-1.533)
	THP-1- Rapa 500nM	ATF4 (-1.619), HGF (-1.745), MAP2K3 (1.662), MAP3K5 (1.741)
Insulin receptor signalling	MV4-11- Rapa 50nM	*BAD* (-1.563), CRK (-1.528), **FOXO3** (1.658), INPPL1 (-1.617), **PPP1R12A** (1.638), **PPP1R14B** (-1.767), **VAMP2** (2.237)
	MV4-11- Rapa 500nM	**FOXO3** (1.674), *FOXO4* (-1.649), **PPP1R12A** (1.533), **PPP1R14B** (-1.592), **VAMP2** (2.075)
	THP-1- Rapa 500nM	*BAD* (-1.583), EIF2B3 (-1.671), FOXO1 (-2.100), *FOXO4* (-2.809), GRB10 (-1.781)
FGF signalling	MV4-11- Rapa 50nM	***ATF4*** (-1.585), **CREB3** (-1.873), CRK (-1.528), *MAP3K5* (1.544)
	MV4-11- Rapa 500nM	***ATF4*** (-1.628), **CREB3** (-1.833)
	THP-1- Rapa 500nM	***ATF4*** (-1.619), HGF (-1.745), MAP2K3 (1.662), *MAP3K5* (1.741)
Protein ubiquitination	MV4-11- Rapa 50nM	**PSMC2** (1.566), PSMD3 (-1.605), ***SKP2*** (-2.507), UBE2E3 (-1.501), UBE2M (-1.676), **USP1** (1.839), **USP12** (1.780), USP15 (1.913)
	MV4-11- Rapa 500nM	**PSMC2** (1.802), ***SKP2*** (-2.063), **USP1** (1.848), **USP12** (1.704)

	THP-1- Rapa 500nM	HLA-C (1.753), HLA-G (2.032), PSMC3 (-1.573), ***SKP2*** (-1.594), UBE2I (-1.503)
Hypoxia signalling	MV4-11- Rapa 50nM	***ATF4*** (-1.585), **ATM** (1.744), **CREB3** (-1.873), UBE2E3 (-1.501), UBE2M (-1.676)
	MV4-11- Rapa 500nM	***ATF4*** (-1.628), **ATM** (1.500), **CREB3** (-1.833)
	THP-1- Rapa 500nM	***ATF4*** (-1.619), UBE2I (-1.503), VEGFA (-1.602)
Selenoamino acid metabolism	MV4-11- Rapa 50nM	**AHCYL1** (1.517), *CTH* (-2.734), FTSJ1 (-1.508), ***PAPSS2*** (-20.990), **SEPHS1** (-1.730)
	MV4-11- Rapa 500nM	**AHCYL1** (1.763), ***PAPSS2*** (-8.694), **SEPHS1** (-1.543)
	THP-1- Rapa 500nM	*CTH* (-1.636), ***PAPSS2*** (-2.466), SCLY (-1.877)

Some of the interesting canonical pathways modulated by rapa and the genes regulated in each pathway, as identified from the microarray study, are listed. The genes highlighted in ***bold italics*** indicate ones that are commonly regulated in all the three samples, while the ones in **bold** represent the genes which are common to both the MV4-11 samples. The genes in *italics* are the ones common to THP-1 and one of the MV4-11 samples.

4.2.5 Validation of the microarray data by quantitative real-time PCR

The change in expression of a chosen set of genes was quantified by real-time PCR. The selected genes were key members of canonical pathways and/or networks. These genes were found to be significantly regulated by rapa in the AML samples and the direction and level of regulation could help explain the observed anti-proliferative effect of rapa. Real-time PCR analysis was performed using the SYBR green technology and the fold-changes were calculated hence. The fold-change values obtained from this study were compared with the levels indicated by the microarray (Table 4.6). Linear regression analysis showed very good correlation between the microarray and real-time PCR data with a R^2 value of 0.8575 (Figure 4.4). The high correlation corroborates the sensitivity of the approach and the veracity of the data.

Table 4.6: Real-Time PCR validation of microarray data

Gene	Cell line	Drug concentration	Microarray fold change	Real time PCR fold change	Pathways involved	Networks involved
FOS	MV4-11	50nM	1.32	1.0795	IGF-1, ERK/MAPK, Acute Phase Response Signaling, TGF-β Signaling, PPAR Signaling	Network- 3- THP-1
		500nM	1.77	1.63		
	THP-1	500nM	2.65	1.975		
FRAT1	MV4-11	50nM	2.14	1.4245	Wnt/β-catenin Signaling	Network 5 - microarray THP-1, Network 7 - microarray MV4-11 50nM
		500nM	2.03	2.215		
	THP-1	500nM	1.83	1.9615		
IGFBP2	MV4-11	50nM	-3.09	-3.735	IGF-1 Signaling	Network 2, 9 – microarray MV4-11 50nM
		500nM	-2.47	-2.16		
	THP-1	500nM	1.32	-1.62		
SKP2	MV4-11	50nM	-2.51	-2.7	Cell Cycle: G1/S Checkpoint Regulation; Cell Cycle: G2/M DNA Damage Checkpoint Regulation; Protein Ubiquitination	Network 1 - microarray THP-1, Network 5 - microarray MV4-11
		500nM	-2.07	-2.19		
	THP-1	500nM	-1.61	-1.715		
TGFβ1	MV4-11	50nM	-2.36	-2.755	Cell Cycle: G1/S Checkpoint Regulation, p38 MAPK Signaling, PPARα/RXRα Activation, TGF-β Signaling, Wnt/β-catenin Signaling	Network 9 - MV4-11 50nM, Network 11 THP-1
		500nM	-2.5	-2.36		
	THP-1	500nM	1.2	-1.215		
IL8Rβ	MV4-11	50nM	-2.29	-2.095	Nil	Network 3, 22 - microarray MV4-11 50nM, Network 11 - THP-1
		500nM	-1.58	-2.235		
	THP-1	500nM	-1.08	-1.195		
TIEG	MV4-11	50nM	2.57	1.325	Nil	Network 5, 9 microarray MV4-11 50nM, Network 4 microarray THP-1 500nM
		500nM	2.5	1.66		
	THP-1	500nM	1.7	1.055		

TNFSF7	MV4-11	50nM	-1.75	-2.865	Nil	Network 1 microarray MV4-11 50nM, Network 4 microarray THP-1
		500nM	- 2.02	-2.33		
	THP-1	500nM	-1.54	-1.475		

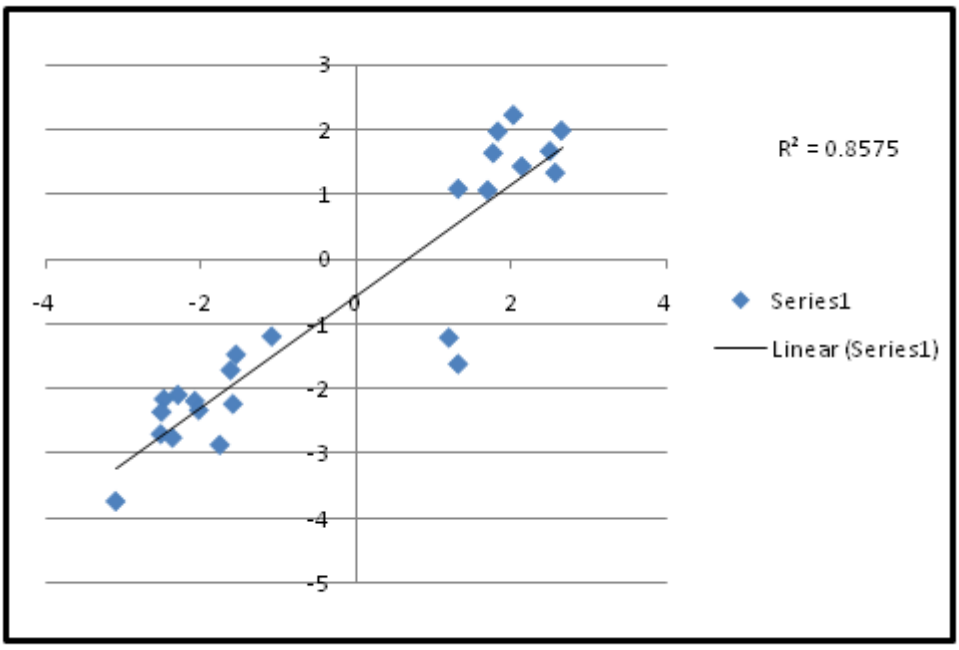

Figure 4.4: Linear regression analysis of fold-changes of regulated genes identified from microarray and real-time PCR studies

Linear regression indicated an R^2 value of 0.8575, which indicates high correlation between the microarray and real-time data.

4.2.6 Rapa causes G1 arrest in AML

Cell cycle: G1/S checkpoint regulation is one of the major pathways found regulated in both the cell lines. Previous studies have shown that G1 arrest is a major mechanism of growth and proliferation arrest employed by rapa. The flow cytometry analysis revealed that upon treatment with rapa, the number of cells in the G1 phase increased with time and peaked at 16 h in both MV4-11 and THP-1 (Figure 4.5). There was a gradual decline in the percentage of G1 cells beyond 24 h suggesting a time dependent cytostatic effect of rapa on AML cells.

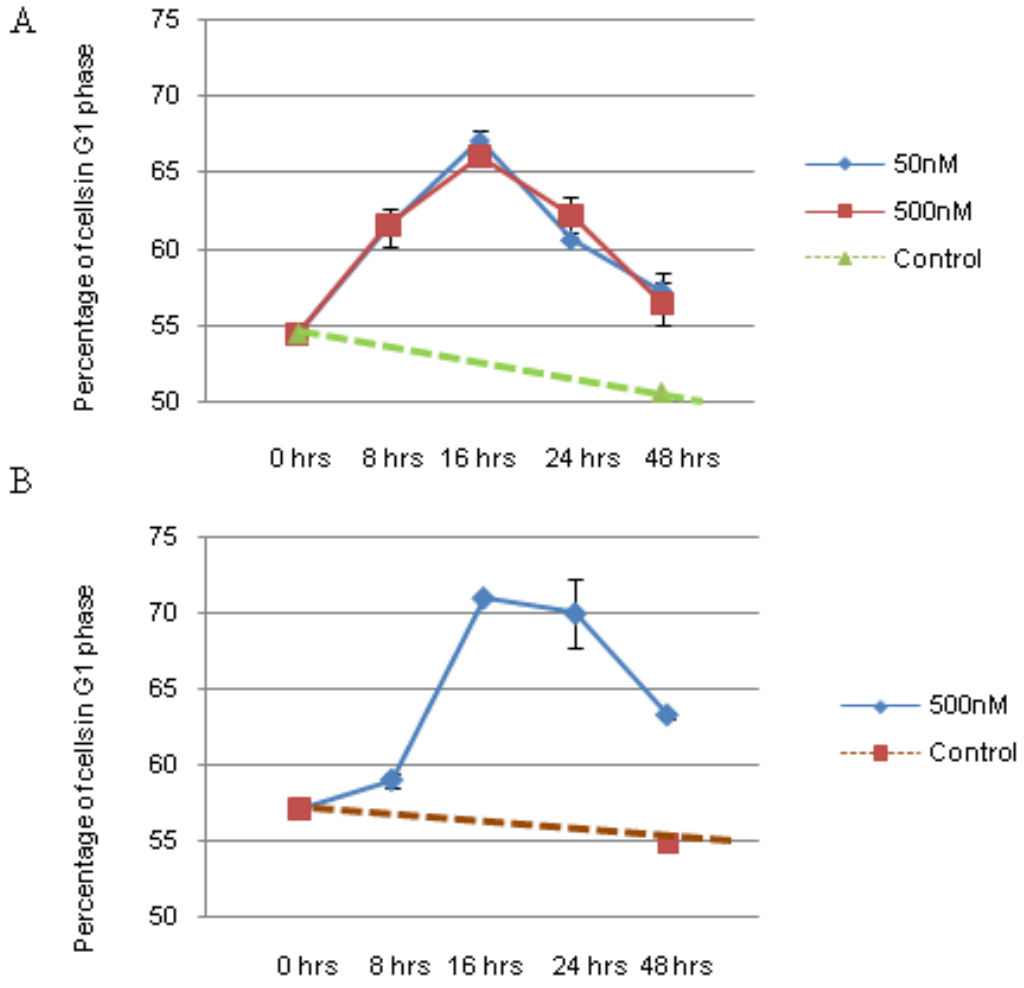

Figure 4.5: Rapa induces time dependent G1 arrest in (a) MV4-11 (b) THP-1

Maximum accumulation of cells in G1 phase was observed at 16 h in both cases. The control was grown for 48 h without drug treatment.

4.2.7 Analysis of the change in the level of cell cycle proteins upon rapa treatment

Dissection of the cellular events orchestrated by rapa to cause such a time dependent G1 arrest was performed using western blotting analysis of the proteins involved in cell cycle: G1/S progression. We found a time dependent decrease in the levels of the Cdk 2 and Cdk 4 and an increase in p27 levels upon rapa treatment in both MV4-11 and THP-1 cells (Figure 4.6). The Cdk 2 and Cdk 4 levels show maximum repression at 16h. The Cdks (cyclin dependent kinases) are essential for the progression of the cell cycle. Hence cell cycle arrest is the direct consequence of their repression. Rapa treatment was also observed to induce up-regulation of the p27 protein, which is a Cdk inhibitor. Thus the decrease in the Cdk levels and increase in the p27 levels act in tandem to cause G1 arrest in AML cells.

A

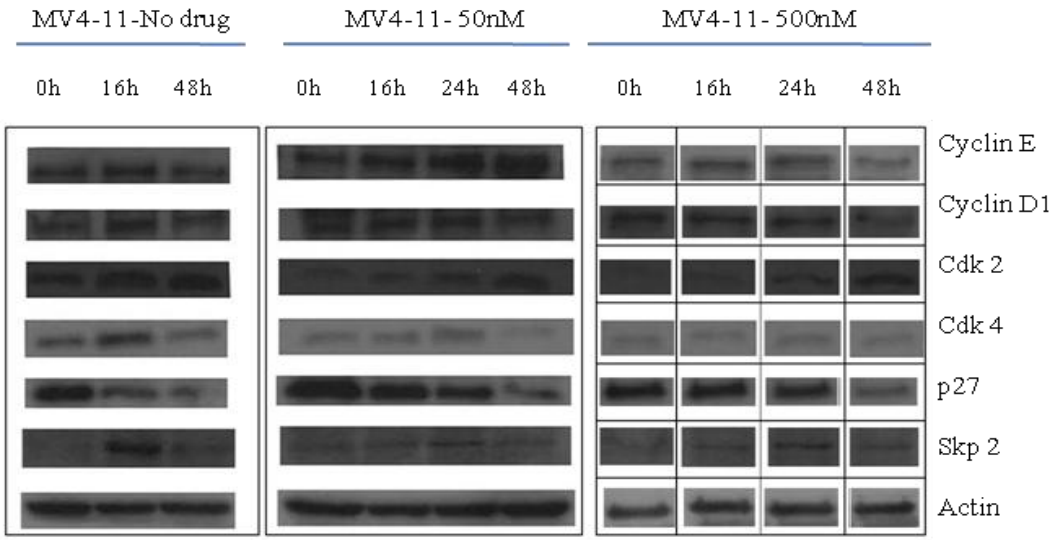
MV4-11-No drug
MV4-11- 50nM
MV4-11- 500nM
0h 16h 48h
0h 16h 24h 48h
0h 16h 24h 48h
Cyclin E
Cyclin D1
Cdk 2
Cdk 4
p27
Skp 2
Actin

B

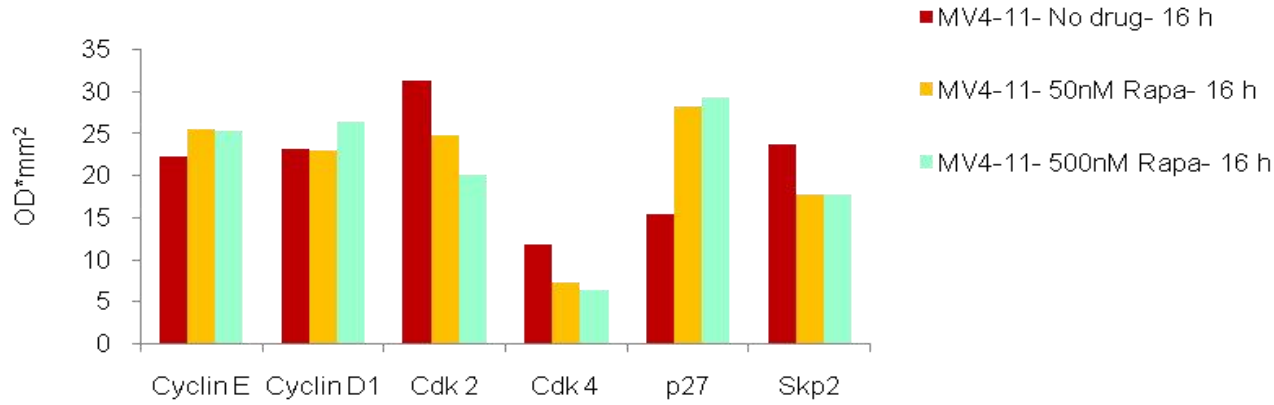
OD*mm2
35
30
25
20
15
10
5
0
Cyclin E
Cyclin D1
Cdk 2
Cdk 4
p27
Skp2
MV4-11- No drug- 16 h
MV4-11- 50nM Rapa- 16 h
MV4-11- 500nM Rapa- 16 h

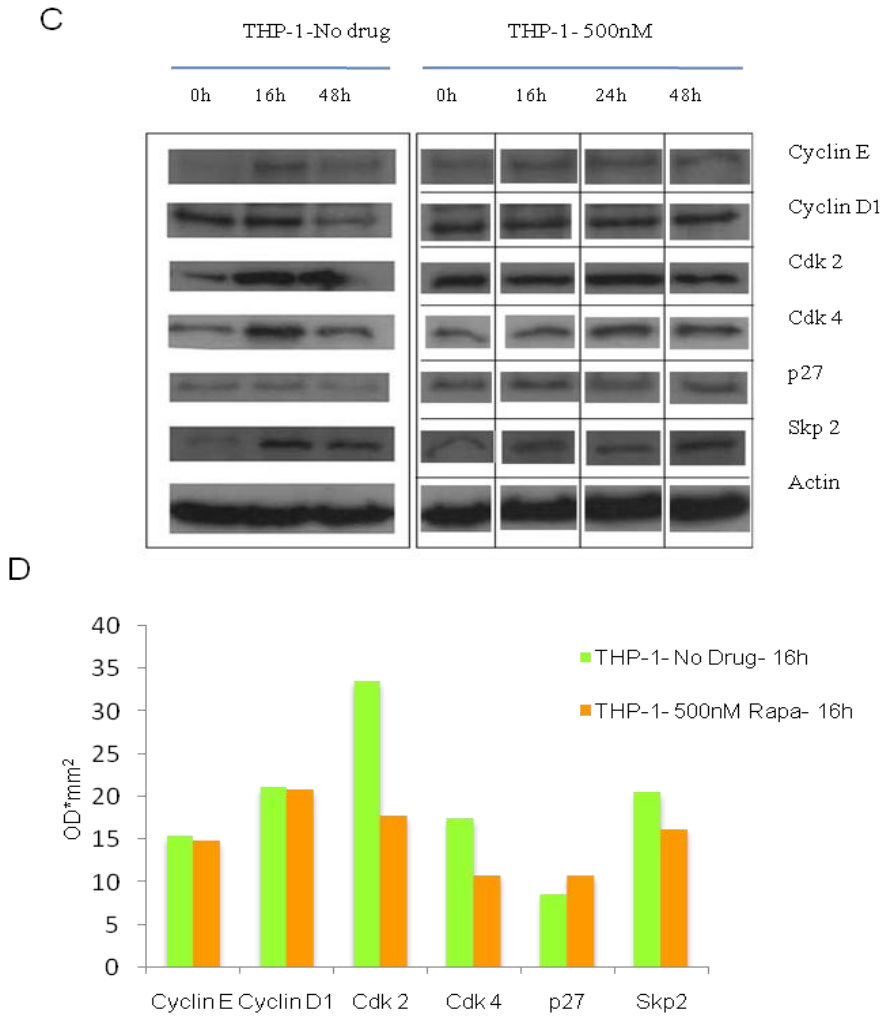

Figure 4.6: Western blots of cell cycle proteins regulated by rapa

Immunoblotting of cell cycle related proteins was done for lysates from both the cell lines (A) MV4-11 and (C) THP-1. The protein levels were compared by densitometry (B) MV4-11 and (D) THP-1.

Interestingly, we found protein ubiquitination among the pathways regulated by rapa. Concurrently, we also observed a down-regulation of Skp2 protein in the microarray study, which was confirmed by real-time PCR (Table 4.6).

4.2.8 Rapa represses Skp2 and hence up-regulates p27 leading to G1 arrest

Skp2 is the specific substrate-recognition subunit of a SCF type ubiquitin ligase complex which is responsible for the ubiquitin-mediated proteolysis of p27 (Yang, et al., 2002; Hershko, et al., 2001). Thus the down-regulation of Skp2, observed in the microarray study, was very intriguing. The observation was validated using western blot analysis, which indicated a down-regulation of Skp2 which correlated with the increased p27 levels and decreased levels of Cdk 2 and Cdk 4. Such a correlation is very significant as the previous reports establish the link between p27 and its regulation by Skp2.

This finding establishes that rapa induces G1 arrest in AML cells through the repression of Skp2 and hence up-regulation of p27, which subsequently causes down-regulation of Cdk 2 and Cdk 4. Hence the results indicate that such a regulation in AML forms the crux of the anti-proliferative activity of rapa.

4.2.9 Confirmation of mTOR arrest by rapa

mTOR has been known to be the prime target of rapa. This is well established and has been discussed at length in Chapter 1, Section 1.4.4. We set about to confirm this effect of rapa on our AML models. As the Figure 4.7 shows, rapa had a potent inhibitory effect on the phosphorylation of 4EBP-1, a key downstream effector of the mTOR pathway.

4.2.10 Rapa regulates the IGF-1 pathway and inhibits IGFBP2- a novel discovery

A number of genes and proteins belonging to the IGF-1 signalling pathway and insulin receptor signalling pathway were found to be significantly regulated by rapa. The microarray and real-time PCR data indicated down-regulation of IGFBP2, an important member of the IGF-1 pathway (Table 4.6). We analysed the protein levels of IGFBP2 and as the western blot indicates, rapa down-regulates IGFBP2 in both the MV4-11 and THP-1 cells (Figure 4.7). This is a very novel and interesting finding as there have been absolutely no reports about such an inhibitory effect of rapa on IGF-1 signalling pathway and IGFBP2 in AML, which lies upstream of mTOR pathway.

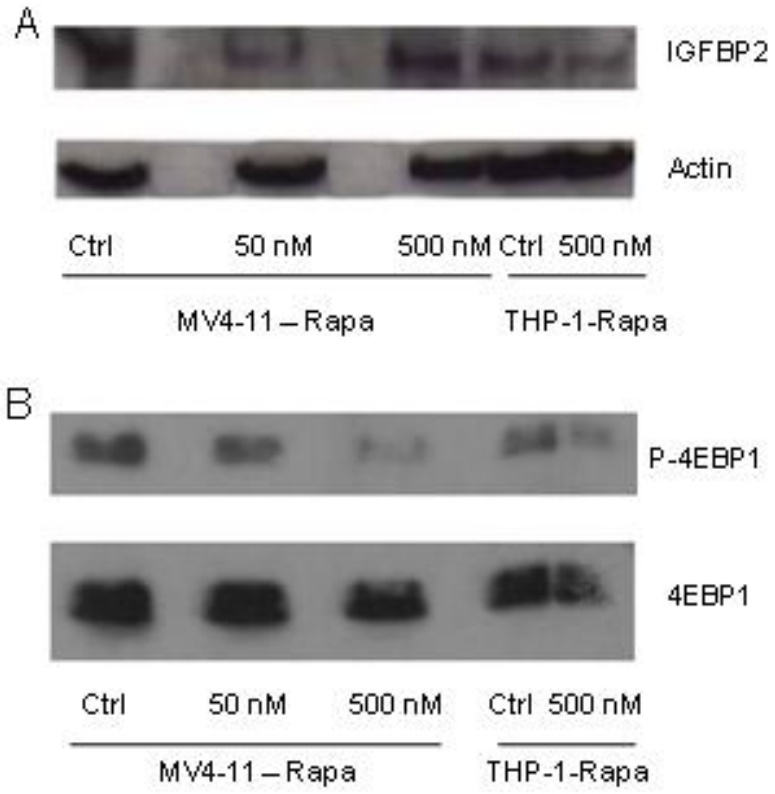

Figure 4.7: Rapa inhibits IGFBP2 and mTOR

(A) Rapa down-regulates expression of IGFBP2 (B) Rapamycin is an mTOR inhibitor. Actin was used as control to compare the IGFBP2 expression change, while unphosphorylated 4EBP-1 served as the control for its phosphorylated counterpart.

4.2.11 Rapamycin does not induce apoptosis in AML

The Annexin V-FITC staining and Caspase-Glo® 3/7 assay results indicate that rapa did not induce apoptosis in AML (Figure 4.8). The Annexin-V-FITC study was conducted at a 48 h time point. The caspase levels were assayed at 12h and 20h time points to probe for early onset of apoptosis. Both the MV4-11 and THP-1 cells did not exhibit significant increase in the percentage of apoptotic cells upon rapa treatment in any of the time points studied. Hence apoptosis does not play a major role in the anti-proliferative effect of rapa. It can thus be concluded that rapa is a cytostatic drug.

(i) Annexin V-FITC assay

MV4-11 Control

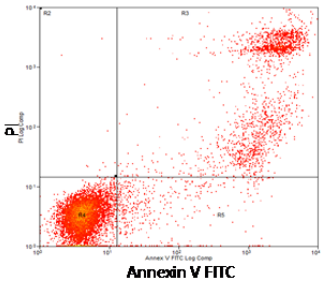

Population	Percentage
R2	0.1
R3	18.86
R4	77.05
R5	3.99

MV4-11 50nM

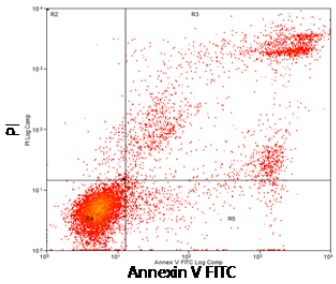

Population	Percentage
R2	1.35
R3	21.87
R4	70.74
R5	6.04

MV4-11 500nM

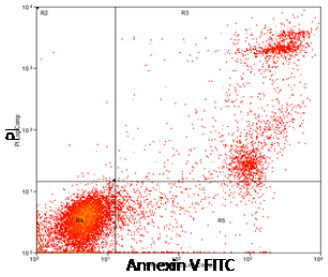

Population	Percentage
R2	0.20
R3	18.81
R4	74.02
R5	6.97

THP-1 Control

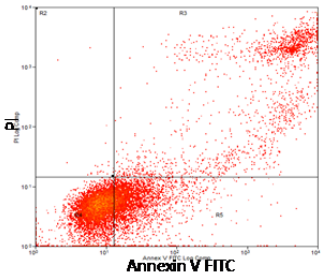

Population	Percentage
R2	0.21
R3	14.88
R4	56.37
R5	28.54

THP-1 500nM

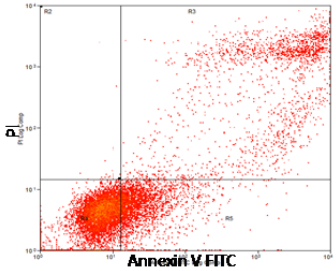

Population	Percentage
R2	0.17
R3	15.93
R4	60.95
R5	22.94

ii) Caspase 3/7 assay

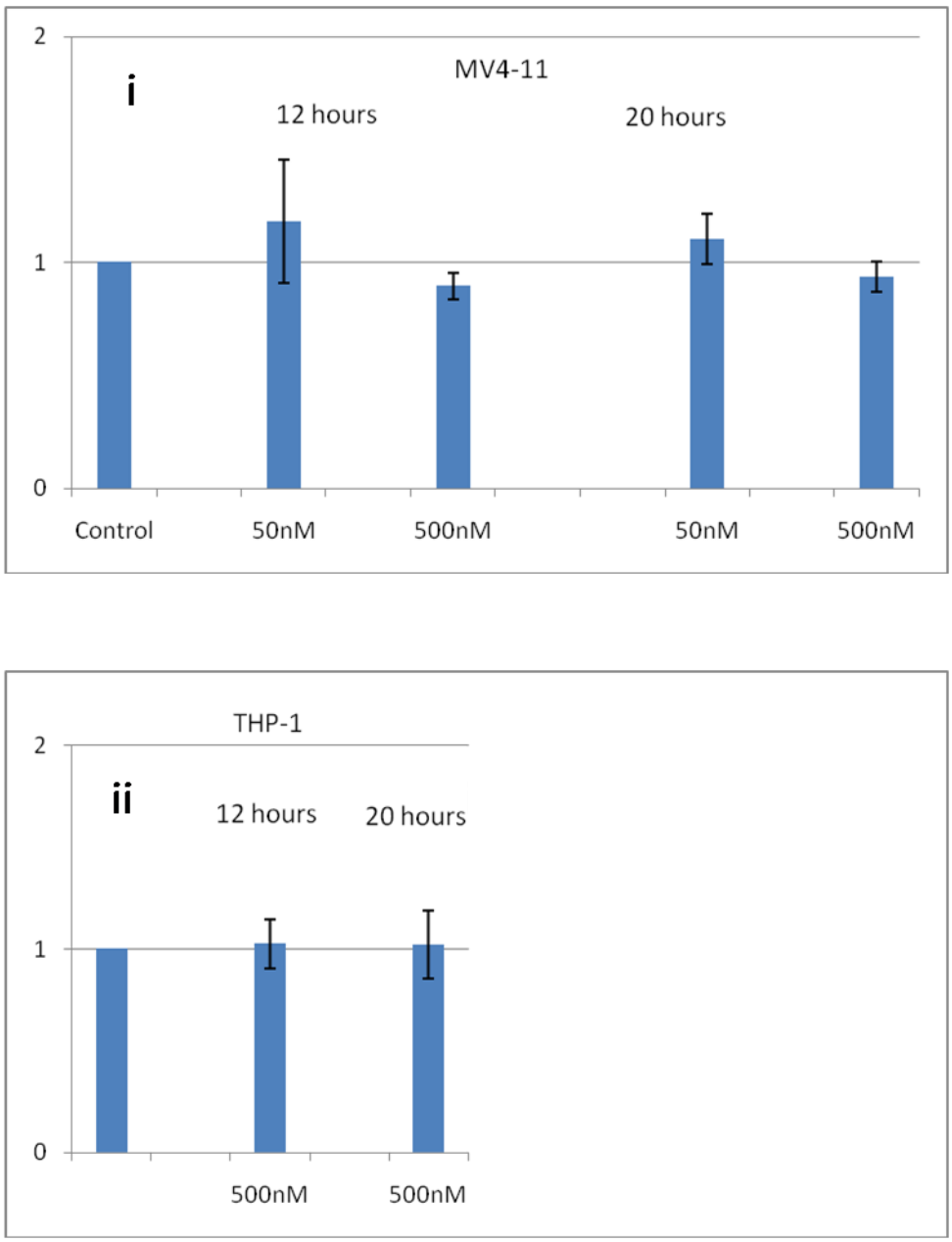

Figure 4.8: Assaying for apoptosis using (a) Annexin-V-FITC (b) Caspase 3/7 assay

Both MV4-11 and THP-1 cells were subjected to rapa treatment and apoptosis was assayed using two different techniques. (A) Cells treated with rapa for 48 h were assayed by Annexin V- FITC method using a flow cytometer. (B) Cells subjected to 12 h and 20 h treatments were assayed for apoptosis using the Caspase-Glo® Reagent. Rapa did not significantly induce apoptosis in both MV4-11 and THP-1 cells.

4.3 Discussion

In this study, we have shown that the potent inhibitory effect of rapa on a variety of AML cell lines is the consequence of the regulation of a multitude of pathways and that mTOR is not its only target as thought of before.

4.3.1 Advantages of the approach

In order to study the mechanism of action of rapa in its totality, we decided that it would be more feasible to adopt a top-down systems biology approach. The use of the microarray technology to study the mode of drug action is a well established high-throughput and robust approach. iTRAQ, though a relatively new technology, has proven to be a useful tool for proteomic research as it captures the relative protein levels and can label multiple samples simultaneously. The Ingenuity Pathway Analysis (IPA) is an application that enables the mining and subsequent discovery of molecular interaction networks in expression data. It is supported by a large Ingenuity Pathway Analysis Knowledge Base- a curated database. The combination of microarray and iTRAQ techniques yielded profiling data, which when analysed with IPA divulged vital clues about the pathways and networks modulated by rapa in AML.

In this era of 'omics', the fact that such a comprehensive profile of the cellular events can be obtained using a high-throughput technologies such as microarrays is a welcome boon to researchers. The efficacy and advantages of such an approach is well established by number of studies (Clarke, et al., 2004; Comuzzi and Sadar, 2006; Hattori, et al., 2006; Qian, et al., 2008).

Functional characterisation of individual pathways is essential to elucidate the intricate role of each molecule involved in the process. Hence an optimal strategy to study the mechanism of action of drugs should obtain a snapshot of the cellular events coordinated by the drug using a

high-throughput approach and use these clues to examine individual pathways in greater detail.

The IPA analysis of the microarray and proteomics data identified a number of canonical pathways to be regulated by rapa treatment as listed in Table 4.5. The power of high-throughput technologies is emphasised by the fact that such a diverse repertoire of regulated pathways and the genes which constitute them could be mapped out using this approach, which would otherwise be impossible.

4.3.2 The cell cycle: G1/S checkpoint regulation pathway

The cell cycle arrest is an interesting target pathway regulated by rapa treatment. Previous studies have shown that rapa induced G1 arrest (Récher, et al., 2005). A number of genes involved in cell cycle checkpoint control were regulated in the microarray study. Additionally, both the iTRAQ and microarray data showed that cell cycle was a major biological function targeted by the drug.

This prompted us to hypothesise that cell cycle arrest might be a prominent feature of the anti-proliferative property of rapa. In accordance to our thought process the flow cytometry based propidium iodide staining results showed that rapa indeed arrested the MV4-11 and THP-1 cells in the G1 phase of the cell cycle. We also observed that such an effect is time dependent. The peak effect occurred at 16h. This is a very interesting observation. Our MTS assay results indicate a 50% killing effect of rapa at 48h. Thus we can conclude that the arrest of AML cells occurs at 16h and the effect manifests at 48h, wherein we observe the reduced cell numbers.

In order to confirm our observation we analysed the levels of some of the important proteins involved in G1 checkpoint regulation. These include certain key components such as the cyclins, Cyclin dependent kinases (Cdks) and Cdk inhibitors as indicated in the Figure 4.9.

Cdks are a family of serine /threonine protein kinases that are activated at specific points of the cell cycle. The Cdk levels remain constant during the cell cycle unlike that of their cyclin counterparts. Cyclin protein levels rise and fall during the cell cycle. Thus they periodically activate the Cdks.

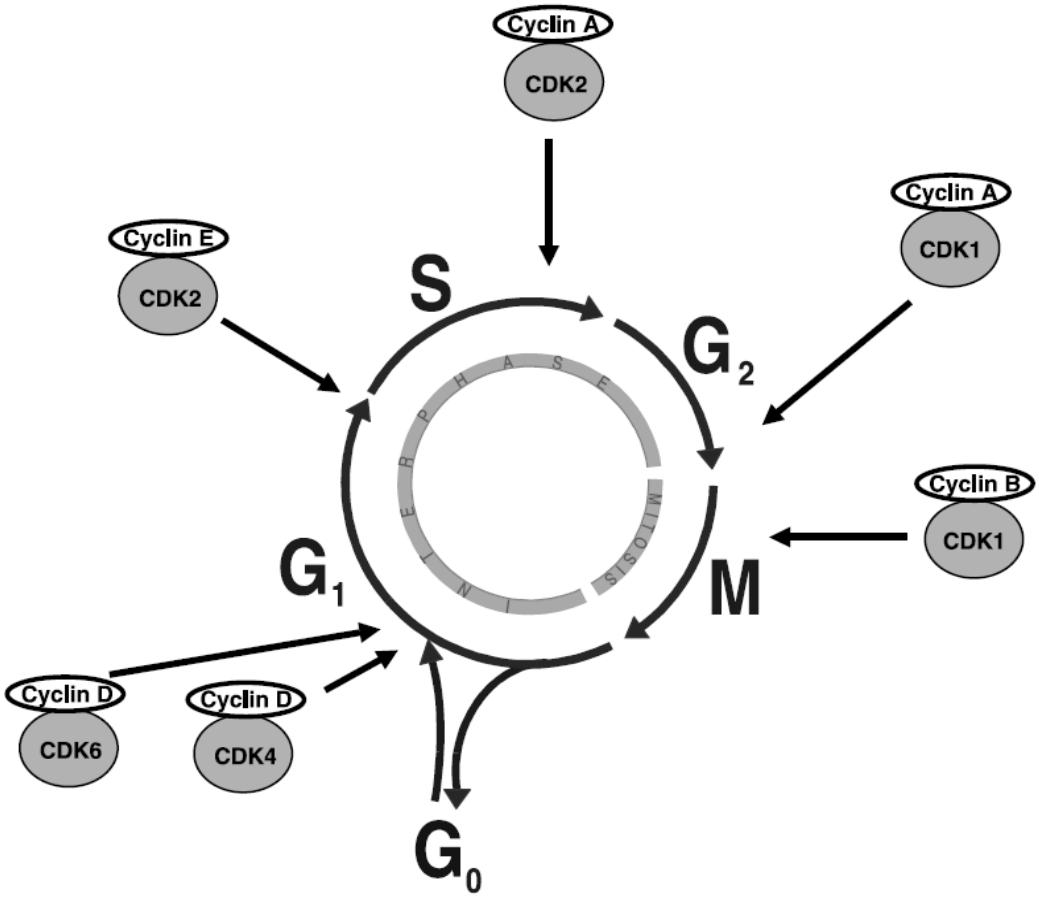

Figure 4.9: Stages of the cell cycle

The cyclins and Cdks work in combination with each other. They tend to form specific pairs.

Progression through the cell cycle and cellular proliferation is under the control of the cyclin-cdk complexes. Each of these cyclin/cdk complexes is activated at a specific point during G1 and has a specific set of substrates. The stage of activity of the Cyclin-Cdk complex is listed in Table 4.7. Thus the Cyclin E- Cdk 2 and Cyclin D- Cdk 4 complexes were chosen as indicators of G1 arrest.

Table 4.7: Cyclin-Cdk protein complexes and their stage of activity

Cdk	**Cyclin**	**Cell cycle phase activity**
Cdk 4	Cyclin D1, D2, D3	G1 phase
Cdk 6	Cyclin D1, D2, D3	G1 phase
Cdk 2	Cyclin E	G1/S phase transition
Cdk 2	Cyclin A	S phase
Cdk 1	Cyclin A	G2/M phase transition
Cdk 1	Cyclin B	Mitosis
Cdk 7	Cyclin H	CAK, all cell cycle phases

The cyclin-Cdk activity can be countered by molecules called Cdk inhibitors (CDKI). The Cip-Kip family of CDKI includes members such as p21 and p27. These inhibitors inactivate Cdk-cyclin complexes. They are active against the G1 Cdk-cyclin complexes, and the Cdk1-cyclin B complexes. The increase in CDKI levels leads to cell cycle arrest at the G1 phase. Hence we chose to study the levels of p27, a quintessential CDKI.

The experiment was conducted on a time-course basis. The idea was to understand the dynamics of cell cycle regulation. Hence studying the cell cycle distribution of the cells over a series of time points would provide a lucid idea about the progression of the cells through the various stages and the effects of rapa on such an event. The PI staining of the cells made it very clear that time is a key player in the G1 arrest exerted by rapa. Hence the western blots were done on protein samples extracted from rapa treated samples extracted at various time points. The protein levels were in complete accordance with the flow cytometry results. The Cdk 2 and Cdk 4 showed maximum down-regulation compared to their control counterparts at 16h. The levels of p27 also showed up-regulation at the same time point as expected. Thus the dynamics of the cell cycle regulation by rapa are explained by the expression pattern of the key determinants.

4.3.3 Linking Protein Ubiquitination to G1 arrest through Skp2 regulation

In our high-throughput study we observed that protein ubiquitination was a major pathway regulated by rapa. This pathway is responsible for the targeted degradation of proteins and the control of protein turnover. The IPA analysis of the microarray data suggested that a number of genes belonging to this pathway showed significant regulation by rapa. Out of these genes, the F-box protein S-phase kinase-associated protein 2 (Skp2) is of particular interest.

Progression through the cell cycle is orchestrated mainly by ubiquitin-mediated proteolysis of cyclins and CDKI. Ubiquitin ligases are special enzymes which function in the last step of a three-enzyme cascade, leading to covalent tagging of ubiquitin or polyubiquitin chains to Lys

residues of substrates. Two types of ubiquitin ligases, SCF complexes and the anaphase-promoting complex/cyclosome (APC/C), ubiquitynate many cell-cycle regulators and are essential for cell-cycle progression. SCF-type ubiquitin ligases are composed of three invariable subunits, Skp1, Cul1 and Rbx1, and one of about 70 different F‑box proteins (Ecker and Hengst, 2009). One such important F-box protein is Skp2.

Among the various substrates of Skp2, p27 is the foremost. Overexpression of Skp2 leads to increased proteolysis of p27 causing deregulation of the cell cycle checkpoint (Hershko, et al., 2001). Skp2 is a proto-oncogene in this respect (Ecker and Hengst, 2009). Skp2 has been found to be up-regulated in several cancers (Kawakami, et al., 2007; Yang, et al., 2002). Increase in Skp2 levels and subsequent loss of p27 have been associated with reduced recurrence free survival in prostate cancer (Yang, et al., 2002). An elevated Skp2 has been observed and implicated in AML progression too (Min, et al., 2004).

In our microarray study we observed that Skp2 is down-regulated by rapa at the transcriptional level in both the cell lines at all the dosages. Real-time PCR analysis validated this result. Western blot analysis showed that the Skp2 protein was indeed down-regulated by rapa especially at 16h. This is a remarkable observation as this paves the way for explaining the mechanism of cell cycle arrest orchestrated by rapa in AML. This is a completely novel effect of rapa.

Recent reports suggest that Akt mediates the regulation of Skp2 in cancer cells (Ecker and Hengst, 2009; Gao, et al., 2009). Cancer cells which usually have elevated Akt levels have increased Skp2 activity, as Akt protects Skp2 from degradation. Rapa is a known inhibitor of PI3K/Akt pathway. Thus we can conclude that this effect of rapa has far reaching effects on the protein ubiquitination pathway. The decrease in Akt levels by rapa treatment leads to reduction of Skp2 protein. Thus there is an elevation in the levels of p27, as they are not targeted for proteolysis by Skp2. The increase in p27 levels in turn leads to G1 arrest and accumulation of cells in this phase of the cell cycle.

Hence the down-regulation of Skp2 by rapa is a key determinant of the cell cycle arrest that it mediates in AML.

4.3.4 The IGF-1 signalling pathway modulation and down-regulation of IGFBP2

The growth and proliferation of cells are highly dependent on the availability of nutrients and growth factors. In this respect it is important to note that pathways such as FGF signalling and IGF-1 signalling were affected by rapa treatment. This suggests that the modulation of these pathways have a causal effect on the cell cycle arrest induced by rapa.

IGF-1 pathway is a very important signalling pathway which lies upstream of PI3K/Akt and mTOR. This pathway was one of the highly regulated pathways in both the cell lines studied. It has been implicated in a number of tumours including breast, colon and prostate cancer prompting the development of anti-IGF-IR therapy to combat cancer (Mitsiades, et al., 2004; Yasui, et al., 2006).

Insulin like growth factor binding proteins (IGFBPs) are key members of the IGF-1 pathway which modulate the availability and biological action of the IGFs (Mohnike, et al., 1996). Among this class of six proteins, IGFBP2 is of particular interest since elevated levels of IGFBP2 have been observed in leukemia patients (Mohnike, et al., 1996), and are associated with increased relapse risk and negative prognosis (Dawczynski, et al., 2006). The elevated levels of IGFBP2 are increasingly being associated with AML progression. Interestingly, in our study we found that rapa down-regulates the expression of IGFBP2 in both MV4-11 and THP-1 cells at the transcriptional (microarray, real-time PCR) and translational (western blot) levels. We hypothesize that the repression of IGFBP2 levels strongly contributes to the anti-leukemic activity of rapa.

A previous study has shown that IGFBP2 is regulated through the PI3K/Akt/mTOR axis in breast cancer cells (Martin and Baxter, 2007). This is in line with our theory since rapa is a known inhibitor of both the PI3K/Akt and mTOR pathway as discussed before. Thus it is

reasonable to suggest a link between the IGFBP2 repression and the mTOR arrest by rapa in AML. This is a very significant finding because there have been no previous reports on such a direct effect of rapa on IGFBP2 in AML.

4.3.5 Rapa is cytostatic- not cytotoxic

Once we established that rapa caused G1 arrest and worked out the underlying molecular mechanism of the cell cycle arrest, we proceeded to investigate whether rapa induced apoptosis in AML cells. We suspected that rapa would indeed induce apoptosis as it had a potent anti-proliferative effect on the AML cells as vouched for by the MTS assays. Also the 'Death receptor signalling pathway', which leads the cells to apoptosis, was among the pathways identified from the IPA analysis. Additionally 'Cell death' was also one of the major functions affected by rapa treatment. Hence it was important to analyse the cytotoxic effects of the drug.

However, the caspase 3/7 and annexin V-FITC staining assays indicated that there was no significant increase in apoptosis observed in the rapa treated cells (Figure 4.8). Thus apoptosis is not a major player in the anti-leukemic effect of rapa. Hence we conclude that rapa is not a cytotoxic drug. Yet, the reason why many apoptosis related genes and proteins were found to be regulated is ambiguous and needs to be studied in greater detail. One possible reason might be that these genes are regulated as part of a greater anti-proliferative effect, but do not translate into cytotoxicity.

4.3.6 Hypoxia signalling regulation by rapamycin

Hypoxia signalling was another pathway modulated by rapa. The critical molecular mediators of this pathway, hypoxia-inducible factors (HIFs), regulate tumour formation, progression and response to drug treatment (Rankin and Giaccia, 2008). This pathway has been known to control cell growth and proliferation by influencing the mTOR signalling (Simon, et al.,

2008), indicating that this pathway could be another upstream signal which contributes to the cell cycle arrest induced by rapa.

4.3.7 Conclusion and Key findings

This is the first comprehensive study to adopt a top-down approach to study the global effects of rapa on AML. The key findings from the study are highly significant. We have established that rapa has potent anti-proliferative effects against AML. It regulates a wide range of pathways ranging from mTOR signalling, IGF-1 signalling, FGF signalling, hypoxia signalling to cell cycle G1 arrest and protein ubiquitination. Thus, the microarray and iTRAQ approaches complement each other and bolster the confidence in the data obtained. Real-time PCR analyses of selected genes indicate high convergence in the fold-change values with their microarray counterparts.

Rapa induced time-dependent cell cycle arrest in both the MV4-11 and THP-1 cells. The peak arrest was achieved at 16h. The classical pathways leading to cell cycle regulation were modulated by rapa. These include PI3K/Akt, mTOR and Protein ubiquitination. Rapa causes down-regulation of Skp2, a SCF-type ubiquitin ligase, leading to p27 elevation. This in turn causes inhibition and concurrent down-regulation of Cdk 2 and Cdk 4 culminating in the arrest of cells in the G1 phase of the cell cycle. Rapa down-regulates IGFBP2, a key member of the IGF-1 signalling pathway, which is known to be elevated in AML. IGF-1 pathway lies upstream of mTOR. IGFBP2 expression portends poor prognosis and increased leukemogenesis. Hence the inhibitory effect of rapa on this key protein is of high significance.

Rapa does not induce apoptosis in AML and is hence a cytostatic drug. The cytostasis induced by rapa on AML is the cumulative effect of its regulation of the PI3K/Akt, mTOR, IGF-1 signalling, FGF signalling, hypoxia signalling and protein ubiquitination pathways. The study strongly endorses the use of high-throughput approaches in partnership with

functional characterisation in deciphering the mode of action of drugs in cancer. The wealth of data generated hence, would greatly help in the selection of combinatorial agents which could synergise the anti-leukemic effects of rapa. Thus, we have proposed a model for the mode of action of rapa based on our study (Figure 4.10).

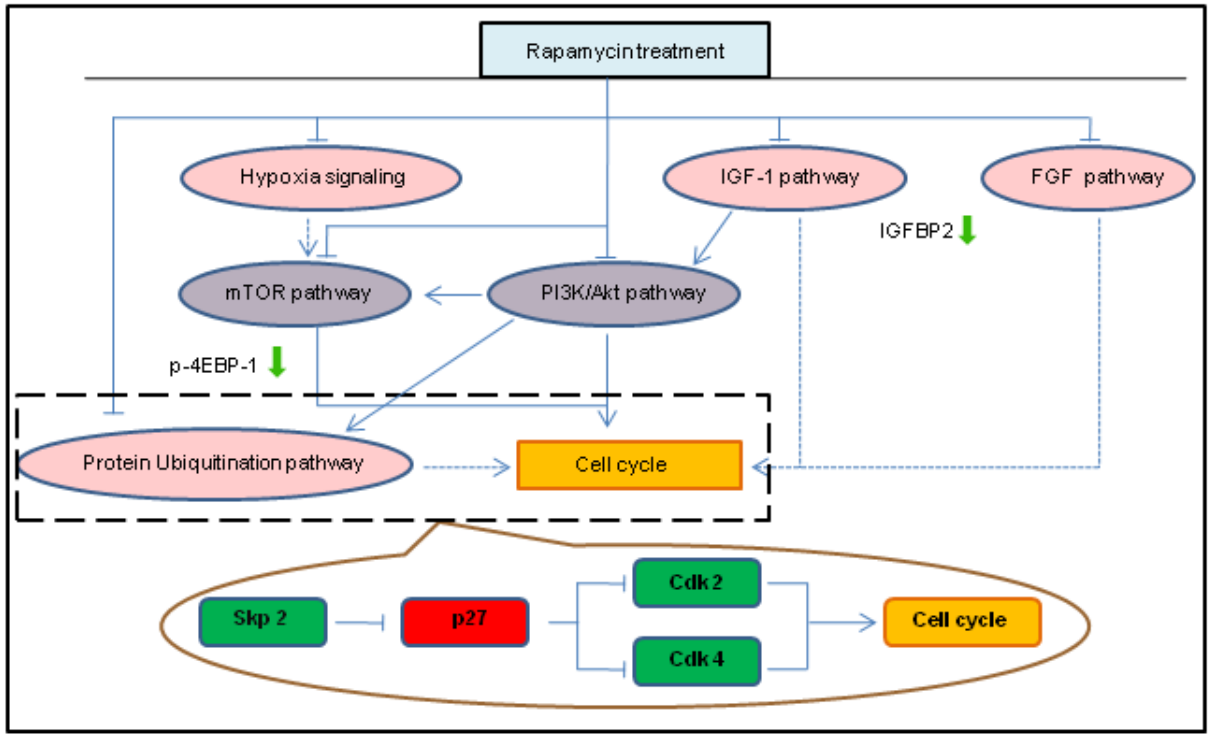

Figure 4.10: Summary of the proposed mechanism of cell growth arrest employed by rapa

The study provides a model for the anti-leukemic effect of rapa based on the findings from the high-throughput studies and functional studies.

- Down-regulated gene

- Up-regulated gene

⋯⋯> Putative effect

CHAPTER 5

PROTEOMIC INVESTIGATION OF THE ANTI-LEUKEMIC ACTIVITY OF GEN

This chapter briefly describes the necessity for a proteomic study of the effects of genistein on AML cells and moves on to describe the results obtained from such a study. The chapter encompasses a detailed analysis of the results leading to an interpretative discussion to elucidate the mechanism of action of GEN.

5.1 Introduction

GEN is a soybean derivative belonging to the isoflavone family of phytochemicals. The fact that GEN has anti-leukemic activity, was identified in the beginning of the previous decade (Traganos, et al., 1992). It is now well established that GEN holds a lot of promise as a potential therapy for AML.

GEN is a multi-targeted receptor tyrosine kinase inhibitor. This interesting characteristic makes it a promising anti-cancer drug candidate, while also leading us to believe that it has a profound effect on the proteome of cancer cells. This has made the study of its mechanism of action a challenge, spawning a number of studies in this direction. Yet the conclusions drawn from these studies are insufficient to map the exact mechanism of action of GEN and leave much to be desired.

We have adopted a proteomic approach to characterise the anti-proliferative activity of GEN in AML cells, using two different cell lines. Although there has been a previous attempt by Zhang et al , wherein they have employed a 2D gel based approach to study the proteome level changes orchestrated by GEN in leukemia cells, it is not conclusive as the method is error prone and the results aren't prolific enough to make a sound judgement (Zhang, et al., 2007).

We have used two different cell lines in our study, one containing an inherent FLT3-ITD mutation and one with the wild-type gene. GEN's effect on the cell lines with FLT3-ITD mutations hasn't been characterised yet. However it is very important to look for this connection, considering the fact that most drugs for AML exert FLT3 status-specific inhibitory effects. A drug which can exert potent anti-leukemic effects irrespective of FLT3 status would be a revolution of sorts, leading to generic AML therapy, without any concerns about the patient sensitivity. The fact that GEN is a known PTK inhibitor provides the reasoning behind our speculation that it might be a FLT3 inhibitor (Akiyama, et al., 1987).

The objective of the study is to identify the various pathways that the drug modulated and piece up the puzzle to accurately pinpoint to its mechanism of functioning. We have used an 8-plex iTRAQ based approach to achieve this goal. The clues obtained from the iTRAQ analysis were followed up and a hypothetical model was formulated to describe GEN's action. The model was empirically validated.

This chapter describes in great detail the results gleaned from the high-throughput proteomic investigative study. The chapter also illustrates the analysis of this data and the subsequent functional assays performed to buttress the claims made by the study.

5.2 Results

5.2.1 Genistein exerts strong anti-proliferative effects on AML cell lines

The anti-leukemic activity of GEN was studied using two AML cell lines, namely, MV4-11 and HL-60 as models. The two cell lines in this case differ in the status of the FLT3 gene mutation. While HL-60 has a wild-type FLT3 gene, MV4-11 possesses a mutant version comprising an ITD mutation, which renders its protein product constitutively phosphorylated and hence activated. In many cases this is the primary cause of leukemogenesis. Such a choice of cell lines provides scope for a broader and more inclusive analysis.

GEN exhibited inhibitory effects on the proliferation of both MV4-11 and HL-60 cells *in vitro*. The effect increased with dosage levels as illustrated in Figure 5.1a. The cytotoxicity of GEN increased with time as observed in Figure 5.1b. While the IC_{50} dosage at 48 h for MV4-11 cells was found to be 20 μM, it was close to 30 μM in the case of HL-60 cells. The cells were seeded in 24-well plates and counted using the trypan blue exclusion staining.

(a)

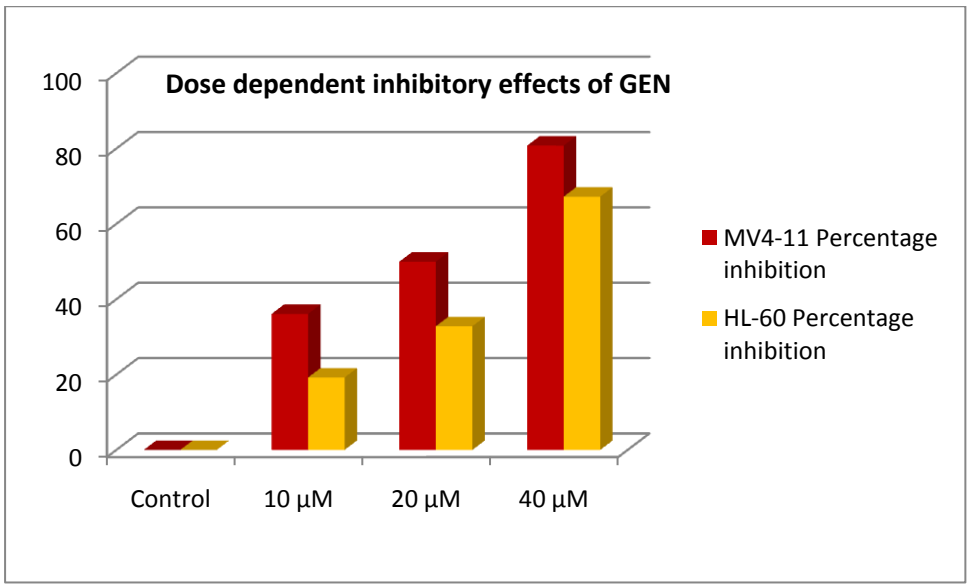

(b)

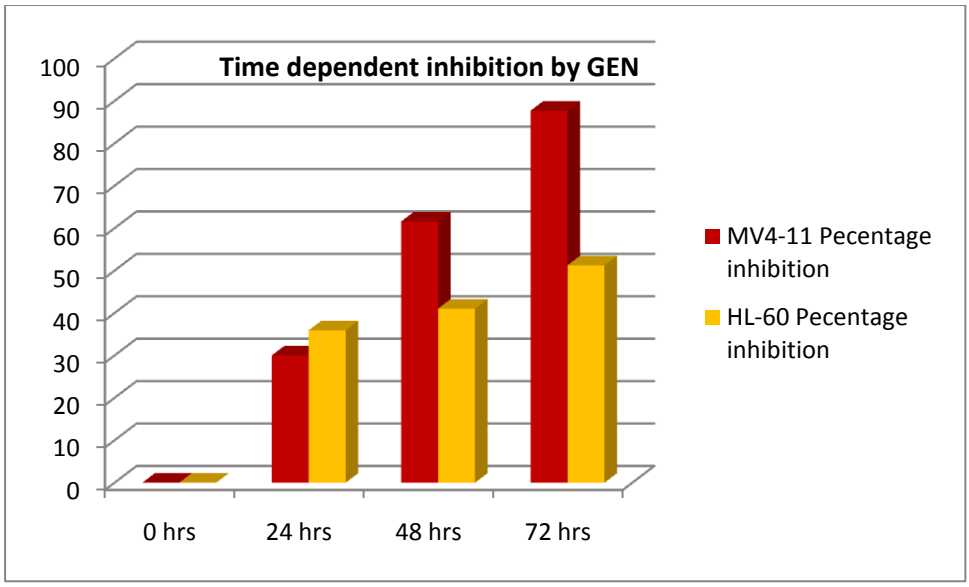

Figure 5.1: Anti-proliferative activity of GEN (a) Dose dependent inhibitory effects at 48h and (b) Time dependent inhibitory effects at 20µM dosage for MV4-11 and 30 µM dosage for HL-60.

The total number of cells at each dosage was counted using trypan blue exclusion staining and the inhibitory effect of GEN was quantified hence. The results show that GEN had an enhanced effect on MV4-11 as compared to HL-60. The IC_{50} dosage was found to be approximately 20µM for MV4-11 and 30 µM for HL-60 at 48h. The data shown is an average of triplicate experiments.

5.2.2 GEN is a FLT3 inhibitor

The inhibitory effect of GEN on PTKs logically led us to examine its effect on FLT3, a tyrosine kinase. Western blotting studies using an antibody specific to the phosphorylated tyrosine residue 591 of the FLT3 gene showed that GEN in fact had a potent inhibitory effect on the phosphorylation status of FLT3 in the MV4-11 cells, which contain the ITD mutation. GEN down-regulated the phosphorylation of FLT3 as indicated in Figure 5.2. This proves that GEN is a FLT3 inhibitor. In the case of HL-60, phosphorylated FLT3 was not detected, consistent with its wild-type status.

Both the cell lines showed positive response to the drug, making it all the more interesting to understand the mechanism of action of GEN in both cases. In order to achieve this, the proteomes of the cells treated with the drug were studied.

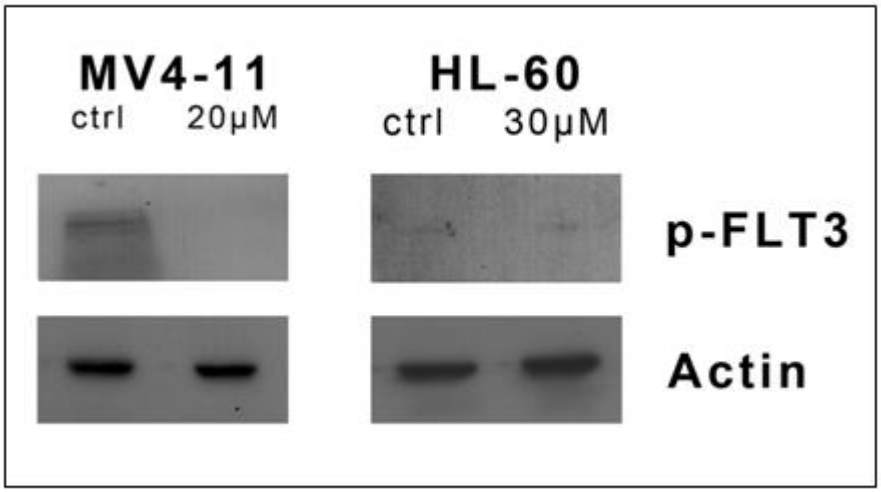

Figure 5.2: GEN is a FLT3 inhibitor

GEN down-regulates the constitutive phosphorylation of FLT3 in the MV4-11 cells and is hence a FLT3 inhibitor. In the case of HL-60, due to the absence of FLT3-ITD mutation, this effect is irrelevant.

5.2.3 8-plex iTRAQ based profiling of the proteome level changes induced by genistein

The optimal dosage of GEN required to kill 50% of the cells was hence determined to be 20 µM for MV4-11 and 30 µM for HL-60 cells at 48h and these fixed dosages were used for all future experiments. Proteomic profiling of the cells was performed by employing the 8-plex iTRAQ strategy. The cells were treated with GEN and proteins were extracted and quantified as described in Chapter 3. The samples were prepared as biological replicates. 100 µg of each sample was used for iTRAQ analysis. Each of the trypsin digested samples was labelled with a unique isobaric tag. The peptides were then identified and quantified by LC/MS/MS analysis. The protein identification performed using the ProteinPilot™ software yielded several hits. A short summary of the results is shown in Table 5.1. An aggregate FDR of 1% was used as the accepted value. This corresponded to an unused score of 2. This was hence set as the cut-off to select significant proteins, which numbered 609 in total.

Table 5.1: Summary of LC/MS/MS results obtained from the iTRAQ study

Protein level data	
Critical Value	**Number of Proteins identified**
Accepted FDR	**Aggregate FDR**
1.0 %	609
5.0 %	774
Peptide level data	
Critical Value	**Number of Peptides identified**
Accepted FDR	**Aggregate FDR**
1.0 %	2907
5.0 %	4171
Spectra level data	
Critical Value	**Number of Spectra identified**
Accepted FDR	**Aggregate FDR**
1.0 %	3511
5.0 %	4975

5.2.3.1 Statistical significance of the iTRAQ data

Since the samples were run as biological duplicates, it is critical to assess the reproducibility of the data. A high level of concordance between the duplicates would bolster the confidence in the data and also lend credibility to the sample preparation methodology and the downstream mass spectrometric analysis. The scatter plot analysis of the duplicates was performed and the R^2 value of the trendline was used as a measure of reproducibility. As the Figure 5.3 shows, the duplicates exhibited high level of conformity, validating the soundness of the data.

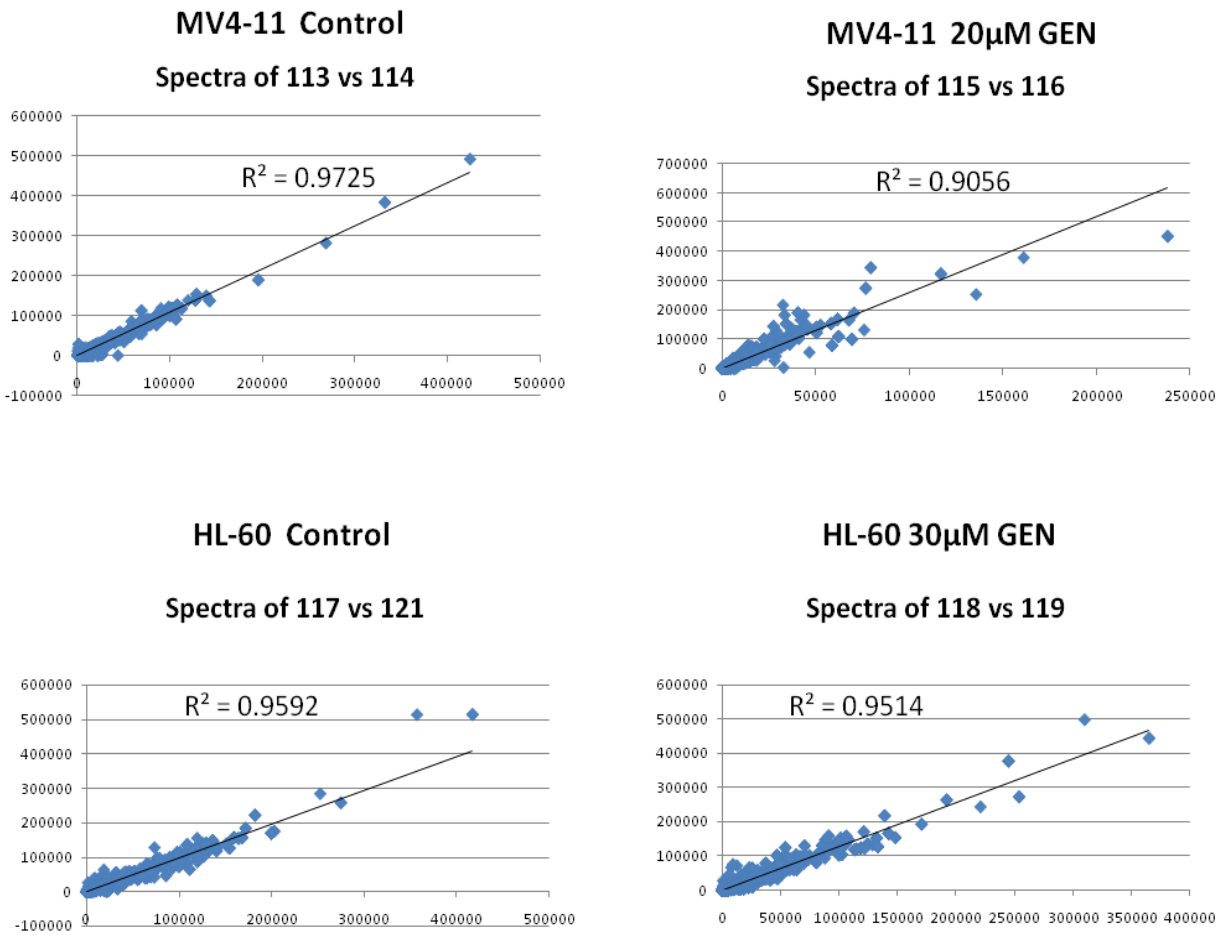

Figure 5.3: Scatter plot analysis of the proteomics data

Comparison of the area under the curve of the spectral profiles of the duplicate pairs indicated high reproducibility. This is justified by the R^2 values of the trendlines. A value of 1 indicates maximum reproducibility.

5.2.3.2 Comparison of the profiles of the two cell lines

Once the veracity of the data was established, it was scrutinised for biological meaning. The data was analysed using the ProteinPilot™ software as mentioned earlier. The fold-changes of the identified proteins in the treated samples, compared to the control samples were calculated. Proteins were considered significantly regulated if they had a fold-change value greater than or equal to +/- 1.3. The ratios of the biological replicates were computed and the average value was taken. Those proteins which exhibit opposite levels of regulation in the replicates were disregarded.

There were more proteins found regulated in MV4-11. Figure 5.4 compares the profiles of proteins regulated in both the cell lines. There was a large percentage of overlap between the two cell lines, indicating a significant similarity in the mechanism of action. However there were still some proteins which were not regulated in the same manner or extent in both cell lines, implying possible divergent effects in some processes.

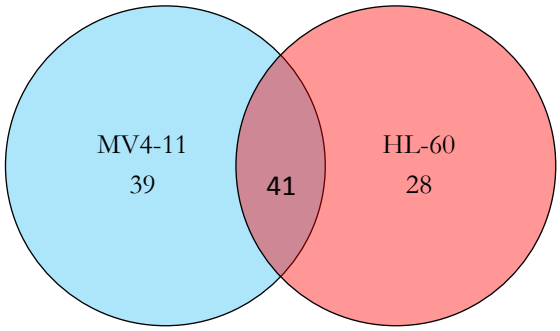

(a) Up-regulated proteins

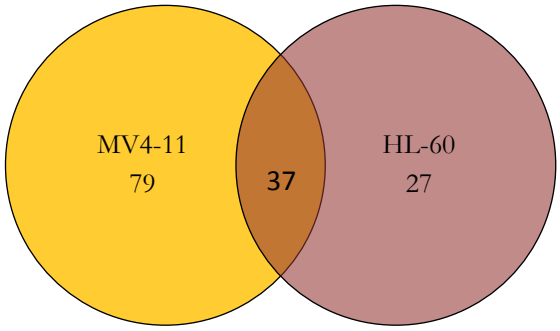

(b) Down-regulated proteins

Figure 5.4: Venn Diagrammatic comparison of the regulated proteins identified from the proteomic study

The intersection represents the proteins commonly up/down regulated in both the cell lines. The data implies a high degree of overlap between the two cell lines, while also signifying unique regulation of a subset of proteins in individual cell lines.

5.2.4 Genistein regulates crucial pathways in MV4-11 and HL-60 cells

Pathway analysis was performed on the proteomics data using the IPA software. The analysis unearthed some very interesting results. A number of signalling and metabolic pathways were found to be regulated by GEN, in line with the fact that GEN is a multi-targeted protein kinase inhibitor. A lot of these pathways, such as mTOR, Akt, protein synthesis, etc have previously not been known to be modulated by GEN.

GEN was found to alter the expression of proteins involved in both signalling and metabolism alike. This implies that the effects of GEN are much more profound and deeper than what is originally known. The top 20 functions regulated in MV4-11 and HL-60 are shown in Figures 5.5 a and 5.5 b respectively.

(a) MV4-11

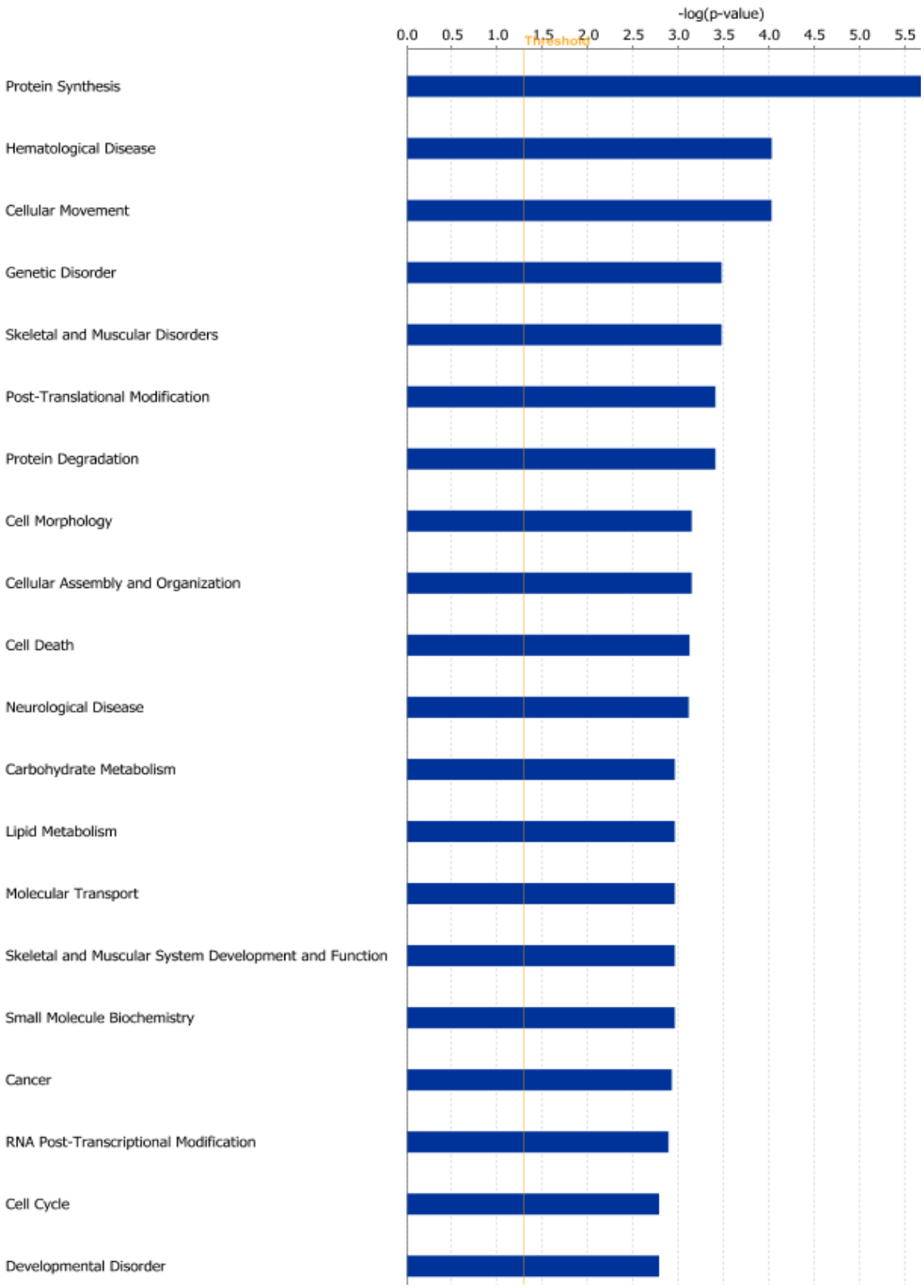
-log(p-value)
0.0
0.5
1.0
1.5
2.0
2.5
3.0
3.5
4.0
4.5
5.0
5.5
Threshold
Protein Synthesis
Hematological Disease
Cellular Movement
Genetic Disorder
Skeletal and Muscular Disorders
Post-Translational Modification
Protein Degradation
Cell Morphology
Cellular Assembly and Organization
Cell Death
Neurological Disease
Carbohydrate Metabolism
Lipid Metabolism
Molecular Transport
Skeletal and Muscular System Development and Function
Small Molecule Biochemistry
Cancer
RNA Post-Transcriptional Modification
Cell Cycle
Developmental Disorder

(b) HL-60

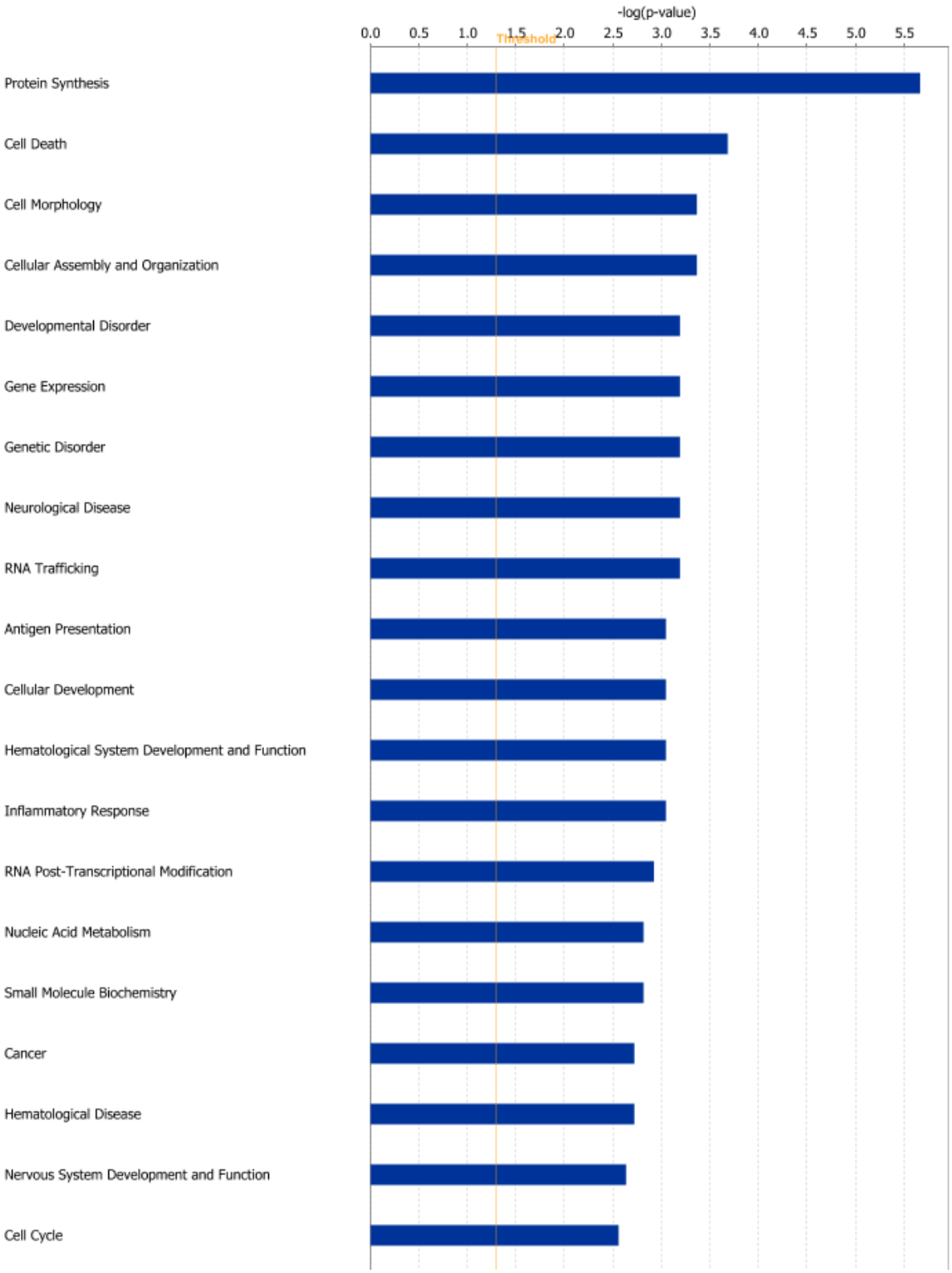

Figure 5.5: Biological functions regulated by GEN in (a) MV4-11 (b) HL-60

As the figure clearly indicates, a number of functions are common to both the cell lines. *Protein synthesis* was the top function targeted by GEN. *PTM, cellular movement, cell death, carbohydrate/lipid metabolism and haematological disease* were among the most regulated functions in both the cell lines.

Although it is important to look at the functions, it is more pertinent and informative to consider the canonical pathways regulated by GEN more closely. Hence we analysed the canonical pathways regulated by GEN using IPA. The Table 5.2 lists the pathways which were regulated in the cell lines. As can be seen, GEN regulated both signalling and metabolic pathways in AML. Only the pathways which cleared the p-value cut-off are shown.

The pathways regulated were of course reflective of the functions found modulated by GEN. There were significant similarities between the two cell lines, indicating a consistent mechanism of action of GEN. However there was significantly more number of pathways regulated in MV4-11 as evidenced by the Table 5.2.

It was interesting to see that GEN regulated mTOR pathway, in both the cell lines, a previously unknown effect. Such a consistent regulation in both the cell lines indicates that mTOR pathway might actually form the crux of GEN's effect.

Table 5.2: Canonical Pathways regulated by GEN in (a) MV4-11 (b) HL-60

(a) MV4-11

Pathway	**-log (p-value)**
Signalling pathways	
Polyamine Regulation in Colon Cancer	4.81E00
Mitochondrial Dysfunction	2.56E00
mTOR Signaling	2.49E00
Induction of Apoptosis by HIV1	2.46E00
Actin Cytoskeleton Signaling	2.2E00
Reelin Signaling in Neurons	2.11E00
RAN Signaling	1.92E00
Leukocyte Extravasation Signaling	1.9E00
Protein Ubiquitination Pathway	1.9E00
Regulation of Actin-based Motility by Rho	1.9E00
Integrin Signaling	1.84E00
ATM Signaling	1.78E00
Death Receptor Signaling	1.63E00
Myc Mediated Apoptosis Signaling	1.61E00
Regulation of eIF4 and p70S6K Signaling	1.6E00
RhoA Signaling	1.56E00
IL-8 Signaling	1.51E00
PI3K/AKT Signaling	1.47E00
Metabolic pathways	
Oxidative Phosphorylation	2.94E00
Purine Metabolism	2.27E00
Phenylalanine Metabolism	2.19E00
Methane Metabolism	1.92E00
One Carbon Pool by Folate	1.65E00
Stilbene, Coumarine and Lignin Biosynthesis	1.58E00
Glutathione Metabolism	1.54E00
Tyrosine Metabolism	1.33E00

(b) HL-60

Pathway	**-log (p-value)**
Signalling pathways	
Polyamine Regulation in Colon Cancer	4.67E00
PI3K/AKT Signaling	3E00
Reelin Signaling in Neurons	2.83E00
mTOR Signaling	2.68E00
Regulation of eIF4 and p70S6K Signaling	2.28E00
Leukocyte Extravasation Signaling	2.15E00
Protein Ubiquitination Pathway	2.15E00
AMPK Signaling	1.95E00
CTLA4 Signaling in Cytotoxic T Lymphocytes	1.68E00
SAPK/JNK Signaling	1.66E00
ERK/MAPK Signaling	1.54E00
p70S6K Signaling	1.35E00
IL-2 Signaling	1.32E00
Metabolic pathways	
Aminoacyl-tRNA Biosynthesis	2.63E00
Purine Metabolism	1.79E00

The canonical pathways regulated are segregated as signalling and metabolic pathways for easier comprehension.

5.2.5 Genistein modulates mTOR pathway- an erstwhile unknown arrow in genistein's quiver

Immunoblotting analysis of 4EBP-1, the downstream effector of the mTOR pathway was performed to ascertain the regulatory effect of GEN on this pathway, which is crucial to cell growth and protein synthesis. The western blots showed that GEN inhibited the phosphorylation of 4EBP-1, hence indicating a shutdown of the mTOR pathway (Figure 5.6). Such a modulation of the mTOR pathway is a novel effect of GEN which has not been observed or even suspected to happen before! This is however very consistent with the fact that in both MV4-11 and HL-60, protein synthesis is the top function regulated by GEN, since mTOR plays a major role in the control of protein translation.

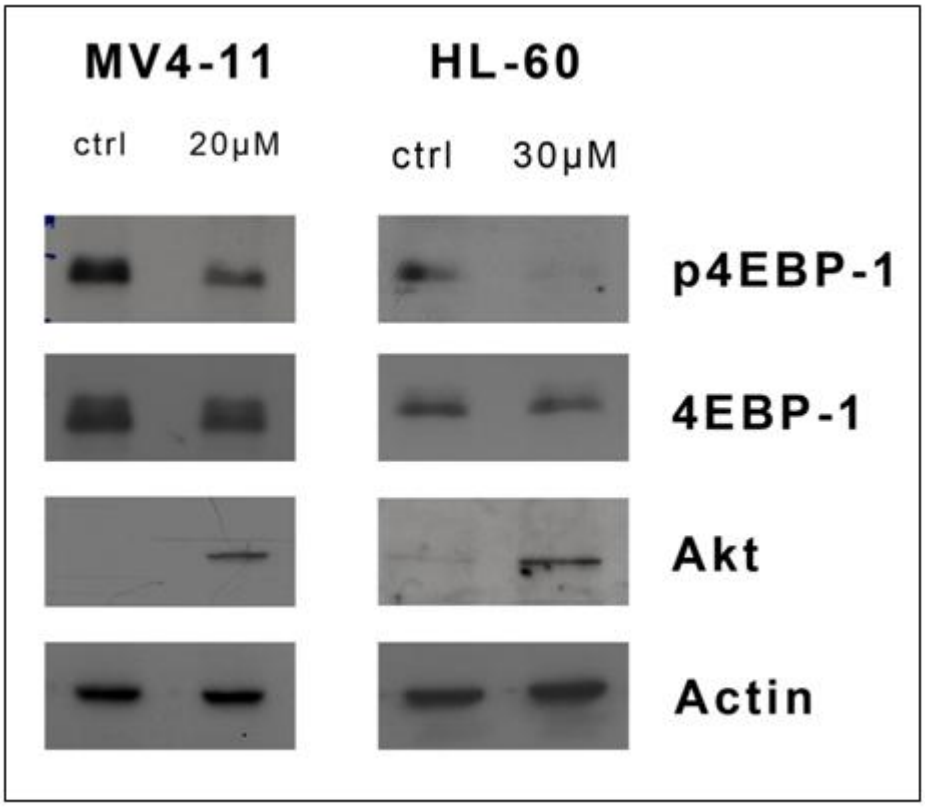

Figure 5.6: Western blot validation of certain key proteins regulated by GEN in AML

The immunoblotting studies indicated that GEN had profound effect on the mTOR and PI3K/Akt pathways in AML. Actin served as the loading control.

5.2.6 Protein synthesis mechanism- an important target of genistein

Considering the strong causal link between the mTOR pathway and protein translation, the rate of nascent protein synthesis was probed. As surmised in the Figure 5.7, GEN was found to severely curtail the rate of protein synthesis in both the MV4-11 and HL-60 cells by a factor of nearly 4-5 folds. Such an emphatic response to GEN is a very interesting observation which is previously unreported.

The experimental procedure adopted is described in detail in the Methods section (Chapter 3). The procedure accommodated an inherent negative control in the form of the cells grown in media containing normal methionine. Such cells technically do not take part in the 'Click chemistry' and would hence account for the basal fluorescence of the cells.

However it is important to note that the effect was manifested at different time points in both the cell lines. MV4-11 cells were quick to react to GEN and exhibited a drop in protein synthesis levels as early as 24h after drug treatment, sustaining the reduction in the levels up to 72h. However the HL-60 cells showed prolific reduction only at 72h, with little or no response at the earlier time points.

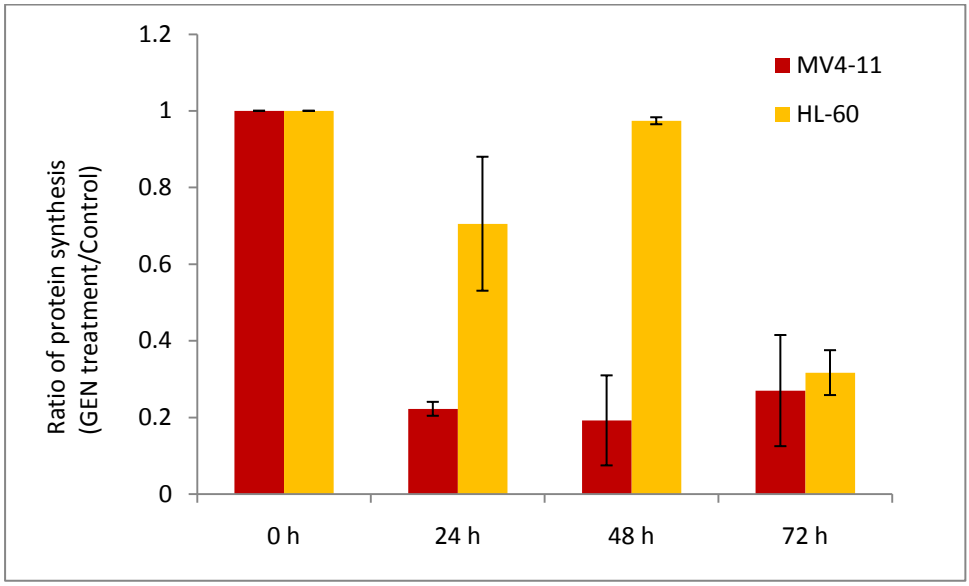

Figure 5.7: GEN arrests protein synthesis in MV4-11 and HL-60.

The dynamics of the inhibitory effect differs between the two cell lines. While there is an immediate and consistent drop in the synthesis rates in the MV4-11 cells treated with 20µM GEN, a delayed effect is observed in the HL-60 cells (treated with 30µM GEN).

5.2.7 Akt regulation- One stop solution to many questions?

The IPA analysis strongly pointed to the regulation of the PI3K/Akt axis in both the cell lines. Hence western blot analysis was performed to characterise the role of GEN in Akt regulation. As seen in Figure 5.6 GEN strongly up-regulated the levels of the Akt protein in both the cell lines. This is very puzzling as Akt is known to promote tumourigenesis and cellular proliferation. Hence such an effect of GEN on this vital pathway is contrary to expectations and is thus intriguing.

However in recent times it has been seen that increase in Akt levels leads to production of reactive oxygen species (ROS). ROS accumulation beyond a certain threshold has been known to promote apoptosis and cell death in a lot of cancer tissues and cells (Simon, et al., 2000; Wei, et al., 2010). It is hence essential to probe this link between Akt and ROS levels to establish a mechanism for the mode of cell death induced by GEN in AML.

5.2.8 Genistein increases ROS levels in leukemia cells

ROS levels were measured using the cell permeant ROS detection indicator carboxy-H_2DCFDA.

As shown in Figure 5.8, GEN caused an accumulation of ROS in the AML cells over time. There was a difference in the pattern of ROS accumulation between the two cell lines. In the case of MV4-11, ROS accumulation followed a uniform upward trend with time, while in HL-60 it exhibited a non-linear pattern. In HL-60 cells, GEN caused a dip in the ROS levels at 24h and 48h before bouncing back to an elevated level at 72h.

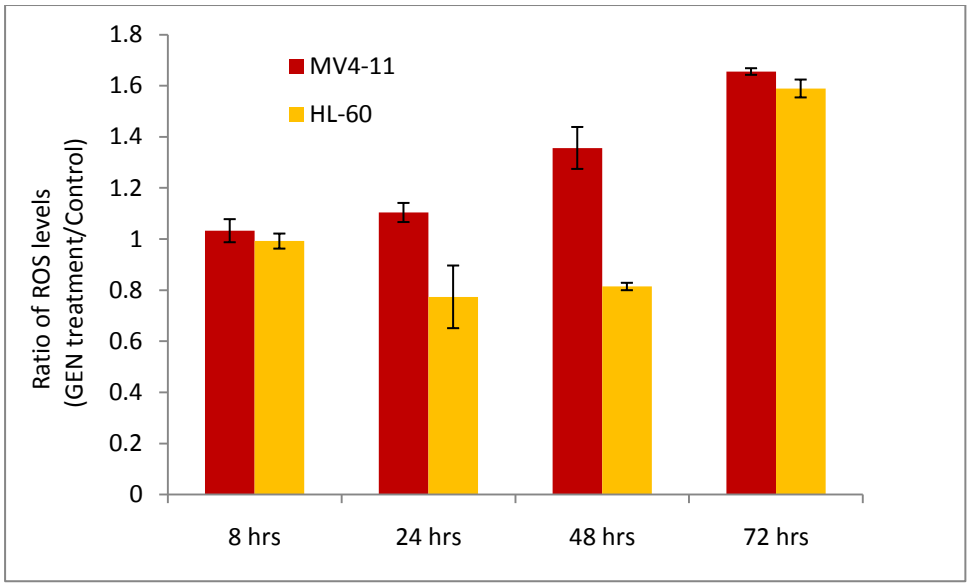

Figure 5.8: GEN induces ROS accumulation in MV4-11 and HL-60.

GEN induces ROS generation in both the cell lines over time. However, while in the MV4-11 cells the trend of ROS accumulation is linear, in the HL-60 it peaks at 72h, with a mild dip at other time points.

5.2.9 Mechanism of cell death caused by genistein

5.2.9.1 GEN induces apoptosis in AML cells

Increase in ROS levels have been known to induce apoptosis and cell death. In order to determine whether such a phenomenon occurs in GEN treatment of AML cells, the cells were assayed for apoptosis using the flow cytometry based Annexin-V FITC staining method. This method involves double staining of the cells with the fluorescent dyes P.I and FITC. GEN was found to induce apoptosis in both the cell lines. The cells which stain positively for FITC, but are negative for P.I are considered apoptotic cells. As the Figure 5.9 indicates, an accumulation of apoptotic cells was observed in both the cell lines.

(a) MV4-11

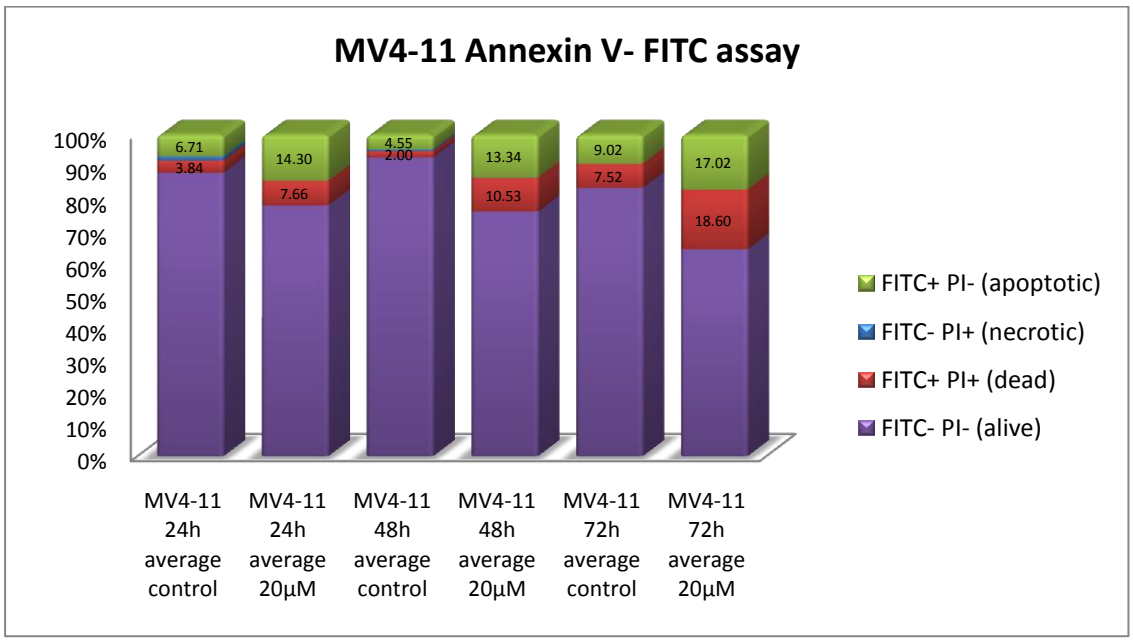

(b) HL-60

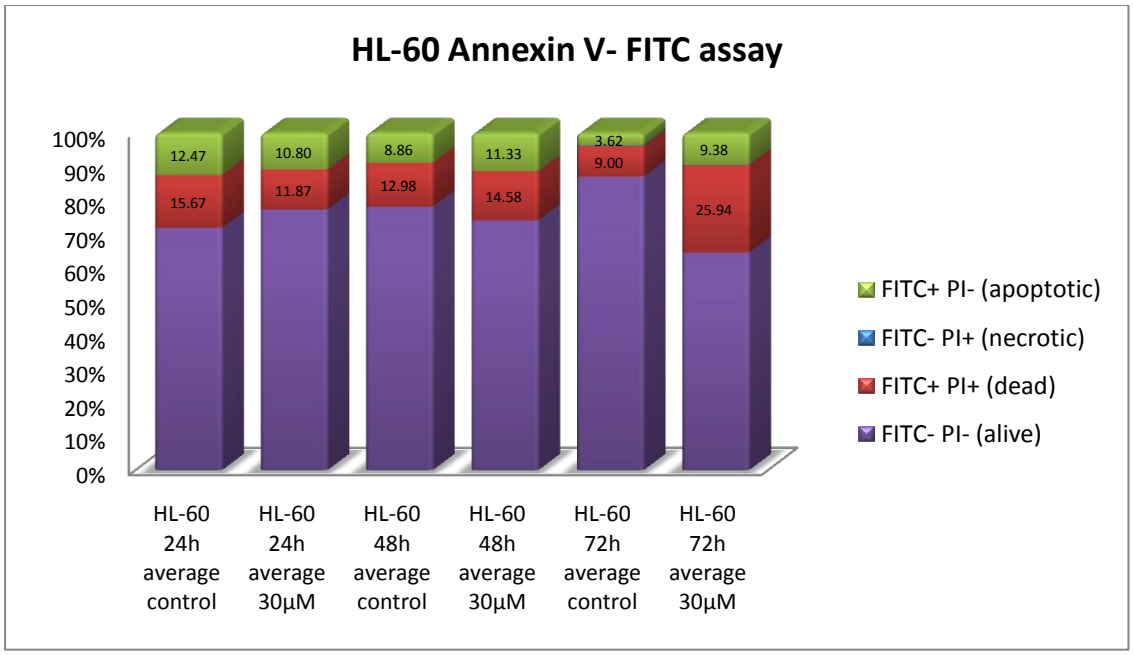

Figure 5.9: GEN causes apoptosis in (a) MV4-11 (b) HL-60.

GEN treatment caused an increase in the proportion of the apoptotic and dead cells in both the cell lines. As is the case with the other observations, the apoptotic response in the MV4-11 cells was faster.

It was also observed that the drug caused an increase in the dead cell population. These cells stain positively for both PI and FITC. However in this subpopulation of cells, it is not possible to discern between those which died via apoptosis and those which died by necrosis. More apoptotic/dead cells were observed at 72h than the other time points, which is concurrent with our *in vitro* cytotoxicity assays, which indicated a peak effect for GEN at 72h in both the cell lines (Figure 5.1). Thus it is apparent that GEN induces apoptosis in both the cell lines, in correlation with the increase in ROS levels.

5.2.9.2 Contrast in the mechanisms of apoptosis in MV4-11 and HL-60

In order to understand the mechanism of apoptosis caused by GEN in AML, the caspase 3/7 levels of AML cells treated with GEN were assayed. Caspase activation is a major mode of apoptosis induction in cells.

Interestingly enough, the results (Figure 5.10) showed that while there was more than a two-fold increase in the activated caspase levels in the HL-60 cells upon treatment with GEN, such a phenomenon does not occur in MV4-11. The dramatic increase in activated caspase levels in HL-60 occurs at 72h, which is consistent with the Annexin-V-FITC results, showing highest degree of apoptosis at the same time point. Such a pattern of regulation is in accordance to the elevation in the ROS levels at 72h.

Yet, in the MV4-11 cells, the activated caspase levels do not conform to the observed increase in apoptosis. The results expound that the apoptosis induction by GEN in MV4-11 is ROS mediated, yet caspase independent and needs further investigation.

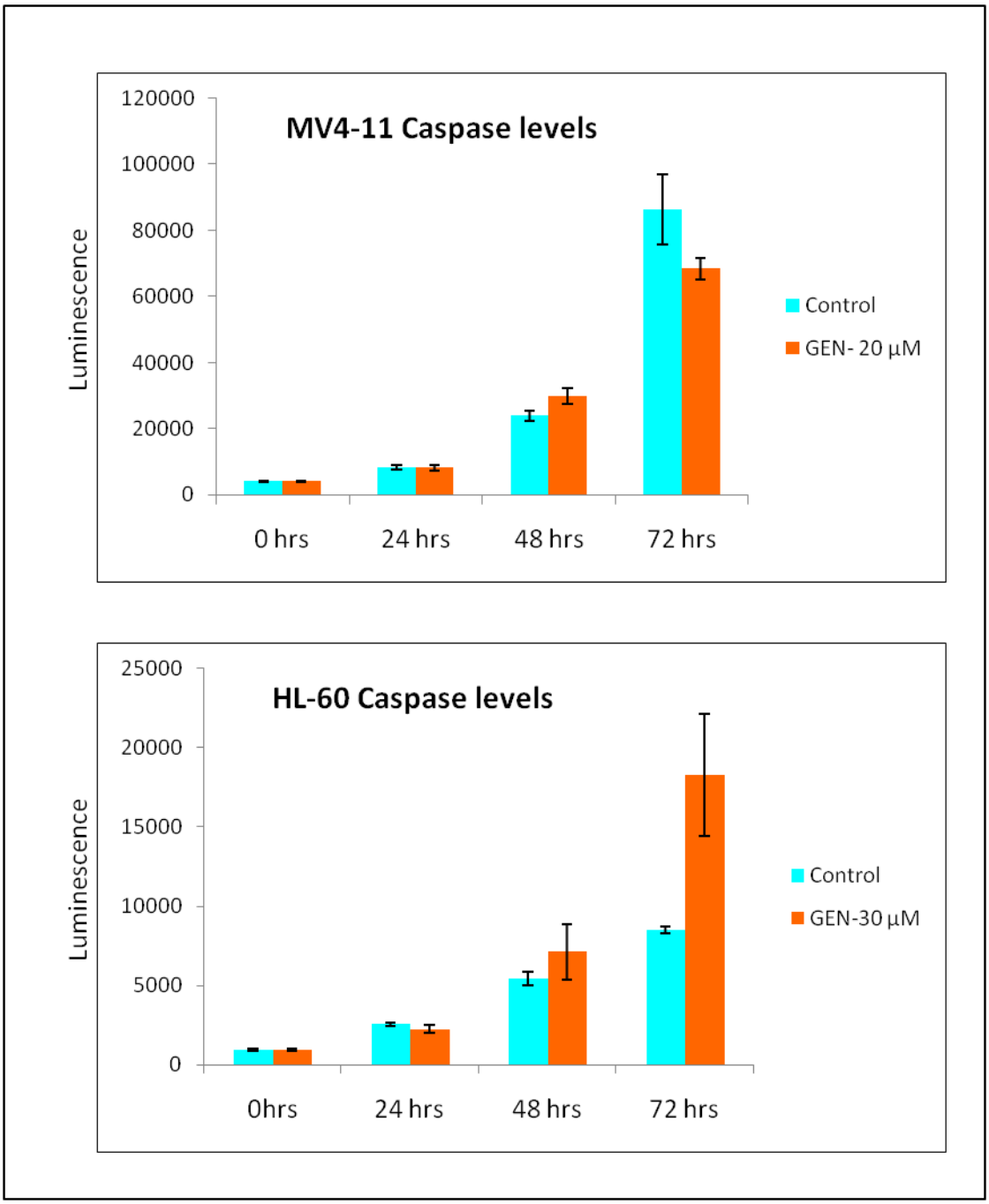

Figure 5.10: GEN exerts a duality in its apoptotic mechanism.

GEN adopts a caspase mediated approach to apoptosis in the HL-60 cells as implied by the increase in the caspase levels. However in the MV4-11 cells, GEN does not have any effect on the caspase levels and the mechanism of apoptosis is hence caspase-independent.

5.2.10 Deciphering the mode of cell cycle arrest caused by GEN

Cell cycle arrest is one of the essential features of inhibition of cellular proliferation by drugs. Cell cycle was among the biological functions regulated by GEN in both the AML cell lines. Hence PI staining of the DNA was performed to study the cell cycle progression of the cells treated with GEN in comparison to the untreated cells. The cell cycle analysis result depicted in Figure 5.11 clearly elucidates that GEN induces G2/M arrest in HL-60 cells. The drug causes a relative accumulation of cycling cells in the G2/M phase with time, thereby blocking cell division and cellular proliferation.

However in the case of the MV4-11 cells, a different phenomenon is observed. The cell cycle of MV4-11 does not show a prolific sensitivity to GEN. The cells show an accumulation in the G1/S phase at 24h, in stark contrast to the observation in the HL-60 cells. This reveals a fundamental difference in the cell cycle regulation by GEN in the two cell lines. This is profoundly significant in the wake of the previous finding that MV4-11 cells undergo caspase independent apoptosis. The results put together indicate that GEN employs a different mode of action to induce growth arrest and cellular death in the AML cells studied, which might be correlated with the difference in their genetic background, namely the presence of wild-type or mutant FLT3 gene.

(a)

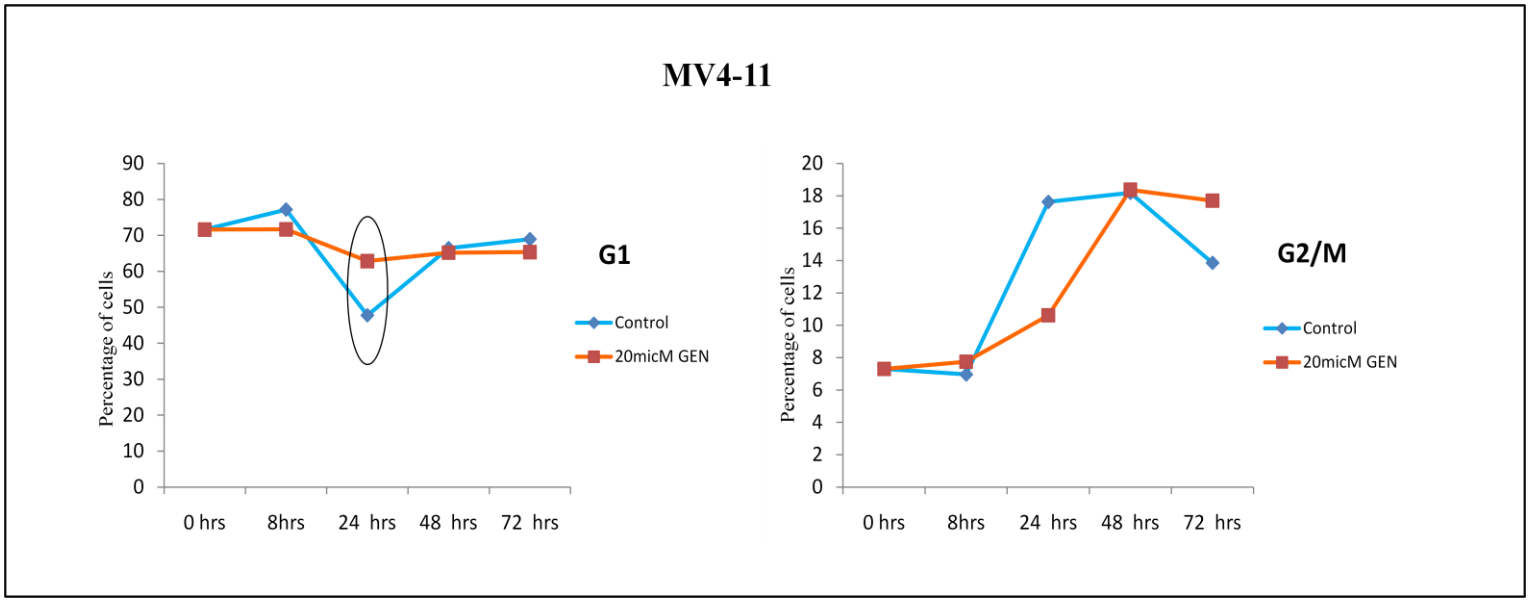
MV4-11
Percentage of cells
90
80
70
60
50
40
30
20
10
0
0 hrs
8hrs
24 hrs
48 hrs
72 hrs
G1
Control
20micM GEN
Percentage of cells
20
18
16
14
12
10
8
6
4
2
0
0 hrs
8hrs
24 hrs
48 hrs
72 hrs
G2/M
Control
20micM GEN

(b)

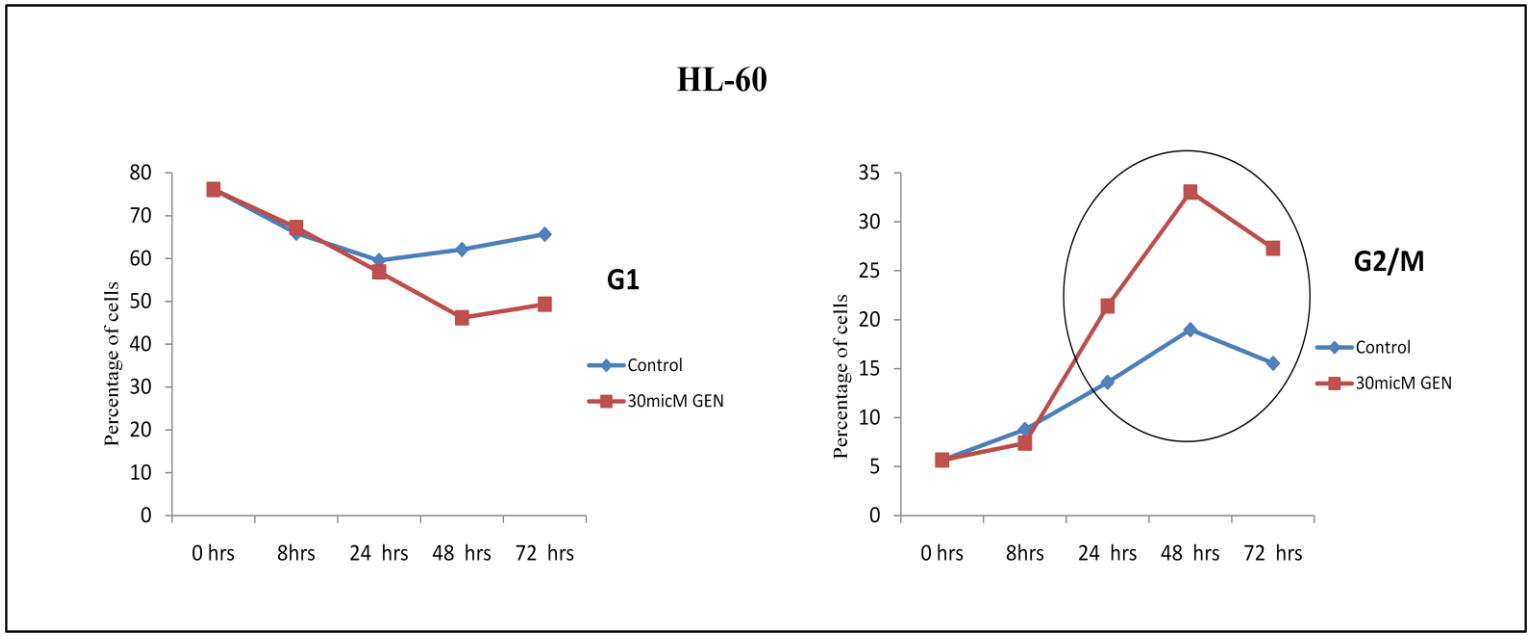

Figure 5.11: Cell cycle regulation by GEN in (a) MV4-11 (b) HL-60

Propidium iodide based flow cytometric assay of cell cycle indicated divergent effects of GEN on MV4-11 and HL-60 cells. The phase and time-points at which GEN induces cell cycle arrest is highlighted by the oval.

5.3 Discussion- Piecing together the puzzle!

5.3.1 Significance of GEN's FLT3 inhibitory effect

The anti-proliferative effect of GEN on tumour cells has been widely reported and is hence well established. There have been many studies characterising the effects of GEN on cancer cells and proposing it as a therapeutic strategy to cure cancer. GEN has been effective in inhibiting the proliferation of AML cells. Various studies have attempted to elucidate the mechanism of action of GEN in AML such as the one by Shen, et al., 2007. However all the studies have restricted themselves to looking at the effects of GEN on just one subset of AML cells. AML is a multifactorial disease and about 24% of the AML cases are exemplified by the presence of an internal tandem duplication in the juxtamembrane of the FLT3 gene, a receptor tyrosine kinase. The presence of this mutation has been known to cause drug resistance and portend to poor prognosis. Hence it is imperative to address the effects of GEN on AML cells containing the FLT3-ITD mutation, in addition to those possessing the wild-type gene, in order to obtain a comprehensive picture of the mechanism of action of GEN on AML cells in its totality.

This is the first high-throughput proteomic study which attempts to characterise the effects of the isoflavone on AML cells, using the cell line MV4-11, containing FLT3-ITD mutation and HL-60, sans the mutation as models. The *in vitro* cytotoxicity assays demonstrated the potent inhibitory effect of GEN on both the cell lines. The MV4-11 cells were seen to be a shade more responsive than HL-60, as typified by the lower IC_{50} dosage values. More interesting is the observation that at 72h, there was nearly 90% inhibition in case of MV4-11. This is all the more significant because there are no previous reports pertaining to GEN's effect on MV4-11 in specific and FLT3-ITD positive cells in general.

The tyrosine kinase inhibitory activity of GEN has been very well characterised decades ago and is hence very well established. This interesting property of GEN formed the basis for our hypothesis that GEN might have a regulatory effect on the FLT3 protein. Indeed, as seen in

Figure 5.2 GEN inhibited the constitutive phosphorylation of FLT3 in MV4-11. This is a landmark discovery as such an effect of GEN is previously unknown and is completely novel. This shows that GEN has an anti-proliferative effect on AML cells, irrespective of the mutational status of their FLT3 gene.

Developing drugs which selectively target leukemia cells containing the FLT3 mutation has been a critical part of therapeutic research in the recent years. A number of FLT3 inhibitors are currently under clinical trials. Thus the fact that GEN can cure both FLT3 dependent and independent leukemia is a highly significant discovery! FLT3 inhibitors have been found to have highly specific cytotoxic effects towards cells harbouring the FLT3 mutation. Drugs such as ABT-869, currently in clinical trials as a FLT3 inhibitor, have little or no effect on cells containing wild-type FLT3 gene (Shankar, et al., 2007; Levis, et al., 2001). In such a climate, the efficacy of GEN on both subsets of AML is remarkable. This widens the scope and application of GEN, which has a directed action, with little side effects, owing to it being a natural product. It is also indicative of a divergent effect of the drug on FLT3 positive and negative cells.

Thus, to study the mechanism of action of GEN on a comprehensive scale a high-throughput proteomic approach was employed. We profiled the proteome of MV4-11 and HL-60 cells treated with the IC_{50} dosage of GEN and compared them with the untreated cells. The iTRAQ platform used for the study was designed in such a manner as to accommodate the labelling of 8 samples in parallel. This allowed us to label each of the samples in duplicate, thus enhancing the statistical power and hence the veracity of the data.

5.3.2 High-throughput study and the story that it presents

High-throughput studies are powerful methods to obtain a large amount of data. However at the end of the day, we would in fact be sitting on a mountain pile of data, completely

overwhelmed by its sheer magnitude. Hence we adopted an IPA based strategy to make sense of our data.

The IPA analysis helped unearth a lot of pathways of considerable significance in explaining GEN's anti-leukemic effects. The pathways identified as regulated by GEN in both the MV4-11 and HL-60 showed significant similarity and correlated well with the biological functions identified. MV4-11 had more number of regulated proteins than HL-60. This might be because of the fact that GEN doubles up as a FLT3 inhibitor in MV4-11. As a consequence of the down-regulation of the phosphorylation of FLT3, a PTK, a host of its downstream targets such as STAT5, RAS/MAPK and PI3K/Akt would be modulated (Gilliland and Griffin, 2002). On the other hand, in the case of HL-60, this action is rendered obsolete due to the absence of the relevant mutation on FLT3.

5.3.2.1 Inhibitory effect of GEN on 'Protein Synthesis'

Delving deeper into the data, we observed that 'Protein Synthesis' ranked consistently as the top function in both the cell lines. This might be indicative of the arrest of protein synthesis by GEN leading to the inhibition of cellular growth and proliferation. In accordance with our hypothesis, mTOR signalling and PI3K/AKT Signalling were found to be regulated by GEN in both the cell lines. In addition to this, metabolic pathways such as Phenylalanine Metabolism, Tyrosine Metabolism in MV4-11 cells and Aminoacyl-tRNA Biosynthesis in HL-60 cells were significantly regulated. These pathways are directly implicated in the protein synthesis events.

Western blotting of p-4EBP-1, the downstream effector of mTOR validated the inhibitory effect of GEN on the mTOR signalling axis. This is a completely novel discovery and to the best of our knowledge there have no previous studies which have reported such an effect of GEN. A detailed description of this pathway is presented in the section 2.4.3.2, Chapter 2.

Among the many functions regulated by this pathway, protein translation and cellular growth are of special significance in explaining the anti-leukemic property of GEN.

Previous studies have reported that targeting translation demonstrated a marked anti-leukemic potential in AML. The phosphorylation of 4EBP-1 was essential for the control of translation initiation (Tamburini, et al., 2009). There are suggestions for development of therapeutic strategies that directly target the eIF4F translation initiating complex in AML, of which 4EBP-1 is an integral component (Tamburini, et al., 2009). Interestingly, GEN exhibited inhibitory effects on protein synthesis in leukemia cells mediated by eIF2α kinase (Ito, et al., 1999).

Thus there is growing evidence to suggest that GEN caused a decrease in the synthesis of proteins mediated by arrest of the mTOR pathway. In order to confirm this, we employed a flow cytometry based approach involving Click-iT® chemistry to study the rate of nascent protein synthesis in cell treated with GEN in comparison to untreated cells at various time points. It is critical to incorporate a series of time points in order to spot the onset of the inhibitory effect at its earliest. This information would help map the events in a sequential fashion. GEN was found to drastically reduce the protein synthesis rate in MV4-11 cells at all time points. In the case of HL-60 the effect was most pronounced at 72h, with the other time points displaying milder reduction in the protein synthesis rates.

The fact that purine metabolism was one of the highly regulated metabolic pathway in both the cell lines indicates that GEN might exert a considerable influence on the transcriptional control too. Such an effect on the nucleic acid biosynthesis needs to be probed further.

Additionally GEN has also been reported to down-regulate the proteosome complex in tumour cells leading to proliferation arrest (Kazi, et al., 2003). Protein Ubiquitination was also among the top functions regulated by GEN in AML. This leads us to speculate that GEN might have an important regulatory role in the protein turnover process in AML.

5.3.2.2 Reactive oxygen species levels

The mTOR pathway is downstream of an important signalling axis- PI3K/Akt. The IPA analysis indicated a regulation of the PI3K/Akt pathway and the related p70S6K signalling axis. Hence we probed the protein levels of Akt in the whole cell lysates in order to glean empirical evidence on this effect. The result was baffling GEN was found to increase the Akt levels in both the cell lines. Genistein has been known to cause repression of Akt activity by the down-regulation of its phosphorylation (Shen, et al., 2007; Zhao, et al., 2009). However in our study we found an increase in the levels of total Akt upon GEN treatment, contrary to all previous observations.

5.3.2.2.1 Akt increases ROS accumulation

The phosphoinositide 3-kinase (PI3-kinase) signalling pathway plays a key role in the regulation of cell survival and proliferation. Activated Akt is then responsible for the phosphorylation of a number of downstream targets, regulating apoptosis and survival, cell growth and the cell cycle. Elevated levels of Akt have long been associated with tumourigenesis and metastasis. Increase in Akt levels is a biomarker for cancer progression (Grandage, et al., 2005). In fact, the PI3K/Akt pathway is an attractive target for several new drugs for various tumour types including leukemia (Martelli, et al., 2006). Hence it is indeed puzzling to see that GEN elevates the expression levels of Akt in our study! However, a recent study reported that Akt stimulated the accumulation of oxygen radicals, which can be exploited to selectively kill cancer cells (Nogueira, et al., 2008; Dolado and Nebreda, 2008). The study terms this property of Akt to generate ROS as the "Achilles' heels of Akt". ROS production by AKT was found to sensitise primary mouse and human fibroblasts to replicative senescence and apoptosis. Replicative senescence is the process by which cells stop dividing after a limited number of passages in culture. The study proposes that the increase in ROS by Akt might be due to a two pronged strategy. Akt stimulates oxidative

metabolism in the mitochondria concurrent with enhanced oxygen consumption, which indirectly increases intracellular ROS. They also found that although the increased Akt level promoted proliferation and inhibited apoptosis in cancer cells, it was ineffective against ROS mediated apoptosis. Thus this study suggests that the increased levels of Akt can actually be exploited to induce the cells to undergo apoptosis.

5.3.2.2.2 ROS mediates apoptosis

ROS plays important roles in cell proliferation, ageing, and cancer development. The reactive chemical properties of ROS may cause a variety of tissue injury in a wide range of human diseases. An excessive amount of ROS can lead to cell death by apoptosis or necrosis. The fact that increased levels of ROS can cause apoptosis is now well established. There is now considerable interest in drugs such as β-phenylethyl isothiocyanate (PEITC) and arsenic trioxide which increase the intrinsic ROS levels of the cells beyond a certain threshold and hence cause apoptosis (Trachootham, et al., 2006; Zhou, et al., 2003). ROS generation was the primary mechanism of cell death induced by 2-methoxyestradiol in AML cells (She, et al., 2007).

GEN is known to cause ROS accumulation in other studies (Salvi, et al., 2002). It is also known to potentiate arsenic trioxide mediated apoptosis in leukemia cells by ROS generation (Sánchez, et al., 2008).

5.3.2.2.3 GEN induces ROS mediated apoptosis by elevating the Akt levels in AML cells

The IPA analysis of the proteomics data showed that Oxidative Phosphorylation and Glutathione Metabolism were among the metabolic pathways highly regulated by GEN in MV4-11 and Mitochondrial Dysfunction was one of the top signalling pathways modulated by the drug. The same pathways were regulated in HL-60 cells too, although they did not

clear the stringent p-value threshold set for the study. This data strongly alludes to a ROS mediated activity by GEN.

Hence we investigated the levels of ROS production in the cells treated with GEN in comparison to the untreated cells. The assay, performed using the carboxy-H_2DCFDA reagent, indicated an elevated ROS production in both MV4-11 and HL-60 cells. The maximum production was at 72h- consistent with the observation that maximum apoptosis occurs at this time point. This is a completely novel finding and adds a completely new dimension to the treatment of AML by GEN, opening up a multitude of possibilities for combinative therapies.

The pattern of ROS increase was linear in the case of MV4-11. This is in concert with the pattern of decrease in the protein synthesis rate observed in this cell line. However in the case of HL-60, the ROS level increased sharply at 72h and showed minor decrease upon GEN treatment at earlier timepoints. This was again in line with the observed drop in protein synthesis in the HL-60 cells.

5.3.3 The tale of two modes of "death"

5.3.3.1 ROS accumulation culminates in apoptosis

The aforementioned arguments based on empirical data obtained from the proteomic study and functional assays indicate that GEN induces apoptosis in both the MV4-11 and HL-60 cells. The IPA analysis unearthed several pathways related to apoptosis in both the cell lines. Pathways related to cell death such as Induction of Apoptosis by HIV1, Death Receptor Signalling and Myc Mediated Apoptosis Signalling were found regulated in both the cell lines, albeit at a milder *p-value* in HL-60, portending to an apoptotic effect of GEN on these cells.

Apoptosis was assayed using Annexin-V-FITC staining, a technique which has the capability to specifically differentiate between apoptotic and necrotic cells. As the results in Figure 5.9 elucidate, GEN induced apoptosis in both MV4-11 and HL-60 cells, with the effect peaking at 72h. This observation is further backed up by the trypan blue counting results, which demonstrate the cytotoxic effect of GEN in AML.

Thus we can conclusively say that GEN potentiated the cells to cell death by shutting down the protein translational machinery, leading to protein synthesis arrest and caused apoptosis in AML cells via ROS mediated mechanism.

5.3.3.2 Caspase dependency paradigm

Apoptosis is the main mode of cell death employed by GEN. We decided to probe deeper into the mechanism of apoptosis initiated by the drug.

Caspase activation is a hallmark of apoptosis. They are so named as they are 'cysteine' proteases that cleave after an 'aspartate' residue in their substrates. They constitute a conserved family of enzymes that irreversibly commit a cell to death. These enzymes participate in a cascade that is triggered in response to proapoptotic signals and culminates in cleavage of a set of proteins, resulting in disassembly of the cell (Thornberry and Lazebnik, 1998). Although there are at least 14 caspases in humans, only a subset of these enzymes is detectably proteolytically activated by various distinct death stimuli in different cell types. Caspase 3 is one of the most important and well studied of this family and is a frequently expressed death protease (Porter and Jänicke, 1999). Caspase 3 and 7 belong to the family of effector caspases, the increased levels of which signal the onset of apoptosis.

The caspase 3/7 levels were assayed in cells treated with GEN. The results were very interesting. We found that while HL-60 cells exhibited a nearly two-fold increase in activated caspase levels upon GEN treatment, while MV4-11 cells showed no such increase. In spite of

the fact that both cell lines underwent apoptosis, caspase activation was restricted to HL-60 cells alone! This shows that MV4-11 cells undergo apoptosis by a caspase independent mechanism.

Several apoptotic mechanisms, independent of caspases have been identified. One such mechanism implicates mitochondria in the release of proapoptotic proteins. The caspase dependent and independent mechanisms can act in tandem in cells (Lorenzo and Susin, 2004). It is important to note that the MV4-11 cells undergo cell death by caspase independent apoptosis and not necrosis as evidenced by the Annexin V FITC staining. Thus there is a duality in the apoptotic effect of GEN in AML. Such a difference arises probably due to the inherent FLT3-ITD mutation in the MV4-11 cells.

5.3.4 Divergent effects of GEN on Cell Cycle Progression

GEN has been known to arrest the cell cycle progression of AML cells and hence inhibit the growth and proliferation of cells (Shen, et al., 2007; Sánchez, et al., 2009). This is characteristic of anti-tumour drugs which cause accumulation of cells in a particular phase of the cell cycle in order to curb the growth of cancer cells.

Literature suggests that GEN effected a G2/M arrest in AML cells, and HL-60 in particular. In our study too, we found that GEN caused a G2/M arrest in HL-60 cells. However in the case of MV4-11, this phenomenon was absent. In fact there was a G1/S arrest at 24 h in MV4-11, in complete contrast to HL-60. This observation is in keeping with the difference in the mode of apoptosis, patterns of ROS increase and protein synthesis decrease observed in the two cell lines.

Thus G2/M arrest induced by GEN is not a generic effect on all AML cells as thought of before. The difference in the FLT3 status of the two cell lines might explain the divergent effects on cell cycle regulation. There have been previous instances of drugs exerting

contradicting effects on the cell cycle based on the presence and absence of FLT3-ITD mutations. In a study conducted on series of AML cells with and without this mutation, it was found that the drug PKC412, a FLT3 inhibitor, arrested the cells with the mutation at the G1 phase and those without the mutation at the G2/M phase of the cell cycle (Odgerel, et al., 2008; Furukawa, et al., 2007). PKC412 was highly cytotoxic to cells containing the mutation, but not very effective against the ones with wild-type FLT3 gene. Thus it is highly possible that the FLT3 mutational status determines to a large degree regulatory effect of GEN on the cell cycle.

5.3.5 Summarising the effects of GEN on AML

Thus, we have studied the effects of GEN on AML in its totality using a two-cell line model. The results are summarised in a tabular form (Table 5.3). The effects of GEN on MV4-11 and HL-60 cells were similar in many ways. The drug generated ROS by elevating the levels of Akt and inhibited protein synthesis by the shutdown the mTOR pathway. These in turn led to cell cycle arrest and apoptosis. However the modes of cell death and growth arrest were divergent in the two cell lines. The processes which differ in the two cell lines by a high degree are highlighted by solid lines and those that differ only by the time of onset are brought into focus by dashed lines.

Table 5.3: Tabular comparison of effects of GEN on the two AML models

EFFECT	MV4-11	HL-60	REMARKS
Cytotoxicity	IC_{50} 20 µm	IC_{50} 30 µm	In the case of MV4-11, GEN exhibits more prolific cytotoxicity
FLT3 status	Abrogates phosphosphorylation of FLT3	p-FLT3 absent	This specific effect on MV4-11 might have a bearing on the downstream effects
mTOR	Down-regulated	Down-regulated	Leads to protein translation arrest
Akt	Up-regulated	Up-regulated	Might lead to increase in ROS levels
ROS levels	Up-regulated (consistently)	Up-regulated (at 72 h, down-regulated or no change at other time points)	HL-60 shows a dip in the ROS levels but bounces back at 72 h. MV4-11 shows an upward trend in the ROS levels consistently
Protein Synthesis rate	Down-regulated (consistently)	Down-regulated (sharply at 72 h, down-regulated or no change at other time points)	Protein synthesis drop dramatically at 72 h in case of HL-60. In MV4-11's case there is a consistent drop in the rate at all time points
Apoptosis – Annexin V FITC assay	Increase in apoptosis	Increase in apoptosis	Consistent with increase in ROS
Caspase assay	No increased caspase activation	More than two-fold increase in activated caspase levels	Mechanism of apoptosis in MV4-11 is caspase independent
Cell cycle analysis	G1 arrest at 24 h	G2/M arrest	Differences in the mode of cell cycle arrest

Compilation of GEN's effects indicated certain key differences in the mode of action of the drug on the two cell lines. The blue dotted line represents those effects which are similar, but vary in their degree between the two cell lines. The solid red lines represent those which are divergent completely.

5.3.6 Examining the role of FLT3 in the story

In spite of the apparent similarity in the overall mechanism of action of GEN in the two model cell lines, the inherent differences surface when we probe in depth. The fact that the two cell lines differ by a mutation in the FLT3 gene, which by itself is capable of leukemogeneis and cancer progression is very significant. Our results prove beyond that the PTK inhibitor GEN is also an effective FLT3 kinase inhibitor and this effect is manifested in the MV4-11 cell line. HL-60 cells are devoid of this mutation and hence such an effect is irrelevant in their context. Hence it is very tempting to view the observed differences through the prism of FLT3 inactivation.

The general mechanism of action of GEN is similar in both the cell lines. Processes such as ROS generation and protein synthesis arrest are common to both cell lines. The causal factors such as mTOR arrest and Akt elevation are also shared by both. However the degree of regulation and time of onset are different for the two models. Previous literature indicates that GEN induces cell cycle arrest and apoptosis in AML. Our study corroborates this fact. However it is very important to note that we found a major difference in the mode of cell cycle regulation and mechanism of apoptosis between the cell lines.

Although baffling, such a difference in the effects of GEN can be explained by incorporating its inhibitory effect on the phosphorylation status of FLT3 in MV4-11. This powerful weapon in GEN's arsenal equips it with an additional method to arrest proliferation of cells. Since FLT3 is a very important kinase for cell growth and proliferation, it has a number of downstream effectors such as STAT5 and RAS/MAPK. Thus a modification to its constitutively activated status would elicit several downstream responses. Such responses would obviously be unique to MV4-11 which contains the mutated FLT3 gene and would not be observed in HL-60 which has the wild-type version.

It is possible that the inhibitory effect of GEN on the FLT3 phosphorylation in MV4-11 makes the cell highly responsive to cytotoxic effects of the drug and hastens the biological

processes such as ROS generation and protein synthesis arrest. The differential effect of drugs on the cell cycle of AML cells with and without FLT3-ITD has been observed previously in a number of studies as cited before (Furukawa, et al., 2007; Odgerel, et al., 2008). The studies also establish that FLT3 inhibitors induce apoptosis in cells with FLT3-ITD cells and not in wild type-FLT3. In our study GEN was effective in inducing apoptosis against both the subsets of AML, albeit by differing mechanisms. Thus the fact that GEN acts as a FLT3 inhibitor in AML adds new meaning to all the observations and provides a plausible explanation to the divergent effects exerted by GEN on certain biological processes in these cell lines.

5.4 Significance and Concluding Remarks

In summary, it is pertinent to note the key findings of this study. GEN exerts anti-proliferative effects on AML cells. It has a novel FLT3 kinase inhibitory function and acts by inhibiting the constitutive phosphorylation of the FLT3 protein in FLT3-ITD cells. Thus, GEN has cytotoxic effects on both the subsets of AML and can hence be used as a generic anti-leukemic drug which would be effective against all patient types irrespective of their mutational status. The drug targets specific functions in AML such as Protein Synthesis, Cell death and Cell growth arrest. It had novel regulatory effects on mTOR (down-regulates); PI3K/Akt (up-regulates); apoptosis related pathways; amino acid biosynthesis pathways, etc. It decreased the protein synthesis levels in both the cell lines. GEN causes ROS mediated apoptosis in AML cells. The apoptosis in MV4-11 cells (FLT3-ITD) was caspase independent while that in HL-60 (wild-type FLT3) was caspase dependent. GEN induced G2/M arrest in the HL-60 cells; it caused G1 arrest in the MV4-11 cells. Hence the drug exhibits a duality in its mode of cell cycle arrest which is dependent on the FLT3 mutational status. Thus with an overall similarity in its mode of action, the dynamics varied between the two cell lines studied. Based upon the empirical data gleaned, we have proposed a mechanism of action of

GEN in AML cells, depicted in Figure 5.12, which summarises the findings from the study in a nutshell.

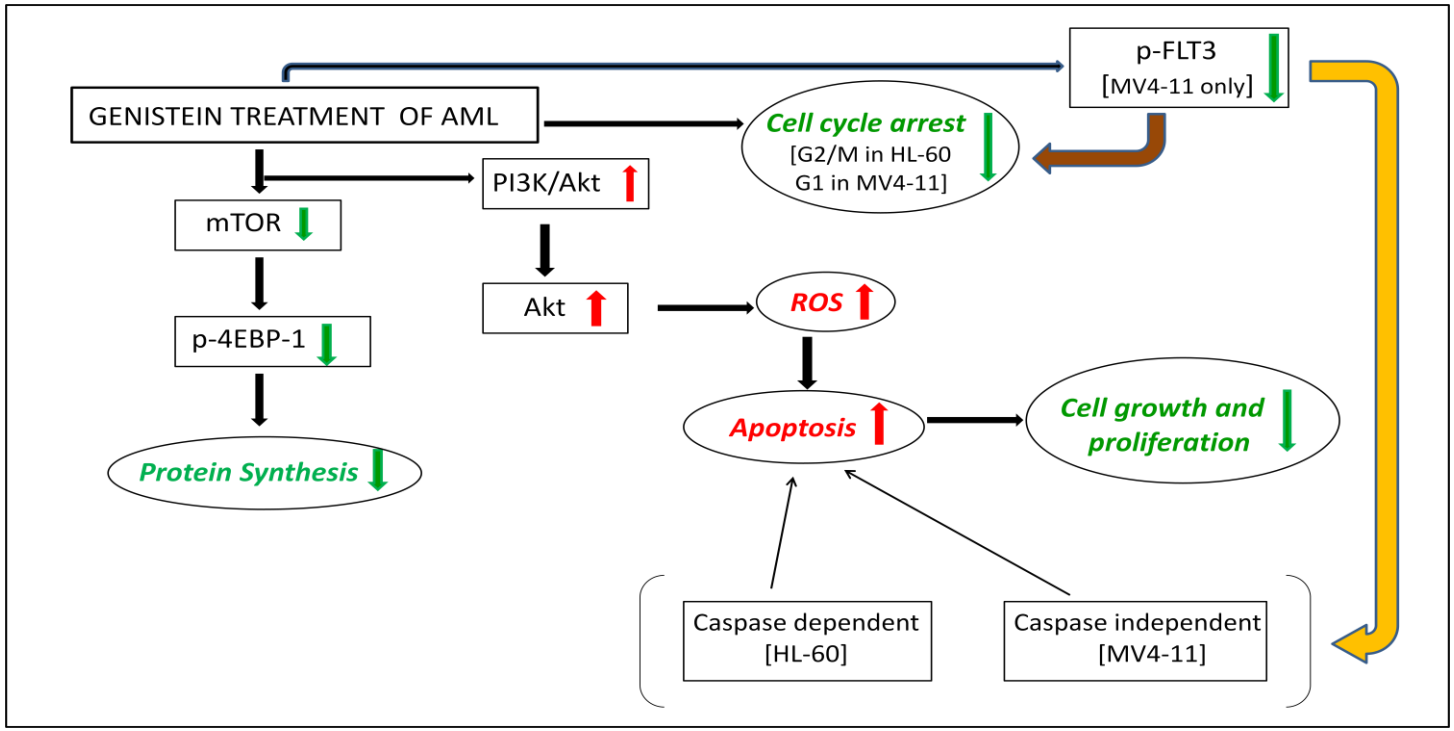

Figure 5.12: Summary of the effects of GEN on AML

Proposed model for the mechanism of action of GEN in AML, based on empirical evidence.

Legend:

Down-regulation

Up-regulation

Putative regulatory effect of FLT3

CHAPTER 6

FUTURE DIRECTIONS

The future augurs well for the development of targeted therapies for AML, which have reduced side-effects, increased cytotoxicity sans drug resistance. Our study helps understand the mechanism of action of two such promising drugs- rapa and GEN. We have used high-throughput methodologies to characterise the anti-leukemic effects of these drugs and have demonstrated the efficacy of such an approach. Hence our study would serve as a template for future studies in this direction. Our investigation provides fresh perspectives to AML therapy and has the potential for further exploration.

6.1 Rapamycin based AML treatment- What lies ahead?

Rapa has far reaching effects on the signalling axis of AML. The fact that its effects are not restricted to just the mTOR pathway is a revelation, paving the way for several future directions.

- Rapa is primarily a cytostatic drug in the context of AML. Hence there are several potential combinatorial strategies that can be tried. Rapa can be coupled to chemotherapeutic agents and apoptosis inducing agents to maximise the anti-cancer effects. Rapa would arrest the cells at the G1 phase and prepare them for cell death by the agent in combination.

- The profiling studies could be carried out on patient samples and primary cells to fathom the effects of rapa in a more fundamental fashion.

- Once the right combinatorial strategy is identified and optimised, clinical trials should be mooted to test its efficacy on patients so that targeted AML therapy can actually become a reality.

6.2 Genistein- Novelties abound and an exciting future!

The discovery that GEN has potent FLT3 inhibitory properties opens the door to a plethora of possibilities.

- Since GEN is primarily a PTK inhibitor which causes reversal of FLT3 phosphorylation, it is imperative to profile the phosphoproteome of the cells treated with the drug. Such a study would throw light on the effects of GEN on the PTM (post-translational modification) of proteins. This would provide more clues to the functional mechanism of the drug as it adds a new dimension to our understanding. We propose to proceed with this set of experiments using a HAMMOC (aliphatic hydroxy acid-modified metal oxide chromatography) technology based mass spectrometric approach (Sugiyama, et al., 2008). The proteins would be labelled intracellularly by SILAC for quantification.

- As the proteomic data implied, metabolic pathways such as oxidative phosphorylation, mitochondrial dysfunction, amino acid biosynthesis and regulation, purine metabolism, etc were highly regulated by GEN. Thus a profile of the metabolites regulated by GEN in AML could pave the way to the understanding of the metabolic functions regulated by the drugs. This would in turn enable the discovery of the intricate link between the signalling and metabolic aspects of the anti-cancer mechanism.

- The metabolic profile thus obtained could be specifically investigated for the regulation of glycolysis, gluconeogenesis and TCA pathways to comprehend the oxygen cycling and energy production dynamics of the cells treated with GEN.

- There is an interesting link between GEN and transcriptional control which needs to be investigated in greater detail. GEN's inhibitory effect on protein translation could imply a similar effect on transcription. Added to this, our observation that purine

metabolism was highly regulated and pentose phosphate pathway was moderately regulated by GEN in both the AML cell lines, bolsters our hypothesis that transcription and gene expression control are important targets of GEN as well.

REFERENCES

Abu-Duhier, F. M., Goodeve, A. C., Wilson, G. A., Gari, M. A., Peake, I. R., Rees, D. C., Vandenberghe, E. A., Winship, P. R. and Reilly, J. T. (2000). FLT3 internal tandem duplication mutations in adult acute myeloid leukaemia define a high-risk group. *Br J Haematol*, **111**(1), 190-195.

Aebersold, R. and Mann, M. (2003). Mass spectrometry-based proteomics. *Nature*, **422**(6928), 198-207.

Agarwala, S. S. and Case, S. (2010). Everolimus (RAD001) in the treatment of advanced renal cell carcinoma: a review. *Oncologist*, **15**(3), 236-245.

Akiyama, T., Ishida, J., Nakagawa, S., Ogawara, H., Watanabe, S., Itoh, N., Shibuya, M. and Fukami, Y. (1987). Genistein, a specific inhibitor of tyrosine-specific protein kinases. *J Biol Chem*, **262**(12), 5592-5595.

Alekel, D. L., Germain, A. S., Peterson, C. T., Hanson, K. B., Stewart, J. W. and Toda, T. (2000). Isoflavone-rich soy protein isolate attenuates bone loss in the lumbar spine of perimenopausal women. *Am J Clin Nutr*, **72**(3), 844-852.

Anderson, N. L. and Anderson, N. G. (1998). Proteome and proteomics: new technologies, new concepts, and new words. *Electrophoresis*, **19**(11), 1853-1861.

Banerjee, S., Li, Y., Wang, Z. and Sarkar, F. H. (2008). Multi-targeted therapy of cancer by genistein. *Cancer Lett*, **269**(2), 226-242.

Bild, A. H., Yao, G., Chang, J. T., Wang, Q., Potti, A., Chasse, D., Joshi, M. B., Harpole, D., Lancaster, J. M., Berchuck, A., Olson, J. A., Marks, J. R., Dressman, H. K., West, M. and Nevins, J. R. (2006). Oncogenic pathway signatures in human cancers as a guide to targeted therapies. *Nature*, **439**(7074), 353-357.

Blackstock, W. P. and Weir, M. P. (1999). Proteomics: quantitative and physical mapping of cellular proteins. *Trends Biotechnol*, **17**(3), 121-127.

Calne, R. Y., Collier, D. S., Lim, S., Pollard, S. G., Samaan, A., White, D. J. and Thiru, S. (1989). Rapamycin for immunosuppression in organ allografting. *Lancet*, **2**(8656), 227.

Cassileth, P. A., Harrington, D. P., Appelbaum, F. R., Lazarus, H. M., Rowe, J. M., Paietta, E., Willman, C., Hurd, D. D., Bennett, J. M., Blume, K. G., Head, D. R. and Wiernik, P. H. (1998). Chemotherapy compared with autologous or allogeneic bone marrow transplantation in the management of acute myeloid leukemia in first remission. *N Engl J Med*, **339**(23), 1649-1656.

Chan, S., Scheulen, M. E., Johnston, S., Mross, K., Cardoso, F., Dittrich, C., Eiermann, W., Hess, D., Morant, R., Semiglazov, V., Borner, M., Salzberg, M., Ostapenko, V., Illiger, H. J., Behringer, D., Bardy-Bouxin, N., Boni, J., Kong, S., Cincotta, M. and Moore, L. (2005). Phase II study of temsirolimus (CCI-779), a novel inhibitor of mTOR, in heavily pretreated patients with locally advanced or metastatic breast cancer. *J Clin Oncol*, **23**(23), 5314-5322.

Clarke, P. A., te Poele, R. and Workman, P. (2004). Gene expression microarray technologies in the development of new therapeutic agents. *Eur J Cancer*, **40**(17), 2560-2591.

Comuzzi, B. and Sadar, M. D. (2006). Proteomic analyses to identify novel therapeutic targets for the treatment of advanced prostate cancer. *Cellscience*, **3**(1), 61-81.

Cruz, M. C., Goldstein, A. L., Blankenship, J., Del Poeta, M., Perfect, J. R., McCusker, J. H., Bennani, Y. L., Cardenas, M. E. and Heitman, J. (2001). Rapamycin and less immunosuppressive analogs are toxic to Candida albicans and Cryptococcus neoformans via FKBP12-dependent inhibition of TOR. *Antimicrob Agents Chemother*, **45**(11), 3162-3170.

Dawczynski, K., Kauf, E., Schlenvoigt, D., Gruhn, B., Fuchs, D. and Zintl, F. (2006). Elevated serum insulin-like growth factor binding protein-2 is associated with a high relapse risk after hematopoietic stem cell transplantation in childhood AML. *Bone Marrow Transplant*, **37**(6), 589-594.

Deschler, B. and Lübbert, M. (2006). Acute myeloid leukemia: epidemiology and etiology. *Cancer*, **107**(9), 2099-2107.

Dixon, R. A. and Ferreira, D. (2002). Genistein. *Phytochemistry*, **60**(3), 205-211.

Dolado, I. and Nebreda, A. R. (2008). AKT and oxidative stress team up to kill cancer cells. *Cancer Cell*, **14**(6), 427-429.

Ecker, K. and Hengst, L. (2009). Skp2: caught in the Akt. *Nat Cell Biol*, **11,** 377-379.

Erasto, P., Bojase-Moleta, G. and Majinda, R. R. T. (2004). Antimicrobial and antioxidant flavonoids from the root wood of Bolusanthus speciosus. *Phytochemistry*, **65**(7), 875-880.

Feller, S. M. and Wong, T. W. (1992). Identification and characterization of a cytosolic protein tyrosine kinase of HeLa cells. *Biochemistry*, **31**(12), 3044-3051.

Fenaux, P., Chastang, C., Chevret, S., Sanz, M., Dombret, H., Archimbaud, E., Fey, M., Rayon, C., Huguet, F., Sotto, J. J., Gardin, C., Makhoul, P. C., Travade, P., Solary, E., Fegueux, N., Bordessoule, D., Miguel, J. S., Link, H., Desablens, B., Stamatoullas, A., Deconinck, E., Maloisel, F., Castaigne, S., Preudhomme, C. and Degos, L. (1999). A randomized comparison of all transretinoic acid (ATRA) followed by chemotherapy and ATRA plus chemotherapy and the role of maintenance therapy in newly diagnosed acute promyelocytic leukemia. The European APL Group. *Blood*, **94**(4), 1192-1200.

Frolov, A., Chahwan, S., Ochs, M., Arnoletti, J. P., Pan, Z. Z., Favorova, O., Fletcher, J., von Mehren, M., Eisenberg, B. and Godwin, A. K. (2003). Response markers and the molecular mechanisms of action of Gleevec in gastrointestinal stromal tumors. *Mol Cancer Ther*, **2**(8), 699-709.

Furukawa, Y., Vu, H. A., Akutsu, M., Odgerel, T., Izumi, T., Tsunoda, S., Matsuo, Y., Kirito, K., Sato, Y., Mano, H. and Kano, Y. (2007). Divergent cytotoxic effects of PKC412 in combination with conventional antileukemic agents in FLT3 mutation-positive versus -negative leukemia cell lines. *Leukemia*, **21**(5), 1005-1014.

Galanis, E., Buckner, J. C., Maurer, M. J., Kreisberg, J. I., Ballman, K., Boni, J., Peralba, J. M., Jenkins, R. B., Dakhil, S. R., Morton, R. F., Jaeckle, K. A., Scheithauer, B. W., Dancey, J., Hidalgo, M., Walsh, D. J. and North Central Cancer Treatment Group (2005). Phase II trial of temsirolimus (CCI-779) in recurrent glioblastoma multiforme: a North Central Cancer Treatment Group Study. *J Clin Oncol*, **23**(23), 5294-5304.

Gan, C. S., Chong, P. K., Pham, T. K. and Wright, P. C. (2007). Technical, experimental, and biological variations in isobaric tags for relative and absolute quantitation (iTRAQ). *J Proteome Res*, **6**(2), 821-827.

Gao, D., Inuzuka, H., Tseng, A. and Wei, W. (2009). Akt finds its new path to regulate cell cycle through modulating Skp2 activity and its destruction by APC/Cdh1. *Cell division*, **4**, 11.

Gilliland, D. G. and Griffin, J. D. (2002). The roles of FLT3 in hematopoiesis and leukemia. *Blood*, **100**(5), 1532-1542.

Gilliland, D. G. and Tallman, M. S. (2002). Focus on acute leukemias. *Cancer Cell*, **1**(5), 417-420.

Golub, T. R., Slonim, D. K., Tamayo, P., Huard, C., Gaasenbeek, M., Mesirov, J. P., Coller, H., Loh, M. L., Downing, J. R., Caligiuri, M. A., Bloomfield, C. D. and Lander, E. S. (1999). Molecular classification of cancer: class discovery and class prediction by gene expression monitoring. *Science*, **286**(5439), 531-537.

Gorin, N. C. (1998). Autologous stem cell transplantation in acute myelocytic leukemia. *Blood*, **92**(4), 1073-1090.

Grandage, V. L., Gale, R. E., Linch, D. C. and Khwaja, A. (2005). PI3-kinase/Akt is constitutively active in primary acute myeloid leukaemia cells and regulates survival and chemoresistance via NF-kappaB, Mapkinase and p53 pathways. *Leukemia*, **19**(4), 586-594.

Griffiths, S. D., Burthem, J., Unwin, R. D., Holyoake, T. L., Melo, J. V., Lucas, G. S. and Whetton, A. D. (2007). The use of isobaric tag peptide labeling (iTRAQ) and mass spectrometry to examine rare, primitive hematopoietic cells from patients with chronic myeloid leukemia. *Mol Biotechnol*, **36**(2), 81-89.

Hainsworth, J. D., Spigel, D. R., Burris, H. A., Waterhouse, D., Clark, B. L. and Whorf, R. (2010). Phase II trial of bevacizumab and everolimus in patients with advanced renal cell carcinoma. *J Clin Oncol*, **28**(13), 2131-2136.

Hattori, H., Matsuzaki, A., Suminoe, A., Koga, Y., Tashiro, K. and Hara, T. (2006). Identification of novel genes with prognostic value in childhood leukemia using cDNA microarray and quantitative RT-PCR. *Pediatr Hematol Oncol*, **23**(2), 115-127.

Hershko, D., Bornstein, G., Ben-Izhak, O., Carrano, A., Pagano, M., Krausz, M. M. and Hershko, A. (2001). Inverse relation between levels of p27(Kip1) and of its ubiquitin ligase subunit Skp2 in colorectal carcinomas. *Cancer*, **91**(9), 1745-1751.

Hwang, J. T., Ha, J. and Park, O. J. (2005). Combination of 5-fluorouracil and genistein induces apoptosis synergistically in chemo-resistant cancer cells through the modulation of AMPK and COX-2 signaling pathways. *Biochem Biophys Res Commun*, **332**(2), 433-440.

Hwang, J., Hodis, H. N. and Sevanian, A. (2001). Soy and alfalfa phytoestrogen extracts become potent low-density lipoprotein antioxidants in the presence of acerola cherry extract. *J Agric Food Chem*, **49**(1), 308-314.

Ito, T., Warnken, S. P. and May, W. S. (1999). Protein synthesis inhibition by flavonoids: roles of eukaryotic initiation factor 2alpha kinases. *Biochem Biophys Res Commun*, **265**(2), 589-594.

Johnson, B. E., Jackman, D. and Jänne, P. A. (2007). Rationale for a phase I trial of erlotinib and the mammalian target of rapamycin inhibitor everolimus (RAD001) for patients with relapsed non small cell lung cancer. *Clin Cancer Res*, **13**(15 Pt 2), s4628-s4631.

Johnston, P. B., Inwards, D. J., Colgan, J. P., Laplant, B. R., Kabat, B. F., Habermann, T. M., Micallef, I. N., Porrata, L. F., Ansell, S. M., Reeder, C. B., Roy, V. and Witzig, T. E. (2010). A Phase II trial of the oral mTOR inhibitor everolimus in relapsed Hodgkin lymphoma. *Am J Hematol*, **85**(5), 320-324.

Jungblut, P. R., Zimny-Arndt, U., Zeindl-Eberhart, E., Stulik, J., Koupilova, K., Pleissner, K. P., Otto, A., Müller, E. C., Sokolowska-Köhler, W., Grabher, G. and Stöffler, G. (1999). Proteomics in human disease: cancer, heart and infectious diseases. *Electrophoresis*, **20**(10), 2100-2110.

Kadara, H., Lacroix, L., Behrens, C., Solis, L., Gu, X., Lee, J. J., Tahara, E., Lotan, D., Hong, W. K., Wistuba, I. I. and Lotan, R. (2009). Identification of gene signatures and molecular markers for human lung cancer prognosis using an in vitro lung carcinogenesis system. *Cancer prevention research (Philadelphia, Pa.)*, **2**(8), 702-711.

Kawakami, K., Enokida, H., Tachiwada, T., Nishiyama, K., Seki, N. and Nakagawa, M. (2007). Increased SKP2 and CKS1 gene expression contributes to the progression of human urothelial carcinoma. *J Urol*, **178**(1), 301-307.

Kazi, A., Daniel, K. G., Smith, D. M., Kumar, N. B. and Dou, Q. P. (2003). Inhibition of the proteasome activity, a novel mechanism associated with the tumor cell apoptosis-inducing ability of genistein. *Biochem Pharmacol*, **66**(6), 965-976.

Kerr, J. R., Barah, F., Cunniffe, V. S., Smith, J., Vallely, P. J., Will, A. M., Wynn, R. F., Stevens, R. F., Taylor, G. M., Cleator, G. M. and Eden, O. B. (2003). Association of acute parvovirus B19 infection with new onset of acute lymphoblastic and myeloblastic leukaemia. *J Clin Pathol*, **56**(11), 873-875.

Kiyoi, H., Towatari, M., Yokota, S., Hamaguchi, M., Ohno, R., Saito, H. and Naoe, T. (1998). Internal tandem duplication of the FLT3 gene is a novel modality of elongation mutation which causes constitutive activation of the product. *Leukemia*, **12**(9), 1333-1337.

Lamartiniere, C. A., Cotroneo, M. S., Fritz, W. A., Wang, J., Mentor-Marcel, R. and Elgavish, A. (2002). Genistein chemoprevention: timing and mechanisms of action in murine mammary and prostate. *J Nutr*, **132**(3), 552S-558S.

Lee, H. P., Gourley, L., Duffy, S. W., Estéve, J., Lee, J. and Day, N. E. (1991). Dietary effects on breast-cancer risk in Singapore. *Lancet*, **337**(8751), 1197-1200.

Levis, M., Tse, K. F., Smith, B. D., Garrett, E. and Small, D. (2001). A FLT3 tyrosine kinase inhibitor is selectively cytotoxic to acute myeloid leukemia blasts harboring FLT3 internal tandem duplication mutations. *Blood*, **98**(3), 885-887.

Li, Z., Lin, Q., Chen, J., Wu, J. L., Lim, T. K., Loh, S. S., Tang, X. and Hew, C. L. (2007). Shotgun identification of the structural proteome of shrimp white spot syndrome virus and iTRAQ differentiation of envelope and nucleocapsid subproteomes. *Mol Cell Proteomics*, **6**(9), 1609-1620.

Look, M., Gao, F., Low, C. H. and Nambiar, R. (2001). Gastric cancer in Singapore. *Gastric Cancer*, **4**(4), 219-222.

Lorenzo, H. K. and Susin, S. A. (2004). Mitochondrial effectors in caspase-independent cell death. *FEBS Lett*, **557**(1-3), 14-20.

Martelli, A. M., Nyåkern, M., Tabellini, G., Bortul, R., Tazzari, P. L., Evangelisti, C. and Cocco, L. (2006). Phosphoinositide 3-kinase/Akt signaling pathway and its therapeutical implications for human acute myeloid leukemia. *Leukemia*, **20**(6), 911-928.

Martin, J. L. and Baxter, R. C. (2007). Expression of insulin-like growth factor binding protein-2 by MCF-7 breast cancer cells is regulated through the phosphatidylinositol 3-kinase/AKT/mammalian target of rapamycin pathway. *Endocrinology*, **148**(5), 2532-2541.

Mayer, R. J., Davis, R. B., Schiffer, C. A., Berg, D. T., Powell, B. L., Schulman, P., Omura, G. A., Moore, J. O., McIntyre, O. R. and Frei, E. (1994). Intensive postremission chemotherapy in adults with acute myeloid leukemia. Cancer and Leukemia Group B. *N Engl J Med*, **331**(14), 896-903.

Meric-Bernstam, F. and Gonzalez-Angulo, A. M. (2009). Targeting the mTOR signaling network for cancer therapy. *J Clin Oncol*, **27**(13), 2278-2287.

Merz-Demlow, B. E., Duncan, A. M., Wangen, K. E., Xu, X., Carr, T. P., Phipps, W. R. and Kurzer, M. S. (2000). Soy isoflavones improve plasma lipids in normocholesterolemic, premenopausal women. *Am J Clin Nutr*, **71**(6), 1462-1469.

Min, Y. H., Cheong, J. W., Lee, M. H., Kim, J. Y., Lee, S. T., Hahn, J. S. and Ko, Y. W. (2004). Elevated S-phase kinase-associated protein 2 protein expression in acute myelogenous leukemia: its association with constitutive phosphorylation of phosphatase and tensin homologue protein and poor prognosis. *Clin Cancer Res*, **10**(15), 5123-5130.

Mita, M. M., Mita, A. and Rowinsky, E. K. (2003). The molecular target of rapamycin (mTOR) as a therapeutic target against cancer. *Cancer Biol Ther*, **2**(4 Suppl 1), S169-S177.

Mita, M. M., Mita, A. C., Chu, Q. S., Rowinsky, E. K., Fetterly, G. J., Goldston, M., Patnaik, A., Mathews, L., Ricart, A. D., Mays, T., Knowles, H., Rivera, V. M., Kreisberg, J., Bedrosian, C. L. and Tolcher, A. W. (2008). Phase I trial of the novel mammalian target of rapamycin inhibitor deforolimus (AP23573; MK-8669) administered intravenously daily for 5 days every 2 weeks to patients with advanced malignancies. *J Clin Oncol*, **26**(3), 361-367.

Mitsiades, C. S., Mitsiades, N. S., McMullan, C. J., Poulaki, V., Shringarpure, R., Akiyama, M., Hideshima, T., Chauhan, D., Joseph, M., Libermann, T. A., García-Echeverría, C., Pearson, M. A., Hofmann, F., Anderson, K. C. and Kung, A. L. (2004). Inhibition of the insulin-like growth factor receptor-1 tyrosine kinase activity as a therapeutic strategy for multiple myeloma, other hematologic malignancies, and solid tumors. *Cancer Cell*, **5**(3), 221-230.

Mohnike, K. L., Kluba, U., Mittler, U., Aumann, V., Vorwerk, P. and Blum, W. F. (1996). Serum levels of insulin-like growth factor-I, -II and insulin-like growth factor binding proteins -2 and -3 in children with acute lymphoblastic leukaemia. *Eur J Pediatr*, **155**(2), 81-86.

Morrison, V. A., Rai, K. R., Peterson, B. L., Kolitz, J. E., Elias, L., Appelbaum, F. R., Hines, J. D., Shepherd, L., Larson, R. A. and Schiffer, C. A. (2002). Therapy-related myeloid leukemias are observed in patients with chronic lymphocytic leukemia after treatment with fludarabine and chlorambucil: results of an intergroup study, cancer and leukemia group B 9011. *J Clin Oncol*, **20**(18), 3878-3884.

Müllner, S., Neumann, T. and Lottspeich, F. (1998). Proteomics--a new way for drug target discovery. *Arzneimittelforschung*, **48**(1), 93-95.

Nakao, M., Yokota, S., Iwai, T., Kaneko, H., Horiike, S., Kashima, K., Sonoda, Y., Fujimoto, T. and Misawa, S. (1996). Internal tandem duplication of the flt3 gene found in acute myeloid leukemia. *Leukemia*, **10**(12), 1911-1918.

Nogueira, V., Park, Y., Chen, C. C., Xu, P. Z., Chen, M. L., Tonic, I., Unterman, T. and Hay, N. (2008). Akt determines replicative senescence and oxidative or oncogenic premature senescence and sensitizes cells to oxidative apoptosis. *Cancer Cell*, **14**(6), 458-470.

Nunoda, K., Tauchi, T., Takaku, T., Okabe, S., Akahane, D., Sashida, G., Ohyashiki, J. H. and Ohyashiki, K. (2007). Identification and functional signature of genes regulated by structurally different ABL kinase inhibitors. *Oncogene*, **26**(28), 4179-4188.

Odgerel, T., Kikuchi, J., Wada, T., Shimizu, R., Futaki, K., Kano, Y. and Furukawa, Y. (2008). The FLT3 inhibitor PKC412 exerts differential cell cycle effects on leukemic cells depending on the presence of FLT3 mutations. *Oncogene*, **27**(22), 3102-3110.

Ouchi, H., Ishiguro, H., Ikeda, N., Hori, M., Kubota, Y. and Uemura, H. (2005). Genistein induces cell growth inhibition in prostate cancer through the suppression of telomerase activity. *Int J Urol*, **12**(1), 73-80.

Panwalkar, A., Verstovsek, S. and Giles, F. J. (2004). Mammalian target of rapamycin inhibition as therapy for hematologic malignancies. *Cancer*, **100**(4), 657-666.

Peterson, G. (1995). Evaluation of the biochemical targets of genistein in tumor cells. *J Nutr*, **125**(3 Suppl), 784S-789S.

Pierce, A., Unwin, R. D., Evans, C. A., Griffiths, S., Carney, L., Zhang, L., Jaworska, E., Lee, C. F., Blinco, D., Okoniewski, M. J., Miller, C. J., Bitton, D. A., Spooncer, E. and Whetton, A. D. (2008). Eight-channel iTRAQ enables comparison of the activity of six leukemogenic tyrosine kinases. *Mol Cell Proteomics*, **7**(5), 853-863.

Porter, A. G. and Jänicke, R. U. (1999). Emerging roles of caspase-3 in apoptosis. *Cell Death Differ*, **6**(2), 99-104.

Qian, M., Sleat, D. E., Zheng, H., Moore, D. and Lobel, P. (2008). Proteomics analysis of serum from mutant mice reveals lysosomal proteins selectively transported by each of the two mannose 6-phosphate receptors. *Mol Cell Proteomics*, **7**(1), 58-70.

Quezada, G., Kopp, L., Estey, E. and Wells, R. J. (2008). All-trans-retinoic acid and arsenic trioxide as initial therapy for acute promyelocytic leukemia. *Pediatr Blood Cancer*, **51**(1), 133-135.

Rankin, E. B. and Giaccia, A. J. (2008). The role of hypoxia-inducible factors in tumorigenesis. *Cell Death Differ*, **15**(4), 678-685.

Raynal, N. J. M., Momparler, L., Charbonneau, M. and Momparler, R. L. (2008). Antileukemic activity of genistein, a major isoflavone present in soy products. *J Nat Prod*, **71**(1), 3-7.

Récher, C., Beyne-Rauzy, O., Demur, C., Chicanne, G., Dos Santos, C., Mas, V. M. D., Benzaquen, D., Laurent, G., Huguet, F. and Payrastre, B. (2005). Antileukemic activity of rapamycin in acute myeloid leukemia. *Blood*, **105**(6), 2527-2534.

Ross, M. E., Mahfouz, R., Onciu, M., Liu, H. C., Zhou, X., Song, G., Shurtleff, S. A., Pounds, S., Cheng, C., Ma, J., Ribeiro, R. C., Rubnitz, J. E., Girtman, K., Williams, W. K., Raimondi, S. C., Liang, D. C., Shih, L. Y., Pui, C. H. and Downing, J. R. (2004). Gene expression profiling of pediatric acute myelogenous leukemia. *Blood*, **104**(12), 3679-3687.

Sabatini, D. M., Erdjument-Bromage, H., Lui, M., Tempst, P. and Snyder, S. H. (1994). RAFT1: a mammalian protein that binds to FKBP12 in a rapamycin-dependent fashion and is homologous to yeast TORs. *Cell*, **78**(1), 35-43.

Salvi, M., Brunati, A. M., Clari, G. and Toninello, A. (2002). Interaction of genistein with the mitochondrial electron transport chain results in opening of the membrane transition pore. *Biochim Biophys Acta*, **1556**(2-3), 187-196.

Sánchez, Y., Amrán, D., de Blas, E. and Aller, P. (2009). Regulation of genistein-induced differentiation in human acute myeloid leukaemia cells (HL60, NB4) Protein kinase modulation and reactive oxygen species generation. *Biochem Pharmacol*, **77**(3), 384-396.

Sánchez, Y., Amrán, D., Fernández, C., de Blas, E. and Aller, P. (2008). Genistein selectively potentiates arsenic trioxide-induced apoptosis in human leukemia cells via reactive oxygen species generation and activation of reactive oxygen species-inducible protein kinases (p38-MAPK, AMPK). *Int J Cancer*, **123**(5), 1205-1214.

Sasco, A. J., Secretan, M. B. and Straif, K. (2004). Tobacco smoking and cancer: a brief review of recent epidemiological evidence. *Lung Cancer*, **45** Suppl 2, S3-S9.

Schinke-Braun, M. and Couget, J. A. (2007). Expression profiling using affymetrix genechip probe arrays. *Methods Mol Biol*, **366**, 13-40.

Schmelzle, T. and Hall, M. N. (2000). TOR, a central controller of cell growth. *Cell*, **103**(2), 253-262.

Sehgal, S. N. (1998). Rapamune (RAPA, rapamycin, sirolimus): mechanism of action immunosuppressive effect results from blockade of signal transduction and inhibition of cell cycle progression. *Clin Biochem*, **31**(5), 335-340.

Sehgal, S. N. (2003). Sirolimus: its discovery, biological properties, and mechanism of action. *Transplant Proc*, **35**(3 Suppl), 7S-14S.

Shankar, D. B., Li, J., Tapang, P., Owen McCall, J., Pease, L. J., Dai, Y., Wei, R. Q., Albert, D. H., Bouska, J. J., Osterling, D. J., Guo, J., Marcotte, P. A., Johnson, E. F., Soni, N., Hartandi, K., Michaelides, M. R., Davidsen, S. K., Priceman, S. J., Chang, J. C., Rhodes, K., Shah, N., Moore, T. B., Sakamoto, K. M. and Glaser, K. B. (2007). ABT-869, a multitargeted receptor tyrosine kinase inhibitor: inhibition of FLT3 phosphorylation and signaling in acute myeloid leukemia. *Blood*, **109**(8), 3400-3408.

She, M. R., Li, J. G., Guo, K. Y., Lin, W., Du, X. and Niu, X. Q. (2007). Requirement of reactive oxygen species generation in apoptosis of leukemia cells induced by 2-methoxyestradiol. *Acta Pharmacol Sin*, **28**(7), 1037-1044.

Shen, J., Tai, Y. C., Zhou, J., Stephen Wong, C. H., Cheang, P. T. S., Fred Wong, W. S., Xie, Z., Khan, M., Han, J. H. and Chen, C. S. (2007). Synergistic antileukemia effect of genistein and chemotherapy in mouse xenograft model and potential mechanism through MAPK signaling. *Exp Hematol*, **35**(1), 75-83.

Sievers, E. L., Larson, R. A., Stadtmauer, E. A., Estey, E., Löwenberg, B., Dombret, H., Karanes, C., Theobald, M., Bennett, J. M., Sherman, M. L., Berger, M. S., Eten, C. B., Loken, M. R., van Dongen, J. J., Bernstein, I. D., Appelbaum, F. R. and Mylotarg Study Group (2001). Efficacy and safety of gemtuzumab ozogamicin in patients with CD33-positive acute myeloid leukemia in first relapse. *J Clin Oncol*, **19**(13), 3244-3254.

Simon, H. U., Haj-Yehia, A. and Levi-Schaffer, F. (2000). Role of reactive oxygen species (ROS) in apoptosis induction. *Apoptosis*, **5**(5), 415-418.

Simon, M. C., Liu, L., Barnhart, B. C. and Young, R. M. (2008). Hypoxia-induced signaling in the cardiovascular system. *Annu Rev Physiol*, **70**, 51-71.

Smith, M., Barnett, M., Bassan, R., Gatta, G., Tondini, C. and Kern, W. (2004). Adult acute myeloid leukaemia. *Crit Rev Oncol Hematol*, **50**(3), 197-222.

Song, G., Ouyang, G. and Bao, S. (2005). The activation of Akt/PKB signaling pathway and cell survival. *J Cell Mol Med*, **9**(1), 59-71.

Tamburini, J., Green, A. S., Bardet, V., Chapuis, N., Park, S., Willems, L., Uzunov, M., Ifrah, N., Dreyfus, F., Lacombe, C., Mayeux, P. and Bouscary, D. (2009). Protein synthesis is resistant to rapamycin and constitutes a promising therapeutic target in acute myeloid leukemia. *Blood*, **114**(8), 1618-1627.

Tamburini, J., Green, A. S., Chapuis, N., Bardet, V., Lacombe, C., Mayeux, P. and Bouscary, D. (2009). Targeting translation in acute myeloid leukemia: a new paradigm for therapy? *Cell Cycle*, **8**(23), 3893-3899.

Tan, H. T., Tan, S., Lin, Q., Lim, T. K., Hew, C. L. and Chung, M. C. M. (2008). Quantitative and temporal proteome analysis of butyrate-treated colorectal cancer cells. *Mol Cell Proteomics*, **7**(6), 1174-1185.

Thornberry, N. A. and Lazebnik, Y. (1998). Caspases: enemies within. *Science*, **281**(5381), 1312-1316.

Trachootham, D., Zhou, Y., Zhang, H., Demizu, Y., Chen, Z., Pelicano, H., Chiao, P. J., Achanta, G., Arlinghaus, R. B., Liu, J. and Huang, P. (2006). Selective killing of oncogenically transformed cells through a ROS-mediated mechanism by beta-phenylethyl isothiocyanate. *Cancer Cell*, **10**(3), 241-252.

Traganos, F., Ardelt, B., Halko, N., Bruno, S. and Darzynkiewicz, Z. (1992). Effects of genistein on the growth and cell cycle progression of normal human lymphocytes and human leukemic MOLT-4 and HL-60 cells. *Cancer Res*, **52**(22), 6200-6208.

Valk, P. J. M., Verhaak, R. G. W., Beijen, M. A., Erpelinck, C. A. J., Barjesteh van Waalwijk van Doorn-Khosrovani, S., Boer, J. M., Beverloo, H. B., Moorhouse, M. J., van der Spek, P. J., Löwenberg, B. and Delwel, R. (2004). Prognostically useful gene-expression profiles in acute myeloid leukemia. *N Engl J Med*, **350**(16), 1617-1628.

Verma, D., O'Brien, S., Thomas, D., Faderl, S., Koller, C., Pierce, S., Kebriaei, P., Garcia-Manero, G., Cortes, J., Kantarjian, H. and Ravandi, F. (2009). Therapy-related acute myelogenous leukemia and myelodysplastic syndrome in patients with acute lymphoblastic leukemia treated with the hyperfractionated cyclophosphamide, vincristine, doxorubicin, and dexamethasone regimens. *Cancer*, **115**(1), 101-106.

Wei, X., Guo, W., Wu, S., Wang, L., Huang, P., Liu, J. and Fang, B. (2010). Oxidative stress in NSC-741909-induced apoptosis of cancer cells. *J Transl Med*, **8**, 37.

Wong, G. K., Griffith, S., Kojima, I. and Demain, A. L. (1998). Antifungal activities of rapamycin and its derivatives, prolylrapamycin, 32-desmethylrapamycin, and 32-desmethoxyrapamycin. *J Antibiot (Tokyo)*, **51**(5), 487-491.

Xu, Q., Simpson, S. E., Scialla, T. J., Bagg, A. and Carroll, M. (2003). Survival of acute myeloid leukemia cells requires PI3 kinase activation. *Blood*, **102**(3), 972-980.

Yang, G., Ayala, G., De Marzo, A., Tian, W., Frolov, A., Wheeler, T. M., Thompson, T. C. and Harper, J. W. (2002). Elevated Skp2 protein expression in human prostate cancer: association with loss of the cyclin-dependent kinase inhibitor p27 and PTEN and with reduced recurrence-free survival. *Clin Cancer Res*, **8**(11), 3419-3426.

Yang, Q. and Guan, K. L. (2007). Expanding mTOR signaling. *Cell Res*, **17**(8), 666-681.

Yasui, H., Hideshima, T., Richardson, P. G. and Anderson, K. C. (2006). Novel therapeutic strategies targeting growth factor signalling cascades in multiple myeloma. *Br J Haematol*, **132**(4), 385-397.

Zhang, D., Tai, Y. C., Wong, C. H. S., Tai, L. K., Koay, E. S. C. and Chen, C. S. (2007). Molecular response of leukemia HL-60 cells to genistein treatment, a proteomics study. *Leuk Res*, **31**(1), 75-82.

Zhao, R., Xiang, N., Domann, F. E. and Zhong, W. (2009). Effects of selenite and genistein on G2/M cell cycle arrest and apoptosis in human prostate cancer cells. *Nutr Cancer*, **61**(3), 397-407.

Zhou, Y., Hileman, E. O., Plunkett, W., Keating, M. J. and Huang, P. (2003). Free radical stress in chronic lymphocytic leukemia cells and its role in cellular sensitivity to ROS-generating anticancer agents. *Blood*, **101**(10), 4098-4104.

Zhu, T. (2003). Global analysis of gene expression using GeneChip microarrays. *Curr Opin Plant Biol*, **6**(5), 418-425.

Zieske, L. R. (2006). A perspective on the use of iTRAQ reagent technology for protein complex and profiling studies. *J Exp Bot*, **57**(7), 1501-1508.

Zittoun, R. A., Mandelli, F., Willemze, R., de Witte, T., Labar, B., Resegotti, L., Leoni, F., Damasio, E., Visani, G. and Papa, G. (1995). Autologous or allogeneic bone marrow transplantation compared with intensive chemotherapy in acute myelogenous leukemia. European Organization for Research and Treatment of Cancer (EORTC) and the Gruppo Italiano Malattie Ematologiche Maligne dell'Adulto (GIMEMA) Leukemia Cooperative Groups. *N Engl J Med*, **332**(4), 217-223.

zur Hausen, H. (2009). Papillomaviruses in the causation of human cancers - a brief historical account. *Virology*, **384**(2), 260-265.

APPENDIX I

TABLE A: Proteins significantly regulated in HL-60 cells upon GEN treatment as identified by 8-plex iTRAQ

ACCESSION #	NAME	HL-60-AVERAGE RATIO
IPI00515061.3	HIST1H2BJ Histone H2B type 1-J	0.213825
IPI00926977.1	PSMC6 proteasome 26S ATPase subunit 6	0.266575
IPI00816460.2	DST Isoform 2 of Bullous pemphigoid antigen 1, isoforms 1/2/3/4/5/8 (Fragment)	0.26945
IPI00291764.5	HIST1H2AH;HIST1H2AI;HIST1H2AK;HIST1H2AJ;HIST1H2AG;HIST1H2AL;HIST1H2AM Histone H2A type 1	0.27375
IPI00032460.3	LSM2 U6 snRNA-associated Sm-like protein LSm2	0.281825
IPI00748149.2	CDC20B Isoform 1 of Cell division cycle protein 20 homolog B	0.301425
IPI00908443.1	DYSF Isoform 2 of Dysferlin	0.3435
IPI00941730.1	ARHGAP1 cDNA FLJ60782, highly similar to Rho-GTPase-activating protein 1	0.38385
IPI00885176.1	C3orf77 Uncharacterized protein C3orf77	0.3853
IPI00019927.2	PSMD7 26S proteasome non-ATPase regulatory subunit 7	0.3934
IPI00290460.3	EIF3G Eukaryotic translation initiation factor 3 subunit G	0.437
IPI00010402.2	SH3BGRL3 Putative uncharacterized protein	0.4979
IPI00026546.1	PAFAH1B2 Platelet-activating factor acetylhydrolase IB subunit beta	0.510225
IPI00873383.1	ST6GALNAC3 Putative uncharacterized protein ST6GALNAC3 (Fragment)	0.5439
IPI00746438.2	RPL11 Isoform 2 of 60S ribosomal protein L11	0.551725
IPI00946481.1	MBNL1 Protein	0.5601
IPI00301058.5	VASP Vasodilator-stimulated phosphoprotein	0.57225
IPI00456758.4	RPL27A 60S ribosomal protein L27a	0.6046
IPI00940423.1	LCK Isoform Long of Proto-oncogene tyrosine-protein kinase LCK	0.610275

IPI00291419.6	ACAT2 cDNA FLJ53975, highly similar to Acetyl-CoA acetyltransferase, cytosolic	0.6127
IPI00645339.2	HP1BP3 39 kDa protein	0.62615
IPI00219446.5	PEBP1 Phosphatidylethanolamine-binding protein 1	0.62995
IPI00216047.3	SMARCC2 Isoform 1 of SWI/SNF complex subunit SMARCC2	0.6314
IPI00945507.1	SUCLG2 48 kDa protein	0.63535
IPI00011913.1	HNRNPA0 Heterogeneous nuclear ribonucleoprotein A0	0.638275
IPI00917298.1	RPL31 Putative uncharacterized protein RPL31	0.641925
IPI00397571.1	NSFL1C Isoform 3 of NSFL1 cofactor p47	0.645225
IPI00900327.2	PCBP2 cDNA FLJ58339, highly similar to Poly(rC)-binding protein 2	0.650025
IPI00942600.1	EIF4B 70 kDa protein	0.671575
IPI00922415.1	SSBP1 cDNA FLJ51825, highly similar to Single-stranded DNA-binding protein, mitochondrial	0.6737
IPI00217950.5	HMGN2 Non-histone chromosomal protein HMG-17	0.67555
IPI00010270.1	RAC2 Ras-related C3 botulinum toxin substrate 2	0.676325
IPI00217030.10	RPS4X 40S ribosomal protein S4, X isoform	0.687875
IPI00106491.3	MRTO4 mRNA turnover protein 4 homolog	0.69085
IPI00216659.1	RBM8A Isoform 2 of RNA-binding protein 8A	0.69115
IPI00872379.1	ANXA5 Putative uncharacterized protein ANXA5 (Fragment)	0.692525
IPI00176637.5	LOC728350;EIF2S2 Eukaryotic translation initiation factor 2 subunit 2-like protein	0.69385
IPI00412607.6	RPL35 60S ribosomal protein L35	0.7008
IPI00068430.1	SNRPEL1 Putative small nuclear ribonucleoprotein polypeptide E-like protein 1	0.7014
IPI00014263.1	EIF4H Isoform Long of Eukaryotic translation initiation factor 4H	0.7031
IPI00220503.9	DCTN2 dynactin 2	0.712225
IPI00005966.6	NDUFA12 13kDa differentiation-associated protein variant (Fragment)	0.714525
IPI00026665.2	QARS cDNA FLJ75085, highly similar to Homo sapiens glutaminyl-tRNA synthetase (QARS), mRNA	0.714575
IPI00420108.5	DLST;DLSTP Dihydrolipoyllysine-residue succinyltransferase component of 2-oxoglutarate dehydrogenase complex, mitochondrial	0.720325
IPI00099550.1	UBQLN1 Isoform 1 of Ubiquilin-1	0.721625

IPI00026781.2	FASN Fatty acid synthase	0.727575
IPI00004839.1	CRKL Crk-like protein	0.7385
IPI00794978.1	MRPL47 Isoform 2 of 39S ribosomal protein L47, mitochondrial	0.73905
IPI00879531.1	- 9 kDa protein	0.744025
IPI00219622.3	PSMA2 Proteasome subunit alpha type-2	0.74715
IPI00903204.1	RPS24 15 kDa protein	0.748
IPI00647915.1	TAGLN2 24 kDa protein	0.7486
IPI00873466.1	HPRT1 Putative uncharacterized protein HPRT1	0.7586
IPI00940950.1	RPL10 Ribosomal protein L10 (Fragment)	0.759
IPI00872814.1	MSN Putative uncharacterized protein MSN (Fragment)	0.761975
IPI00643317.3	HMGB3 21 kDa protein	0.767075
IPI00006658.4	PIN4 Isoform 2 of Peptidyl-prolyl cis-trans isomerase NIMA-interacting 4	0.768525
IPI00945691.1	PRPS1 Ribose-phosphate pyrophosphokinase (Fragment)	0.769625
IPI00303882.2	PLIN3 Isoform B of Mannose-6-phosphate receptor-binding protein 1	0.772075
IPI00908543.1	PPP2R1A cDNA FLJ56133, highly similar to Serine/threonine-protein phosphatase 2A 65 kDa regulatory subunit A alpha isoform	1.3003
IPI00815770.2	SNX3 Isoform 1 of Sorting nexin-3	1.301825
IPI00000816.1	YWHAE 14-3-3 protein epsilon	1.303925
IPI00878984.1	DDT 14 kDa protein	1.31175
IPI00947458.1	PCMT1 protein-L-isoaspartate (D-aspartate) O-methyltransferase 1	1.31645
IPI00947554.1	RP6-213H19.1 cDNA FLJ90669 fis, clone PLACE1005519, moderately similar to Homo sapiens STE20-like kinase 3 (mst-3) mRNA	1.319175
IPI00412737.1	WARS tryptophanyl-tRNA synthetase isoform b	1.321975
IPI00002569.3	EIF4EBP1 Eukaryotic translation initiation factor 4E-binding protein 1	1.322325
IPI00165393.1	ANP32E Acidic leucine-rich nuclear phosphoprotein 32 family member E	1.32335
IPI00853163.1	TYMP 46 kDa protein	1.34025
IPI00399142.5	SURF4 Surfeit 4	1.36515
IPI00789285.1	TXNDC17 11 kDa protein	1.366775

IPI00375380.4	PSMD13 proteasome 26S non-ATPase subunit 13 isoform 2	1.374175
IPI00026833.4	ADSS Adenylosuccinate synthetase isozyme 2	1.376875
IPI00893362.1	RYR3 Putative uncharacterized protein RYR3	1.3773
IPI00556451.2	ETFB Isoform 2 of Electron transfer flavoprotein subunit beta	1.3788
IPI00783982.1	COPG Coatomer subunit gamma	1.383225
IPI00395617.5	ARID1B Isoform 2 of AT-rich interactive domain-containing protein 1B	1.40015
IPI00007163.1	LSM7 U6 snRNA-associated Sm-like protein LSm7	1.4041
IPI00788055.3	THAP4 Isoform 1 of THAP domain-containing protein 4	1.40415
IPI00032313.1	S100A4 Protein S100-A4	1.4077
IPI00003419.1	C11orf58 Small acidic protein	1.411175
IPI00657724.1	NPTN Isoform 3 of Neuroplastin	1.412625
IPI00383680.3	RPN2 ribophorin II isoform 2 precursor	1.4145
IPI00939431.1	RELN 368 kDa protein	1.4183
IPI00795292.1	NME2;NME1-NME2 Isoform 3 of Nucleoside diphosphate kinase B	1.420875
IPI00028004.2	PSMB3 Proteasome subunit beta type-3	1.421425
IPI00910593.1	CNN2 cDNA FLJ52765, highly similar to Calponin-2	1.425425
IPI00059139.1	ATP6V1E2 V-type proton ATPase subunit E 2	1.43245
IPI00015602.1	TOMM70A Mitochondrial import receptor subunit TOM70	1.439425
IPI00927101.1	RPSAP15;RPSA 30 kDa protein	1.440125
IPI00177728.3	CNDP2 Isoform 1 of Cytosolic non-specific dipeptidase	1.456575
IPI00894213.1	RTN4 Isoform 6 of Reticulon-4	1.4684
IPI00013122.1	CDC37 Hsp90 co-chaperone Cdc37	1.4926
IPI00418169.3	ANXA2 Isoform 2 of Annexin A2	1.51015
IPI00744851.2	HMGA1 cDNA FLJ54188, moderately similar to High mobility group protein HMG-I/HMG-Y	1.514425
IPI00940656.1	ANP32A;LOC723972 Putative uncharacterized protein ANP32A	1.529875
IPI00790115.1	SLC25A3 cDNA FLJ90278 fis, clone NT2RP1000325, highly similar to Phosphate carrier protein, mitochondrialprecursor	1.530125

IPI00009950.1	LMAN2 Vesicular integral-membrane protein VIP36	1.558975
IPI00871954.2	LARS cDNA FLJ58466, highly similar to Leucyl-tRNA synthetase, cytoplasmic	1.56735
IPI00939523.1	DDX46 117 kDa protein	1.63585
IPI00646241.1	CIRBP 18 kDa protein	1.650375
IPI00304925.5	HSPA1A;HSPA1B Heat shock 70 kDa protein 1	1.680575
IPI00299404.1	LAMB3 Laminin subunit beta-3	1.688175
IPI00465211.1	PPP3R1;WDR92 HZGJ	1.740825
IPI00942171.1	PRPSAP2 cDNA FLJ52829, highly similar to Phosphoribosyl pyrophosphatesynthetase-associated protein 2	1.76285
IPI00939315.1	- 37 kDa protein	1.76625
IPI00872855.1	EWSR1 Isoform EWS of RNA-binding protein EWS	1.83685
IPI00012382.3	SNRPA U1 small nuclear ribonucleoprotein A	1.8451
IPI00395939.4	PITPNB Phosphatidylinositol transfer protein, beta, isoform CRA_a	1.853325
IPI00550069.3	RNH1 Ribonuclease inhibitor	1.879725
IPI00746770.4	LOC728129 Putative LRRC3-like protein ENSP00000367157	1.88255
IPI00941900.1	CALU Isoform 1 of Calumenin	1.977975
IPI00328754.6	ZFHX4 zinc finger homeodomain 4	2.0119
IPI00943889.1	LOC100129103 similar to hCG2038970	2.15715
IPI00027409.1	PRTN3 Myeloblastin	2.186275
IPI00293276.10	MIF Macrophage migration inhibitory factor	2.292175
IPI00847759.2	DENND4B DENN domain-containing protein 4B	2.3784
IPI00385250.1	PRSS3 Protease serine 4 isoform B	2.698
IPI00218448.4	H2AFZ Histone H2A.Z	2.74285
IPI00793234.1	- 395 kDa protein	2.750125
IPI00009030.1	LAMP2 Isoform LAMP-2A of Lysosome-associated membrane glycoprotein 2	2.87545
IPI00031489.1	EIF1B Eukaryotic translation initiation factor 1b	2.97935
IPI00941463.1	NAP1L4 Nucleosome assembly protein 1-like 4	3.3569

IPI00022630.1	AIF1 Allograft inflammatory factor 1	3.977825
IPI00031696.4	FASTKD3 FAST kinase domain-containing protein 3	5.4235
IPI00644529.1	ZNF615;ZNF432 Isoform 1 of Zinc finger protein 615	6.91355
IPI00477040.1	NUP188 Isoform 1 of Nucleoporin NUP188 homolog	6.931175
IPI00479186.7	PKM2 Isoform M2 of Pyruvate kinase isozymes M1/M2	10.38615

TABLE B: Proteins significantly regulated in MV4-11 cells upon GEN treatment as identified by 8-plex iTRAQ

ACCESSION #	NAME	MV4-11-AVERAGE RATIO
IPI00926977.1	PSMC6 proteasome 26S ATPase subunit 6	0.232475
IPI00291764.5	HIST1H2AH;HIST1H2AI;HIST1H2AK;HIST1H2AJ;HIST1H2AG;HIST1H2AL;HIST1H2AM Histone H2A type 1	0.25295
IPI00515061.3	HIST1H2BJ Histone H2B type 1-J	0.292025
IPI00816460.2	DST Isoform 2 of Bullous pemphigoid antigen 1, isoforms 1/2/3/4/5/8 (Fragment)	0.368725
IPI00885176.1	C3orf77 Uncharacterized protein C3orf77	0.374425
IPI00216659.1	RBM8A Isoform 2 of RNA-binding protein 8A	0.4275
IPI00619914.2	U2AF1 U2 small nuclear RNA auxillary factor 1 isoform b	0.431375
IPI00010414.4	PDLIM1 PDZ and LIM domain protein 1	0.438025
IPI00004839.1	CRKL Crk-like protein	0.44925
IPI00793205.1	SFRS9 cDNA FLJ56571, highly similar to Splicing factor, arginine/serine-rich 9	0.45385
IPI00019927.2	PSMD7 26S proteasome non-ATPase regulatory subunit 7	0.460175

IPI00908443.1	DYSF Isoform 2 of Dysferlin	0.46565
IPI00299254.3	EIF5B Eukaryotic translation initiation factor 5B	0.468225
IPI00301058.5	VASP Vasodilator-stimulated phosphoprotein	0.472225
IPI00008418.6	DIABLO Diablo homolog, mitochondrial precursor	0.47235
IPI00909453.2	HSPB1 cDNA FLJ52243, highly similar to Heat-shock protein beta-1	0.484375
IPI00301561.1	TRIP6 Thyroid receptor-interacting protein 6	0.497025
IPI00783862.2	BLVRB Flavin reductase	0.50615
IPI00414684.7	SEMG1 Isoform 2 of Semenogelin-1	0.51215
IPI00946481.1	MBNL1 Protein	0.52285
IPI00017342.1	RHOG Rho-related GTP-binding protein RhoG	0.537975
IPI00026546.1	PAFAH1B2 Platelet-activating factor acetylhydrolase IB subunit beta	0.5461
IPI00942600.1	EIF4B 70 kDa protein	0.566325
IPI00604710.2	LOC442497;SLC3A2 Isoform 1 of 4F2 cell-surface antigen heavy chain	0.569
IPI00900327.2	PCBP2 cDNA FLJ58339, highly similar to Poly(rC)-binding protein 2	0.576725
IPI00221035.4	BTF3 Isoform 1 of Transcription factor BTF3	0.593775
IPI00005537.2	MRPL12 39S ribosomal protein L12, mitochondrial	0.595375
IPI00843996.1	SFRS3 Splicing factor, arginine/serine-rich 3, isoform CRA_a	0.60135
IPI00026519.1	PPIF Peptidyl-prolyl cis-trans isomerase, mitochondrial	0.602825
IPI00746438.2	RPL11 Isoform 2 of 60S ribosomal protein L11	0.603275
IPI00450855.1	HMGA1 HMGA1 protein	0.61485
IPI00748149.2	CDC20B Isoform 1 of Cell division cycle protein 20 homolog B	0.6159
IPI00412492.3	PLXND1 Isoform 1 of Plexin-D1	0.617675
IPI00219953.5	CMPK1 UMP-CMP kinase 1 isoform a	0.62145
IPI00217950.5	HMGN2 Non-histone chromosomal protein HMG-17	0.6233
IPI00008986.1	SLC7A5 Large neutral amino acids transporter small subunit 1	0.6301
IPI00011913.1	HNRNPA0 Heterogeneous nuclear ribonucleoprotein A0	0.631225

IPI00016513.5	RAB10 Ras-related protein Rab-10	0.632825
IPI00301434.4	BOLA2;BOLA2B BolA-like protein 2	0.634425
IPI00221224.6	ANPEP Aminopeptidase N	0.640525
IPI00420108.5	DLST;DLSTP Dihydrolipoyllysine-residue succinyltransferase component of 2-oxoglutarate dehydrogenase complex, mitochondrial	0.654725
IPI00219446.5	PEBP1 Phosphatidylethanolamine-binding protein 1	0.6565
IPI00026314.1	GSN Isoform 1 of Gelsolin	0.658975
IPI00922914.1	EPB41L3 cDNA FLJ58675, highly similar to Band 4.1-like protein 3	0.6629
IPI00853163.1	TYMP 46 kDa protein	0.668325
IPI00941730.1	ARHGAP1 cDNA FLJ60782, highly similar to Rho-GTPase-activating protein 1	0.66885
IPI00106491.3	MRTO4 mRNA turnover protein 4 homolog	0.669
IPI00025019.3	PSMB1 Proteasome subunit beta type-1	0.670975
IPI00031801.4	CSDA Isoform 1 of DNA-binding protein A	0.67155
IPI00787306.1	RCC1 regulator of chromosome condensation 1 isoform b	0.6721
IPI00013297.1	PDAP1 28 kDa heat- and acid-stable phosphoprotein	0.672275
IPI00456925.3	DBNL Isoform 1 of Drebrin-like protein	0.67765
IPI00006052.3	PFDN2 Prefoldin subunit 2	0.678725
IPI00002569.3	EIF4EBP1 Eukaryotic translation initiation factor 4E-binding protein 1	0.68335
IPI00935729.1	HBXIP Hepatitis B virus X-interacting protein	0.68905
IPI00375531.2	NME1 Isoform 2 of Nucleoside diphosphate kinase A	0.690675
IPI00021840.1	RPS6 40S ribosomal protein S6	0.692025
IPI00872952.1	UQCRH Ubiquinol-cytochrome c reductase hinge protein, isoform CRA_c	0.6942
IPI00412607.6	RPL35 60S ribosomal protein L35	0.70145
IPI00916535.1	P4HA1 prolyl 4-hydroxylase, alpha I subunit isoform 3 precursor	0.702575
IPI00456758.4	RPL27A 60S ribosomal protein L27a	0.70735
IPI00021924.1	H1FX Histone H1x	0.707575
IPI00290460.3	EIF3G Eukaryotic translation initiation factor 3 subunit G	0.7103

IPI00815642.1	TMSB4X TMSB4X protein (Fragment)	0.71265
IPI00220487.4	ATP5H Isoform 1 of ATP synthase subunit d, mitochondrial	0.71605
IPI00940263.1	LPXN 44 kDa protein	0.71715
IPI00015891.1	PFDN4 Prefoldin subunit 4	0.717875
IPI00945507.1	SUCLG2 48 kDa protein	0.7207
IPI00010270.1	RAC2 Ras-related C3 botulinum toxin substrate 2	0.721275
IPI00942171.1	PRPSAP2 cDNA FLJ52829, highly similar to Phosphoribosyl pyrophosphatesynthetase-associated protein 2	0.722425
IPI00303882.2	PLIN3 Isoform B of Mannose-6-phosphate receptor-binding protein 1	0.722825
IPI00027834.3	HNRNPL Heterogeneous nuclear ribonucleoprotein L	0.725125
IPI00176637.5	LOC728350;EIF2S2 Eukaryotic translation initiation factor 2 subunit 2-like protein	0.72895
IPI00217236.4	TBCA Tubulin-specific chaperone A	0.731425
IPI00873383.1	ST6GALNAC3 Putative uncharacterized protein ST6GALNAC3 (Fragment)	0.73335
IPI00025273.1	GART Isoform Long of Trifunctional purine biosynthetic protein adenosine-3	0.7336
IPI00005260.4	PSME4 Isoform 1 of Proteasome activator complex subunit 4	0.737675
IPI00936284.1	LOC100291317 hypothetical protein XP_002346735	0.737725
IPI00011200.5	PHGDH D-3-phosphoglycerate dehydrogenase	0.740125
IPI00014263.1	EIF4H Isoform Long of Eukaryotic translation initiation factor 4H	0.740525
IPI00647915.1	TAGLN2 24 kDa protein	0.74235
IPI00218319.3	TPM3 Isoform 2 of Tropomyosin alpha-3 chain	0.74525
IPI00025086.4	COX5A Cytochrome c oxidase subunit 5A, mitochondrial	0.746925
IPI00031708.1	FAH Fumarylacetoacetase	0.7485
IPI00219445.1	PSME3 Isoform 2 of Proteasome activator complex subunit 3	0.7494
IPI00941907.1	STRAP Serine-threonine kinase receptor-associated protein	0.749525
IPI00003419.1	C11orf58 Small acidic protein	0.75335
IPI00794978.1	MRPL47 Isoform 2 of 39S ribosomal protein L47, mitochondrial	0.75475
IPI00298547.3	PARK7 Protein DJ-1	0.7586

IPI00011569.2	ACACA Isoform 1 of Acetyl-CoA carboxylase 1	0.758975
IPI00010402.2	SH3BGRL3 Putative uncharacterized protein	0.75905
IPI00013452.10	EPRS Bifunctional aminoacyl-tRNA synthetase	0.75935
IPI00643317.3	HMGB3 21 kDa protein	0.75965
IPI00413611.1	TOP1 DNA topoisomerase 1	0.7599
IPI00386119.4	SF1 Isoform 5 of Splicing factor 1	0.76005
IPI00647786.1	ARHGEF1 Isoform 1 of Rho guanine nucleotide exchange factor 1	0.7623
IPI00879531.1	- 9 kDa protein	0.76255
IPI00337541.3	NNT NAD(P) transhydrogenase, mitochondrial	0.7628
IPI00219034.3	NDUFA8 NADH dehydrogenase [ubiquinone] 1 alpha subcomplex subunit 8	0.765725
IPI00026105.1	SCP2 Isoform SCPx of Non-specific lipid-transfer protein	0.766575
IPI00220362.5	HSPE1 10 kDa heat shock protein, mitochondrial	0.766825
IPI00021266.1	RPL23A 60S ribosomal protein L23a	0.76865
IPI00879702.2	RBBP7 Retinoblastoma binding protein 7	0.76875
IPI00376005.2	EIF5A Isoform 2 of Eukaryotic translation initiation factor 5A-1	0.770075
IPI00798025.1	C21orf33 Protein	0.770875
IPI00783982.1	COPG Coatomer subunit gamma	1.311425
IPI00789457.1	KPNA2 Karyopherin alpha 2	1.3168
IPI00847759.2	DENND4B DENN domain-containing protein 4B	1.319025
IPI00939174.1	OTUB1 Isoform 1 of Ubiquitin thioesterase OTUB1	1.320725
IPI00479191.2	HNRNPH1 51 kDa protein	1.324325
IPI00646241.1	CIRBP 18 kDa protein	1.3329
IPI00220503.9	DCTN2 dynactin 2	1.334425
IPI00009950.1	LMAN2 Vesicular integral-membrane protein VIP36	1.345175
IPI00478410.2	ATP5C1 Isoform Liver of ATP synthase subunit gamma, mitochondrial	1.357275
IPI00007244.1	MPO Isoform H17 of Myeloperoxidase	1.36145

IPI00220301.5	PRDX6 Peroxiredoxin-6	1.365
IPI00007163.1	LSM7 U6 snRNA-associated Sm-like protein LSm7	1.36535
IPI00641334.3	CYB5B Putative uncharacterized protein DKFZp686M0619	1.3658
IPI00375380.4	PSMD13 proteasome 26S non-ATPase subunit 13 isoform 2	1.3667
IPI00293655.3	DDX1 ATP-dependent RNA helicase DDX1	1.36765
IPI00943215.1	BID 22 kDa protein	1.377575
IPI00790115.1	SLC25A3 cDNA FLJ90278 fis, clone NT2RP1000325, highly similar to Phosphate carrier protein, mitochondrialprecursor	1.381575
IPI00759715.1	FH Isoform Cytoplasmic of Fumarate hydratase, mitochondrial	1.3822
IPI00945846.1	PRSS1 28 kDa protein	1.392275
IPI00927101.1	RPSAP15;RPSA 30 kDa protein	1.393575
IPI00894213.1	RTN4 Isoform 6 of Reticulon-4	1.396275
IPI00639819.1	TARDBP TAR DNA binding protein	1.4045
IPI00878984.1	DDT 14 kDa protein	1.413525
IPI00023542.6	TMED9 Transmembrane emp24 domain-containing protein 9	1.41695
IPI00945622.1	NAT13 15 kDa protein	1.42115
IPI00939315.1	- 37 kDa protein	1.422875
IPI00893362.1	RYR3 Putative uncharacterized protein RYR3	1.42985
IPI00023302.2	SYN2 Isoform IIa of Synapsin-2	1.4363
IPI00328754.6	ZFHX4 zinc finger homeodomain 4	1.44505
IPI00827658.1	CD44 Isoform 7 of CD44 antigen	1.448625
IPI00910419.1	DDOST cDNA FLJ52929, highly similar to Dolichyl-diphosphooligosaccharide--proteinglycosyltransferase 48 kDa subunit	1.448975
IPI00003217.3	PSMB7 Proteasome subunit beta type-7	1.458875
IPI00903204.1	RPS24 15 kDa protein	1.461875
IPI00872855.1	EWSR1 Isoform EWS of RNA-binding protein EWS	1.469025
IPI00795292.1	NME2;NME1-NME2 Isoform 3 of Nucleoside diphosphate kinase B	1.474
IPI00220416.3	UQCRB Cytochrome b-c1 complex subunit 7	1.4765

IPI00514530.5	ACTA1 Putative uncharacterized protein ACTA1	1.493825
IPI00013122.1	CDC37 Hsp90 co-chaperone Cdc37	1.498125
IPI00000816.1	YWHAE 14-3-3 protein epsilon	1.50145
IPI00940656.1	ANP32A;LOC723972 Putative uncharacterized protein ANP32A	1.513525
IPI00027409.1	PRTN3 Myeloblastin	1.515325
IPI00550917.3	TWF2 Twinfilin-2	1.51825
IPI00910593.1	CNN2 cDNA FLJ52765, highly similar to Calponin-2	1.519975
IPI00744851.2	HMGA1 cDNA FLJ54188, moderately similar to High mobility group protein HMG-I/HMG-Y	1.533025
IPI00007188.5	SLC25A5 ADP/ATP translocase 2	1.5607
IPI00420014.2	SNRNP200 Isoform 1 of U5 small nuclear ribonucleoprotein 200 kDa helicase	1.5767
IPI00219525.10	PGD 6-phosphogluconate dehydrogenase, decarboxylating	1.584975
IPI00105598.3	PSMD11 Proteasome 26S non-ATPase subunit 11 variant (Fragment)	1.586
IPI00015602.1	TOMM70A Mitochondrial import receptor subunit TOM70	1.58615
IPI00059139.1	ATP6V1E2 V-type proton ATPase subunit E 2	1.59565
IPI00743626.1	MTHFD2 Methylenetetrahydrofolate dehydrogenase (NADP+ dependent) 2, methenyltetrahydrofolate cyclohydrolase, isoform CRA_b	1.622525
IPI00908424.1	CDC2 cell division cycle 2 isoform 3	1.64165
IPI00550069.3	RNH1 Ribonuclease inhibitor	1.645675
IPI00657659.1	BNC2 Basonuclin 2	1.66475
IPI00399142.5	SURF4 Surfeit 4	1.667925
IPI00893258.1	SMC1B Isoform 3 of Structural maintenance of chromosomes protein 1B	1.70635
IPI00293276.10	MIF Macrophage migration inhibitory factor	1.71975
IPI00514622.2	RANBP6 Ran-binding protein 6	1.732075
IPI00383680.3	RPN2 ribophorin II isoform 2 precursor	1.7333
IPI00031411.3	FAT1 507 kDa protein	1.8685
IPI00022246.1	AZU1 Azurocidin	1.890675
IPI00914061.1	TCOF1 Treacher Collins-Franceschetti syndrome 1 isoform e	1.92545

IPI00746770.4	LOC728129 Putative LRRC3-like protein ENSP00000367157	1.926975
IPI00013163.1	MNDA Myeloid cell nuclear differentiation antigen	2.036625
IPI00220271.3	AKR1A1 Alcohol dehydrogenase [NADP+]	2.043675
IPI00793234.1	- 395 kDa protein	2.087575
IPI00006377.4	POMP Proteasome maturation protein	2.0987
IPI00759542.1	TTN Isoform 8 of Titin	2.102375
IPI00022643.2	TRIM36 E3 ubiquitin-protein ligase TRIM36	2.183625
IPI00385250.1	PRSS3 Protease serine 4 isoform B	2.197475
IPI00937077.1	hCG_2011852 hypothetical protein LOC643677	2.2041
IPI00218448.4	H2AFZ Histone H2A.Z	2.251175
IPI00939523.1	DDX46 117 kDa protein	2.2599
IPI00009030.1	LAMP2 Isoform LAMP-2A of Lysosome-associated membrane glycoprotein 2	2.269725
IPI00941463.1	NAP1L4 Nucleosome assembly protein 1-like 4	3.0814
IPI00939431.1	RELN 368 kDa protein	3.17255
IPI00022630.1	AIF1 Allograft inflammatory factor 1	3.278075
IPI00031696.4	FASTKD3 FAST kinase domain-containing protein 3	4.0252
IPI00644529.1	ZNF615;ZNF432 Isoform 1 of Zinc finger protein 615	6.2289
IPI00477040.1	NUP188 Isoform 1 of Nucleoporin NUP188 homolog	6.65625
IPI00479186.7	PKM2 Isoform M2 of Pyruvate kinase isozymes M1/M2	9.518775

LIST OF PUBLICATIONS

Publications in International peer-reviewed journals:

- **Karthik Narasimhan**, Teck Kwang Lim, Jin-Hua Han, Qingsong Lin. Rapamycin regulates multiple signalling pathways in AML and induces G1 arrest by an ingenious mechanism- revelations from a high-throughput study. *Under review.*

- **Karthik Narasimhan**, Teck Kwang Lim, Qingsong Lin. Characterization of the anti-leukemic effects of genistein- an iTRAQ based proteomic study. *Manuscript under preparation.*

Presentations at Conferences:

- **Karthik Narasimhan**, Teck Kwang Lim, Jin-Hua Han, Qingsong Lin. Rapamycin regulates multiple signaling pathways in AML and induces G1 arrest by an ingenious mechanism - revelations from a high-throughput study. Human Proteome Organisation (HUPO), 8th Annual World Congress, 2009, Toronto, Canada, 26th-30th September, 2009. Was awarded the **Young Investigator Award**.

- **Karthik Narasimhan**, Teck Kwang Lim, Jin-Hua Han, Qingsong Lin. Rapamycin mediated Acute Myeloid Leukemia therapy- a high-throughput study. Singapore Society for Mass Spectrometry, 1st Annual Seminar, 2008, Singapore.

- **Karthik Narasimhan**, Teck Kwang Lim, Jin-Hua Han, Qingsong Lin. Rapamycin mediated Acute Myeloid Leukemia therapy- a microarray study. 12th Biological Sciences Graduate Congress, University of Malaya, Kuala Lumpur, Malaysia, 17-19 December, 2007- Won **best oral presentation runner-up award**.

- **Karthik Narasimhan**, Jin-Hua Han. Rapamycin as a therapy for Acute Myeloid Leukemia- an investigative study. 11th Biological Sciences Graduate Congress, Chulalongkorn University, Bangkok, Thailand, 14-17 December, 2006- Won **best oral presentation award**.

- **Karthik Narasimhan**, Jin-Hua Han. Rapamycin as a therapy for Acute Myeloid Leukemia- an investigative study. Joint third AOHUPO and fourth structural biology and genomics conference, National University of Singapore, 4-7 December, 2006.